

© 2019

Stephanie Michelle Marco

ALL RIGHTS RESERVED

**DISPOSITION AND MOLECULAR ACTIONS OF  
ORGANOPHOSPHATE FLAME RETARDANTS**

By

STEPHANIE MICHELLE MARCO

A dissertation submitted to

The School of Graduate Studies

Rutgers, The State University of New Jersey

In partial fulfillment of the requirements

For the degree of

Doctor of Philosophy

Graduate Program in Toxicology

Written under the direction of

Brian Buckley, Ph.D.

And approved by

---

---

---

---

---

New Brunswick, New Jersey  
May 2019

## **ABSTRACT OF THE DISSERTATION**

Disposition and Molecular Actions of Organophosphate Flame Retardants

By STEPHANIE MICHELLE MARCO

Dissertation Director:

Brian Buckley, Ph.D.

Organophosphate flame retardants (OPFRs) are a class of chemicals applied to clothing, electronics, plastics, furniture, and building materials to reduce the flammability of commercial products. Over the past 15 years, global use of OPFRs has increased significantly, as they replace other persistent bioaccumulative compounds such as polybrominated diphenyl ethers. OPFRs are chemicals of emerging toxicological and environmental concern due to reports of endocrine disruption, neurotoxicity, and reproductive and developmental toxicity in animals; as well as their environmental persistence. Although research on the adverse effects of OPFR exposure has increased over the past decade, there are still several gaps in our understanding of their behavior *in vivo* and their potential toxicity, especially in mammals. The purpose of this dissertation was to investigate whether OPFRs interact with molecular targets (acetylcholinesterase, AChE), metabolic enzymes (carboxylesterase, CES), and transporters (multi-drug resistance protein 1, MDR1) that influence their overall disposition and potential for neurotoxicity. The findings in this dissertation demonstrate that OPFRs do not

behave like the structurally similar organophosphate pesticides in terms of inhibiting enzyme activity and that OPFRs are more effective inhibitors of CES than AChE. Although, the OPFRs did not demonstrate adverse effects on brain and liver enzymatic activity *in vitro*, the brain and liver, as well as the kidneys, placenta, and fetus, were identified as targets of toxicity due to their preferential accumulation of OPFRs. Finally, MDR1 was shown to potentially influence the *in vivo* disposition of TPP in the brain suggesting that MDR1 may protect the brain from TPP accumulation. The results of this study will help guide future research into OPFR-induced organ-specific adverse effects, especially in the brain and in the developing fetus.

## **DEDICATION**

This dissertation is dedicated to my parents, Timothy and Nelly Marco.

## ACKNOWLEDGMENTS

Throughout my graduate career, I have been fortunate to receive overwhelming support from mentors, colleagues, staff, friends, and family alike. Each one has played an important role in helping me to complete my doctorate.

To my advisor, Dr. Brian Buckley, thank you for being such a supportive and encouraging mentor. You have always been a champion for my success, guiding me through many aspects of my professional and personal life. I am profoundly grateful to have been a part of your lab.

To all the past and present members of the Buckley lab who I have had the privilege to work with over the course of my graduate career: Dr. Hilly Yang, Dr. Anita Brinker, Dr. Cathleen Doherty, Nicole Renkel, Brittany Karas, Melody Wren, Abby Lazofsky, Dr. Saowanee Norkaew, Dr. Elizabeth McCandlish, and Dr. Min Liu. Hilly, thank you for all that you have taught me. You always made yourself available to me whether it be to discuss analytical methods or to review data, and I am grateful for your guidance. To my officemates, Elizabeth, Min, Saowanee, Cathleen, and Abby, thank you for all the wonderful conversations we have shared and for the many laughs that came with them. Anita, Nicole, Melody, and Brittany, you have never hesitated to lend a helping hand and I am so appreciative.

Thank you, Drs. Lauren Aleksunes, Troy Roepke, Jason Richardson, and Jeehiun Lee, for serving on my thesis committee. I am grateful for all the time, energy, and resources you have invested in me and my research. It has been a privilege to

work with each of you. I also want to thank the Aleksunes, Roepke, and Richardson lab members especially Dr. Xia Wen, Dr. Diana You, Ludwik Gorczyca, Ali Yasrebi, Dr. Ashley Green, Dr. Angela Baker, and Angela Tiethof for all your help.

Dr. Ken Reuhl, thank you for everything. I have learned so much from you both in and out of the classroom. You have always been in my corner, and I cannot thank you enough for that. Drs. Grace Guo and Mike Gallo, thank you for your support and encouragement.

To Liz, Linda, Eva, Sandi and Perry, the kindest and most supportive administrative staff, thank you for being your caring selves and for all your help over the years. To Lisa, Sam, Dave, Maria, Mario, TJ, and Wilson, thank you for all the work that you do. Without your efforts, things would not run nearly as smoothly as they do.

Thank you, Drs. Sheryse Taylor, Diana You, and Blessy George for being the best classmates turned friends anyone could ask for. Thank you, Breann Coffaro, Brittany Karas, and Nicole Renkel for making me smile and laugh even through the most challenging of times. Gabby Wahler, Talia Planes-Fontanez, Dr. Laura Armstrong, Dr. Sara Fournier, Dr. Justin Schumacher, Dr. John Szilagyi, Dr. Cody Smith, Dr. Amy Kohtz, Alexa Murray, and Dan Rizzolo, thank you for the wonderful memories. To the RATS, thank you for being such a great group of colleagues. I always enjoyed our get-togethers and look forward to seeing you all again soon.

To Vishwa, Caity, Sharana, and Stacey—my Rutgers/UNH family—thank you for all the laughs but most importantly thank you for always being there. To my Rockland family—Meagan, Tom, Lorraine, Kristen, Jimmy, Coop, Lauren, Nicole, Matt, Tim, John, Joe, Anthony, Jackie, Liz, and Katie—thank you for keeping me sane all these years. I am so lucky to have friends like you.

I am forever grateful to my family for helping me to get where I am today. Mom and Dad, thank you for your love and unwavering support. Thank you for believing in me even when I did not believe in myself. Jen, thank you for being there when I needed you most. Thank you, Uncle Ken, Grandma, Elena, Aunt Vicky, Uncle Tony, Uncle Danny, Patricia, Danny, and Uncle Tony for your constant prayers and encouragement. Grandpa, thank you for watching over me and reminding me to say a little prayer, take a deep breath, and do my best.



## ACKNOWLEDGMENT OF PUBLICATIONS

*In preparation for submission to Toxicology:*

### CHAPTER 2

**Marco SM**, Richardson JR, Buckley BT (2019) Comparative Assessment of the Organophosphate Flame Retardants for Acetylcholinesterase and Carboxylesterase Inhibitory Activity In Vitro. *In preparation for submission to Toxicology.*

*In preparation for submission to Environmental Toxicology and Pharmacology:*

### CHAPTER 4

**Marco SM**, Wen X, Yang I, Richardson JR, Aleksunes LA, Buckley BT (2019) Assessment of Organophosphate Flame Retardant Interactions with the MDR1 Transporter In Vitro and In Vivo. *In preparation for submission to Environmental Toxicology and Pharmacology.*

### APPENDIX 1

Krumm EA, Patel VJ, Tillery TS, Yasrebi A, Shen J, Guo GL, **Marco SM**, Buckley BT, Roepke TA (2018) Organophosphate flame-retardants alter adult mouse homeostasis and gene expression in a sex-dependent manner potentially through interactions with ERalpha. *Toxicol Sci.* 162(1):212-224.

## TABLE OF CONTENTS

|  |      |
|--|------|
| ABSTRACT OF THE DISSERTATION .....                     | ii   |
| DEDICATION .....                                       | iv   |
| ACKNOWLEDGMENTS .....                                  | v    |
| ACKNOWLEDGMENT OF PUBLICATIONS .....                   | viii |
| TABLE OF CONTENTS .....                                | ix   |
| LIST OF FIGURES .....                                  | xii  |
| LIST OF TABLES .....                                   | xiv  |
| CHAPTER 1: INTRODUCTION .....                          | 1    |
| 1.1    General Overview .....                          | 1    |
| 1.2    Distribution of OPFRs in the Environment .....  | 3    |
| 1.3    Human Exposure to OPFRs .....                   | 4    |
| 1.4    OPFR Pharmacokinetics and Toxicokinetics .....  | 8    |
| 1.4.1    Metabolism .....                              | 8    |
| 1.4.2    Distribution, Excretion, and Half-Lives ..... | 9    |
| 1.4.3    Molecular Targets .....                       | 11   |
| 1.5    OPFR Toxicities .....                           | 14   |
| 1.5.1    Humans .....                                  | 14   |
| 1.5.2    Rodents .....                                 | 19   |

|  |   |    |
|--|---|----|
| 1.5.3  | Fish .....                              | 24 |
| 1.6  | Research Objective and Hypothesis ..... | 32 |
| CHAPTER 2: COMPARATIVE ASSESSMENT OF THE                   |   |    |
| ORGANOPHOSPHATE ESTERS FOR ACETYLCHOLINESTERASE AND        |   |    |
| CARBOXYLESTERASE INHIBITORY ACTIVITY <i>IN VITRO</i> ..... |   |    |
| 2.1  | Abstract .....                          | 38 |
| 2.2  | Introduction.....                       | 41 |
| 2.3  | Materials and Methods .....             | 45 |
| 2.4  | Results .....                           | 49 |
| 2.5  | Discussion .....                        | 53 |
| CHAPTER 3: DISPOSITION OF ORGANOPHOSPHATE FLAME            |   |    |
| RETARDANTS IN MICE.....                                    |   |    |
| 3.1  | Abstract .....                          | 64 |
| 3.2  | Introduction.....                       | 67 |
| 3.3  | Materials and Methods .....             | 70 |
| 3.4  | Results .....                           | 74 |
| 3.5  | Discussion .....                        | 78 |
| CHAPTER 4: ASSESSMENT OF ORGANOPHOSPHATE FLAME             |   |    |
| RETARDANT INTERACTIONS WITH THE MDR1 TRANSPORTER <i>IN</i> |   |    |
| <i>VITRO</i> AND <i>IN VIVO</i> .....                      |   |    |
|  |   | 89 |

|   |                             |     |
|---|-----------------------------|-----|
| 4.1   | Abstract .....              | 90  |
| 4.2   | Introduction.....           | 93  |
| 4.3   | Materials and Methods ..... | 97  |
| 4.4   | Results .....               | 102 |
| 4.5   | Discussion .....            | 107 |
| CHAPTER 5: OVERALL DISCUSSION.....                                    |                             | 122 |
| APPENDIX 1: Organophosphate flame-retardants alter adult mouse        |                             |     |
| homeostasis and gene expression in a sex-dependent manner potentially |                             |     |
| through interactions with ERalpha .....                               |                             |     |
|   |                             | 131 |
| A-1.1   | Abstract .....              | 132 |
| A-1.2   | Introduction .....          | 133 |
| A-1.3   | Materials and Methods ..... | 137 |
| A-1.4   | Results.....                | 145 |
| A-1.5   | Discussion .....            | 153 |
| REFERENCES .....  |                             | 171 |

## LIST OF FIGURES

|  |     |
|--|-----|
| Figure 2.1. Inhibition of AChE activity by OPEs.....   | 60  |
| Figure 2.2. Inhibition of CES activity by OPEs .....   | 62  |
| Figure 3.1. Names, acronyms, and structures of the OPFRs used in this study.   | 83  |
| Figure 3.2. OPFR disposition in adult male and female mice .....   | 84  |
| Figure 3.3. Maternal-fetal transfer of OPFRs <i>in utero</i> .....   | 86  |
| Figure S3.1. Representative gas chromatogram of the OPFRs.....   | 88  |
| Figure 4.1. Names, acronyms, and structures of the OPFRs used in this<br>study.....  | 111 |
| Figure 4.2. OPFR-induced cell death .....  | 112 |
| Figure 4.3. OPFR effects on MDR1 efflux function.....  | 113 |
| Figure 4.4. OPFR disposition in wild-type (WT) and Mdr1a/1b-null (KO) mice.  | 114 |
| Figure S4.1. Representative gas chromatogram of the OPFRs.....   | 116 |
| Figure S4.2. Confirmation of MDR1 protein expression in HEK293 cells<br>stably-transfected with the human <i>MDR1</i> gene ..... | 118 |
| Figure S4.4. OPFR disposition in the kidneys of wild-type (WT) and<br>Mdr1a/1b-null (KO) mice .....                              | 120 |
| Figure A-1.1. Serum concentrations of TDCPP, TPP, TCP, and PBDE-47 .....   | 162 |
| Figure A-1.2. Percent weight gain and body weight in mice. ....  | 163 |

|   |     |
|---|-----|
| Figure A-1.3. Weekly energy intake, feeding efficiency, and fasting glucose in mice ..... | 164 |
| Figure A-1.4. Glucose and insulin tolerance in mice.....                                  | 165 |
| Figure A-1.5. Plasma levels of peptide hormone ghrelin, leptin, and insulin.....          | 166 |
| Figure A-1.6. Illustration of our hypothesis .....  | 170 |

## LIST OF TABLES

|  |     |
|--|-----|
| Table 1.1. Names and acronyms of OPFRs and metabolites reviewed.....   | 33  |
| Table 1.2. OPFR metabolite concentrations in human urine (ng/mL) .....   | 35  |
| Table 2.1. Names, acronyms, classes, and structures of OPEs screened for inhibition of AChE and CES activity .....                               | 58  |
| Table S3.1. Molecular weights (MW), retention times (RT), and quantitation ions (Q) for each OPFR.....   | 87  |
| Table 4.1. Tissue/serum partitioning of OPFRs in WT and MDR1 KO mice .....   | 115 |
| Table S4.1. Molecular weights (MW), retention times (RT), and quantitation ions (Q) for each OPFR. TPP-D15 was used as an internal standard..... | 117 |
| Figure S4.3. Confirmation of MDR1 function in HEK293 cells transfected with the human <i>MDR1</i> gene .....                                     | 119 |
| Table S4.2. Kidney/serum ratios for wild-type (WT) and Mdr1a/1b-null (KO) mice.....  | 121 |
| Table A-1.1. Arcuate expression of neuropeptides and hormone receptors from WT and ERKO male and females .....                                   | 167 |
| Table A-1.2. Arcuate expression of cation channels from WT and ERKO male and females.....  | 168 |
| Table A-1.3. Liver expression of xenobiotic receptor target genes from WT and ERKO male and females.....   | 169 |

## CHAPTER 1: INTRODUCTION

### 1.1 General Overview

Flame retardants are material additives that prevent combustion and delay the spread of fire after ignition. U.S. manufacturers began adding flame retardants to plastics, construction material, textiles, furniture, and electronics to meet flammability standards in the 1970s. One of the initial classes of flame retardants on the market was polybrominated diphenyl ethers (PBDEs). However, beginning in 2005, PBDEs were phased out due to their environmental persistence, bioaccumulation, and risk to human health creating a demand for alternative chemicals such as organophosphate flame retardants (OPFRs).

Over the past two decades, the use of OPFRs has increased. In 1992, 17% of the estimated 600,000 tons of flame retardants used worldwide were OPFRs (OECD 1995) and 70% of the 300,000 tons of organophosphorus compounds utilized in 2004 were OPFRs (Wei et al. 2015). The U.S. Environmental Protection Agency (EPA) reported more recently that chlorinated OPFRs are high production chemicals with greater than 50 million pounds per year produced or imported into the U.S. (EPA 2015). Like PBDEs, OPFRs are additives and are not chemically bound to materials. As a result, OPFRs can easily leach into the environment via volatilization, abrasion, and dissolution.

OPFRs have been detected in the environment suggesting that human and wildlife exposure to these chemicals is likely widespread (Dishaw et al. 2014). Several studies have reported the detection of OPFRs in sediment/soil, water, biota, indoor



air, and dust. A detailed review of these external environment studies was previously published in 2012, 2015, and 2016 (Greaves and Letcher 2016; Hou et al. 2016; van der Veen and de Boer 2012). OPFRs have also been detected in household consumables such as furniture and baby products (Patisaul et al. 2013; Stapleton et al. 2011). Indoor exposures to OPFRs are often higher than outdoor exposures, which may suggest that humans could be at risk of adverse health effects due to direct interaction with chemicals on a daily basis (Dishaw et al. 2014; van der Veen and de Boer 2012). In particular, young children (ages 1-5 years old) are exposed to environmental contaminants during normal oral and manual exploration of their environment (e.g. crawling and hand-to-mouth activity). Since young children spend a significant amount of time indoors and in close proximity to carpets that accumulate potentially contaminated dust and dirt, they are estimated to ingest 2-10 times more mg of dust per day compared to adults (EPA 2008). These exploratory behaviors put young children at greater risk of exposure to OPFRs than adults.

Numerous studies have monitored human exposure to OPFRs using urinary metabolites as biomarkers. The ubiquitous detection of OPFR metabolites in toddlers, children, pregnant women, and adults justify cause for concern (Castorina et al. 2017a; Castorina et al. 2017b; Chen et al. 2018; He et al. 2018; Hoffman et al. 2017a; Hoffman et al. 2017b; Ospina et al. 2018; Thomas et al. 2017). Over the past decade, scientists have begun to focus on delineating the potential adverse effects of OPFR exposure. Studies have suggested that OPFR exposure can cause adverse effects including neurotoxicity, carcinogenicity,

reproductive toxicity, and endocrine disruptions. OPFRs have been shown to alter sperm and hormone concentrations in humans (Meeker and Stapleton 2010), induce metabolic syndrome in rats (Patisaul et al. 2013), affect testis organization in mice (Chen et al. 2015b), and induce neurodevelopmental toxicity in zebrafish (Dishaw et al. 2014). The purpose of this Introduction will be to provide an update on recent human exposure and human, rodent, aquatic, and *in vitro* toxicity studies concerning OPFRs.

## **1.2 Distribution of OPFRs in the Environment**

OPFRs have been detected in air, soil, and water globally. A detailed review of OPFRs in the environment can be found in van der Veen and de Boer (2012). Recent studies characterizing the distribution of OPFRs in abiotic matrices indicate that OPFR concentrations continue to rise. Air samples collected via passive air sampling of rural, agricultural, suburban, urban, and industrial regions of Bursa, Turkey ranged from 529 to 19,139 pg OPFR/m<sup>3</sup> (Kurt-Karakus et al. 2017). Higher concentrations of alkyl OPFRs (such as tris(2-butoxyethyl) phosphate, TBOEP), with much lower concentrations of chlorinated and aryl OPFRs (such as tris (2-chloroethyl) phosphate (TCEP) and triphenyl phosphate (TPP), respectively). Additionally, levels of OPFRs were much higher than levels of PBDEs, which reflects the shift toward the use of alternative flame retardants. Overall, nonchlorinated OPFRs dominated every other type in the sampled locations. By comparison, a study in the U.S. Great Lakes basin showed that urban sites (Cleveland and Chicago) were dominated by chlorinated OPFRs (such as TCEP and tris(1,3-dichloro-2-propyl) phosphate, [TDCPP]) whereas nonchlorinated

OPFRs (such as TBOEP and TPP) were most abundant in rural sites (Eagle Harbor and Sleeping Bear Dunes) (Salamova et al. 2014b). Similarly, air concentrations of nonchlorinated OPFRs, such as TPP, have increased relative to PBDEs and other brominated flame retardants by orders of magnitude in the Northern Pacific, European Arctic, and Canadian Arctic regions (Moller et al. 2012; Salamova et al. 2014a; Suhring et al. 2016).

As aforementioned, indoor exposures tend to be higher than outdoor exposure because of the use of OPFRs in household, commercial, and workplace products. Analysis of dust from multiple fire stations across U.S. state lines indicated that OPFR levels, including TBP, TCPP, and TDCPP, were higher in firehouses than in other occupational and residential settings (Shen et al. 2017). In these fire stations, the OPFR concentrations in dust were on the same order of magnitude as PBDE concentrations (maximum OPFR: 218,000 ng/g; maximum PBDE: 351,000 ng/g). In Brazil where flame retardant use is not regulated to the standards in the U.S., OPFRs were detected at higher concentrations in indoor dust than PBDEs and newer brominated flame retardants (Cristale et al. 2018). Notably, TBOEP, TPP, TDCPP, and TCPP were the most abundant OPFRs detected.

### **1.3 Human Exposure to OPFRs**

Due to the ubiquitous nature of the OPFRs in the environment, numerous studies have been conducted to quantify human exposures to these compounds. The primary routes of human exposure to OPFRs are reported to occur via inhalation, ingestion, and dermal contact (Hou et al. 2016). Multiple studies have quantified

human exposure in diverse populations using OPFR metabolites as biomarkers for detection (**Table 1.1, Fig. 1.1**). A summary of these findings published since the most recent review by Wei et al. (2015) is presented in **Table 1.2**.

As previously mentioned, toddlers and children have been historically considered as a vulnerable population to OPFR exposure due to their frequent hand-to-mouth contact, increased time spent indoors, and lower body weights compared to adults (EPA 2015). In a study of infants and children (0-5 years old) from Australia, pooled female urine (n=10 pooled samples from 200 individuals) had significantly higher concentrations of diphenyl phosphate (DPP) and lower concentrations of TEHP than the pooled male urine (n=10 pooled samples from 200 individuals) (He et al. 2018). Additionally, a decrease in TCEP, BCEP, TEHP, and DBP concentrations in urine was observed with advancing age. Moreover, a preliminary assessment of the estimated daily intake of OPFRs from breast milk suggested that breastfeeding is the major route of exposure for TCEP, TEHP, and TBP in infants and toddlers. OPFRs have previously been detected in breast milk in two studies (n=87 Kim et al., n=286 Sundkvist et al.) at concentrations ranging from 46 to 180 ng/g lipid weight (Kim et al. 2014; Sundkvist et al. 2010). In a U.S.-based study, OPFR metabolites were detected in a 100% of urine samples from toddlers (15- to 18-months old, n=41), which supports previous findings indicating widespread exposure to OPFRs (Thomas et al. 2017). Average urine DPP concentrations were greater than median concentrations in German toddlers (22-80 months, n=312), which is consistent with previous reports of higher OPFR exposures in U.S. populations relative to European (Fromme et al. 2014; Thomas et al. 2017).

BDCPP concentrations were similar to cohorts in North Carolina (2-18 months, n=43) and New Jersey (1-5 years old, n=23), but lower than in a California (2-70 months, n=33) cohort, which may be due to California's stricter furniture flammability standards (Butt et al. 2014; Butt et al. 2016; Hoffman et al. 2015). In China, BCEP and DPP were most frequently detected in the urine of children 6-14 years old (n=411) (Chen et al. 2018). OPFR metabolite levels were generally lower compared to similar studies in other countries, except for BCEP suggesting that children in South China have a relatively high exposure level to TCEP. Investigators also saw a relatively high level of TCEP in Chinese adults (n=757) where the mean concentration of blood-TCEP increased 13% from 2011 to 2015 (Ma et al. 2017). Similar to the cohort in Australia, a negative correlation with age for urinary concentrations of BCEP ( $r=-0.277$ ), BDCPP ( $r=-0.157$ ), DCP ( $r=-0.112$ ), and DPP ( $r=-0.270$ ) was observed (Chen et al. 2018; He et al. 2018). This trend was also observed in the 2013-2014 National Health and Nutrition Examination Survey (NHANES) study of the U.S. general population (6 years and older; n=2244) for OPFR exposure (Ospina et al. 2018). Children (6-11 years; n=421) were found to have higher urinary concentrations of BDCPP and DPP than adults ( $\geq 60$  years; n=552). Additionally, BDCPP and DPP were detected in approximately 92% of study participants, BCEP in 89%, DBP in 81%, and BCPP in 61%. Moreover, females had significantly higher DPP and BDCPP concentrations than males. Overall, the results of these studies corroborate previous findings suggesting that OPFR exposure is extensive.

Exposure of pregnant women to OPFRs has also been investigated. In a recent publication investigating a cohort of pregnant women in California (n=310), BDCPP and TPP were detected in 78% and 79% of urine samples collected between 2000 and 2001 (Castorina et al. 2017b). By comparison, these women had lower median OPFR metabolite levels (BDCPP: 0.4 ng/mL, DPP: 0.9 ng/mL) than pregnant women in a North Carolina cohort (BDCPP: 1.8 ng/mL, DPP: 1.4 ng/mL) collected between 2002 and 2005 (Castorina et al. 2017b; Hoffman et al. 2017b). Interestingly, urine DPP and BDCPP concentrations from the North Carolina cohort were similar to those measured in a 2011-2012 cohort of pregnant women from the same state (BDCPP: 1.3 ng/mL, DPP: 1.9 ng/mL), despite the phase-out of PBDEs, which was thought to have resulted in increased OPFR usage (Hoffman et al. 2014; Hoffman et al. 2017b). Akin to the California and North Carolina cohorts, investigators frequently detected DPP (95%) and BDCPP (93%) in urine samples collected from pregnant women in Rhode Island (n=59) from 2014-2015 (Romano et al. 2017). Additionally, urinary concentrations of these metabolites were relatively reproducible from weeks 12 to 35 of gestation. The greater detection frequency of OPFR metabolites may be indicative of the increase in OPFR usage following the PBDE phase-out, as the study took place approximately three years after the 2011-2012 North Carolina cohort.

Recently, temporal trends in OPFR exposure across multiple age groups and populations in the U.S. have been studied. Investigators combined data from 14 U.S.-based epidemiological studies conducted between 2002 and 2015 to assess exposure to TDCPP and TPP (Hoffman et al. 2017a). Urine BDCPP concentrations

were shown to have increased dramatically since 2002. Samples collected in 2014 and 2015 had 15-fold higher urine BDCPP concentrations compared to those collected in 2002 and 2003. Furthermore, there was a significant elevation in urine DPP levels albeit smaller than what was observed for BDCPP. It also appears that exposure varies seasonally with significantly higher levels of exposure in summer for both TDCPP and TPP compared to winter suggesting that OPFR exposure may be temperature-dependent as well as a reflection of seasonal behavior changes (Hoffman et al. 2017a). The increase in exposure levels by the general population underscore the necessity of determining the potential for adverse health outcomes.

## 1.4 OPFR Pharmacokinetics and Toxicokinetics

### 1.4.1 Metabolism

Several studies have investigated the metabolic pathways of OPFRs *in vivo* and *in vitro*. OPFRs have been shown to be rapidly metabolized via Phase I and Phase II reactions (Van den Eede et al. 2013a; Van den Eede et al. 2013b). Although information is quite limited, several possible metabolic pathways have been proposed (**Fig. 1.2**). Cytochrome P450s (CYPs)—a superfamily of isozymes responsible for the biotransformation of a variety of xenobiotic and endobiotic compounds—are thought to be the primary enzymes responsible for OPFR metabolism. However, NADPH-independent pathways involving paraoxonases and arylesterases have also been shown to catalyze OPFR metabolism (Chapman et al. 1991; Sasaki et al. 1984; Van den Eede et al. 2013a). Chlorinated OPFRs (such as TDCPP and TCEP) undergo Phase I metabolism by ether bond cleavage

(O-dealkylation) or by terminal carbon oxidative dehalogenation (Hou et al. 2016; Van den Eede et al. 2013a). Phase I metabolites of chlorinated OPFRs include diesters, hydroxylated metabolites, and carboxylic acids, which have been observed in human liver microsomes and S9 fractions as well as in rats and rat liver homogenates (Burka et al. 1991; Hou et al. 2016; Nomeir et al. 1981; Van den Eede et al. 2013a). Chlorinated OPFRs also undergo Phase II metabolism, resulting in glutathione conjugates via substitution of the chlorine (Burka et al. 1991; Van den Eede et al. 2013a). Alkyl OPFRs (such as TBP and TBOEP) can be dealkylated to their diester metabolites by hydrolysis or form hydroxylated metabolites in rats and rat liver microsomes (Hou et al. 2016; Sasaki et al. 1984; Suzuki et al. 1984). This was corroborated by studies in human liver microsomes and S9 fractions (Van den Eede et al. 2013a). Unlike chlorinated OPFRs, Phase II metabolites of alkyl OPFRs were shown to only undergo Phase II metabolism on the hydroxylated metabolites produced after Phase I metabolism (Hou et al. 2016). Aryl OPFRs (such as TPP and TCP) have similar metabolic pathways to alkyl OPFRs. O-dealkylation, hydroxylation, oxidation, and conjugation (sulfate and glucuronide conjugates) reactions were observed in chicken embryonic hepatocytes, human liver microsomes and S9 fractions, and rats (Kurebayashi et al. 1985; Su et al. 2014; Van den Eede et al. 2013a).

#### 1.4.2 Distribution, Excretion, and Half-Lives

General distribution and accumulation data for OPFRs are limited (Greaves and Letcher 2016). Studies investigating the *in vivo* distribution of OPFRs have generally been done in rats and fish. TDCPP and TCEP have been shown to be



rapidly and extensively absorbed following acute dosing and distribute throughout the body without preferential treatment in specific organs or tissues in rats (Herr et al. 1991; Nomeir et al. 1981). In another study, 5-week-old male Wistar rats were given a single dose of 50  $\mu\text{mol/kg}$  ( $\sim 14 \text{ mg/kg}$ ) of  $^{14}\text{C}$ -labeled TCEP or TDCPP by gavage and sacrificed at different times over a period of 7 days (ASTDR 2012; Minegishi et al. 1988). Low tissue/blood ratios were detected in the brain (0.05-0.08), heart (0.29-1.13), muscle (0.12-1.35), and testis (0.20-1.86), moderate ratios in adipose (0.12-2.08), spleen (0.18-2.35), and lung (0.39-3.50), and high ratios in the liver (0.62-8.16) and kidneys (0.90-10.60). The highest amount of radioactivity was found in the liver and kidney after 12 hours (67.08 nmol TDCPP/g liver and 26.31 nmol TCEP/g kidney) and the liver after 7 days (2.27 nmol TDCPP g/liver and 1.00 nmol TCEP g/liver). The biological half-lives ( $t_{1/2}$ ) for TCEP and TDCPP exhibited a biphasic response with the longest  $t_{1/2}$  occurring in phase two for TDCPP and TCEP in adipose at 92 and 87 hours, respectively. Elimination of TDCPP primarily occurred in urine (43.2% of  $^{14}\text{C}$ -labeled dose) followed by feces (39.2%), and expired air (16.2%). By comparison, TCEP was eliminated at 96% in urine, 6% in feces, and 2% in expired air. In general, dichlorinated alkyl OPFRs (TDCPP) were more slowly absorbed, distributed, and excreted than monochlorinated alkyl OPFRs (TCEP) (Minegishi et al. 1988). Killifish exposed to TCEP (1-3 ppm) and TDCPP (1 ppm) as well as TBP (3-4 ppm) and TPP (0.25 ppm) in water were shown to have  $t_{1/2}$  of 0.7 hours (TCEP), 31 hours (TDCPP), 58 hours (TBP), and 5 hours (TPP) (Sasaki et al. 1981). Goldfish exposed to the same treatment paradigm—except TCEP—exhibited longer  $t_{1/2}$  for TDCPP (42 hours),

TBP (100 hours), TPP (>100 hours). These data suggest that chlorinated OPFRs (such as TDCPP and TCEP) have rapid elimination rates compared to alkyl (TBP) and aryl (TPP) OPFRs in fish. Despite the aforementioned data on OPFR metabolism, distribution, and excretion, a comprehensive study of OPFRs would be necessary to fully understand their toxicokinetics.

### 1.4.3 Molecular Targets

#### 1.4.3.1 *Serine Hydrolases*

Serine hydrolases are a class of enzymes known to metabolize xenobiotic (e.g. pesticides) and endogenous compounds (e.g. acetylcholine) via hydrolysis at the active site serine. This family of enzymes includes esterases such as acetylcholinesterase (AChE) and carboxylesterase (CES). AChE is primarily responsible for hydrolysis of the neurotransmitter acetylcholine. Organophosphate pesticides (OPs)—a structurally similar class of compounds that have been consistently referred to when exploring potential OPFR-induced adverse effects—are potent AChE inhibitors (Casida 1964). When AChE is inhibited in insects—the primary target of OPs—rapid twitching of voluntary muscles and paralysis occurs. Unfortunately, OPs also inhibit AChE in humans resulting in the continuous stimulation of the muscles, glands, and central nervous system. Anticholinergic effects of OP intoxication in humans include hypotension, hypersecretion, bradycardia, bronchoconstriction, gastrointestinal hypermotility, and death (Casida 1964; King and Aaron 2015). In mammals, symptoms of cholinergic overstimulation also include salivation, lacrimation, gastrointestinal hypermotility,

muscular tremors or convulsions, culminating in death by respiratory failure (Moser and Padilla 2011).

OPs such as dichlorvos (DDVP) and chlorpyrifos oxon (CPO)—the toxic metabolite of the OP chlorpyrifos (CPF)—inhibit AChE (Casida 1964). OPs also act on other enzymes within the serine hydrolase superfamily such as carboxylesterases (CES) (Casida and Quistad 2004). Inhibition of CES itself does not cause toxicity; however, the reactions of OPs with CES are important as potential detoxification processes and can influence the overall disposition of OPs (Chanda et al. 1997; Maxwell 1992; Ross et al. 2010). CES detoxifies OPs by hydrolysis to form carboxylic acid and alcohol metabolites (Ross et al. 2010). An OP can act as both a substrate and an inhibitor for serine hydrolases (Casida and Quistad 2004). For example, CES metabolizes the OP malathion to the toxic metabolite maloxon, which in turn inhibits detoxification via CES (Hodgson and Rose 2006). Based on the structural similarities of the OPFRs, it is hypothesized that the OPFRs interact with AChE and CES in a manner similar to the OPs. However, limited or conflicting data assessing these interactions and thus necessitate further analysis (EPA 2015).

#### *1.4.3.2 Drug Transporters*

Multi-drug resistance 1 (MDR1) is a member of the ATP-binding cassette (ABC) family of efflux transporters localized on apical membranes of numerous tissues including the luminal membrane of enterocytes and endothelial cells of brain microcapillaries, the brush border membrane of renal proximal tubules, and the

canalicular membrane of hepatocytes. ABC transporters use primary active transport to function as efflux pumps that remove xenobiotics to limit intestinal absorption, blood-brain barrier (BBB) penetration, facilitate biliary and renal excretion, and protect against xenobiotic exposure (Klaassen and Aleksunes 2010; Mao and Unadkat 2015; Stieger and Gao 2015).

There is some evidence suggesting that OPs interact with MDR1 (Lanning et al., 1994; Leslie et al., 2005). CPO was shown to bind to mammalian MDR1 in competition experiments with [<sup>3</sup>H]azidopine and to stimulate cellular ATPase activity (Lanning et al. 1996). In another study, 250 µM CPF inhibited 51-80% of MDR1-mediated efflux of doxorubicin in B16/Hmdr1 cells—B16/F10 murine melanoma cells transfected with the human MDR1 gene—which may occur due to direct protein binding (Bain and LeBlanc 1996). Additionally, CPF (100 µM) was not shown to be appreciably transported by MDR1 compared to doxorubicin—containing an efflux ratio of 1.06 and 7.05, respectively, by HPLC. In human Caco2 intestinal cells, 8-hour treatment with CPF induced MDR1 activity indicated by a higher rate of verapamil efflux from the CPF-treated cells as compared to the control group (Agarwala et al. 2004). In addition, MDR1 gene expression in Caco2 cells was increased upon CPF exposure. CPF exhibited a maximal increase in MDR1 expression at 8 hours, which decreased at 24 hours. CPO exposure, however, only increased MDR1 expression at 4 hours. These results suggest that CPF may alter the bioavailability of drugs by changing the expression and function of MDR1.

Thus far, only one study has investigated OPFR interaction with ABC transporters. Following exposure of adult Asian clams (*C. fluminea*) to TBOEP and TBP for 28 days *abcc1* (the gene encoding multidrug resistance-associated protein 1 [MRP1]) and *abcb1* (gene encoding MDR1) levels were altered (Yan et al. 2017). TBP significantly increased *abcc1* expression at 20 ug/L but inhibited expression at 2000 µg/L. Additionally, *abcb1* levels were significantly increased at 20 µg/L and then significantly decreased at 200 µg/L and 2000 µg/L. Alternatively, TBOEP was shown to significantly enhance *abcb1* and *abcc1* at all concentrations tested. These results suggest that TBP (20 µg/L) and TBOEP (20, 200, and 2000 µg/L) may activate MRP1 and MDR1 thereby mediating xenobiotic efflux in clams. In order to get a better understanding of the potential interactions of OPFRs and ABC transporters, further studies must be conducted, especially in mammalian models.

## **1.5 OPFR Toxicities**

### **1.5.1 Humans**

Although data regarding human exposure to OPFRs is accumulating, studies investigating the potential toxicity of OPFRs to humans is limited. To date, OPFRs have been associated with altered endocrine function, reproductive health measures, and cognitive function (Carignan et al. 2017; Carignan et al. 2018; Castorina et al. 2017a; Meeker et al. 2013a; Meeker and Stapleton 2010; Preston et al. 2017). Additionally, *in vitro* studies using human-derived cell lines and proteins suggest that OPFRs may act as metabolic disruptors, cytotoxicants,

enzyme inhibitors, and nuclear receptor activity modifiers (Belcher et al. 2014; Saboori et al. 1991).

#### 1.5.1.1 *Endocrine and Reproduction*

Recently, urine OPFR metabolite levels and their effects on pregnancy outcomes was studied in couples recruited from a U.S. fertility clinic (Carignan et al. 2017; Carignan et al. 2018). BDCPP (87%), DPP (94%), and ip-PPP (80%) were detected with high frequency in maternal urine (N=201) and the sum of the metabolite concentrations were associated with decreased success for several *in vitro* fertilization outcomes including successful fertilization, implantation, clinical pregnancy, and live birth (Carignan et al. 2017). As in maternal urine, BDCPP (84%), DPP (87%), and ip-PPP (76%) were detected at high frequencies in paternal urine (n=201) (Carignan et al. 2018). Paternal urinary BDCPP concentrations were associated with a significant 12% reduction in fertilization as well. However, no associations with successful implantation, clinical pregnancy, or live birth were observed suggesting that female preconception exposure to a sum of OPFRs may be more relevant for these outcomes (Carignan et al. 2017; Carignan et al. 2018).

The potential for OPFRs to alter normal patterns of DNA methylation in sperm has also been investigated. Men with higher concentrations of urinary OPFR metabolites had a significantly higher fraction of aberrantly methylated sperm cells at the differentially methylated regions (DMRs) of multiple growth regulating genes in the early embryo and fetus including *MEG3*, *NDN*, *SNRPN*, *GRB10*, and *H19*

(Soubry et al. 2017). ip-PDPP exposure was significantly correlated to hypermethylation at the *MEG3*, *NDN*, and *SNRPN* DMRs. Increased TPP exposure was associated with hypermethylation at the *GRB10* DMR. Lastly, TDCPP exposure was associated with hypomethylation at the *MEG3-IG* and *H19* DMRs. These findings suggest that fertilization by one of these aberrantly methylated sperm cells could pass on these epigenetic modifications thereby affecting offspring's health (Soubry et al. 2017).

A few epidemiological studies have investigated the potential health risks of OPFR exposure on male reproduction. In a small study (N=50), TDCPP and TPP were measured in house dust and relationships with hormone levels and semen quality parameters were assessed (Meeker and Stapleton 2010). TDCPP and TPP were detected in nearly 100% of house dust samples and their concentrations were found to be on the same order of magnitude as PBDEs (Meeker and Stapleton 2010; Stapleton et al. 2009). The authors observed that an interquartile range (IQR) increase TPP was associated with increased prolactin (10%) and decreased sperm concentration (19%), while an IQR increase in TDCPP was associated with greater prolactin (17%) and reduced free T4 (3%) and free androgen index (6%) (Meeker and Stapleton 2010). In a subset of this cohort, urine concentrations (N=33) were measured for associations between metabolites of TDCPP (BDCPP) and TPP (DPP) and male reproductive health and thyroid hormones (Meeker et al. 2013a). Urinary BDCPP was associated with decreased semen quality (37%) and sperm motility (15%) and increased TSH (40%) and total T3 concentrations (7%) in serum. Similar to its parent compound TPP, DPP was associated with

decreased sperm concentration (57%) as well as decreased sperm motility (20%) and increased total T3 levels (8%). In a separate study, women (N=26) were found to have mean DPP concentrations that were 43% greater than men (N=26) (Preston et al. 2017). These levels were associated with an increase in total T4 levels, particularly in women (0.91 µg/dL). Taken together, these findings suggest that OPFRs can alter endocrine function, thyroid levels, and reproductive health in men and thyroid levels in women. However, studies using larger sample sizes are necessary to determine whether these findings can be generalized to populations at-large.

Studies in animal-derived cell lines transfected with human nuclear receptors suggest that OPFRs possess agonistic and/or antagonistic activities toward these receptors. Nuclear receptors are a family of ligand-activated transcriptional regulators that function as xenobiotic sensors—such as pregnane X receptor (PXR), constitutively active receptor (CAR), aryl hydrocarbon receptor (AhR) and peroxisome proliferator-activated receptor (PPAR $\alpha$ )—as well as steroid sensors (estrogen receptor  $\alpha/\beta$  [ER $\alpha/\beta$ ], androgen receptor [AR], glucocorticoid receptor [GR]), thyroid sensors (thyroid hormone receptor  $\alpha_1/\beta_1$  [TR $\alpha_1/\beta_1$ ]), and endobiotic sensors (retinoic acid receptor  $\alpha$  [RAR $\alpha$ ], retinoid X receptor  $\alpha$  [RXR $\alpha$ ]). In CHO (hamster; epithelial) and COS-7 (monkey; fibroblast-like) cells expressing human nuclear receptors, TPP and TCP exhibited agonistic activity towards PXR and ER $\alpha$ —and ER $\beta$  in the case of TPP—while showing AR and GR antagonistic activity (Kojima et al. 2013). TPP and TCP were also shown to be ER ligands in human-derived breast cancer MVLN cells (Liu et al. 2012). TBP and TDCPP



appeared to be AR and GR antagonists and PXR agonists (Kojima et al. 2013). TEHP presented GR antagonistic and PXR agonistic activities. TCPP and TBOEP acted as agonists of PXR. None of the OPFRs displayed agonistic and/or antagonistic activity against  $TR\alpha_1/\beta_1$ ,  $RAR\alpha$ ,  $RXR\alpha$ , or peroxisome  $PPAR\alpha/\gamma$  suggesting that OPFRs alter endocrine pathways via  $ER\alpha/\beta$ , AR, GR, or PXR.

#### 1.5.1.2 *Neurological*

Since young children are thought to be exposed to higher concentrations of OPFRs than adults it is imperative that toxicologists determine the potential effects of OPFR exposure on perinatal and postnatal development. However, studies regarding outcomes in children exposed to OPFRs are limited. A study investigating neurodevelopmental outcomes in children exposed to OPFRs *in utero* showed that higher maternal urine DPP and total OPFR concentrations were associated with decreased IQ (-2.9 points for DPP; -3.8 points for total OPFR) and working memory (-3.9 points for DPP; -4.6 points for total OPFR) in children (n=310) for each 10-fold increase in prenatal urinary metabolite concentration (Castorina et al. 2017a). In another study, a modest association between OPFR exposure and social behaviors in pre-school children (3-5 years old, n=72) was observed after adjusting for gender, age, family context, and child's exposure to adverse experiences (Lipscomb et al. 2017). Children with higher exposure levels to OPFRs were rated by their teachers as behaving more irresponsibly ( $\beta=-0.25$ ) and exhibiting more externalizing behavior problems (i.e. bullying, aggression, defiance, inattention, and hyperactivity;  $\beta=0.31$ ) suggesting that higher OPFR exposure may negatively impact a child's ability to succeed academically and

socially. While these initial data point to a potential impact of OPFRs on neurodevelopment, clearly additional investigation is warranted.

### 1.5.2 Rodents

Studies conducted in rodents have suggested that OPFR exposure can cause adverse effects including reproductive toxicity and endocrine disruption. In mice, OPFRs have been shown to affect testis organization, cause liver injury, and alter homeostasis and gene expression (Chen et al. 2015a; Krumm et al. 2017; Xu et al. 2016).

#### 1.5.2.1 *Hepatic*

Male mice administered diets containing TPP (100 or 300 mg/kg/day) and TCEP (100 or 300 mg/kg/day) for 35 days experienced an induction in markers of oxidative stress and endocrine disruption (Chen et al. 2015a). TPP treatment resulted in a dose-dependent elevation of hepatic malondialdehyde (MDA), a biomarker of oxidative stress, while TCEP had no effect on MDA content. Liver concentrations of glutathione (GSH), an antioxidant, were reduced in mice exposed to 300 mg/kg TPP and both concentrations of TCEP, which could explain the observed decline in glutathione *S*-transferase activity and its transcription levels. Additionally, TPP and TCEP, especially at the 300 mg/kg dose, stimulated antioxidant enzymes superoxide dismutase (SOD), catalase, and glutathione peroxidase (GPX) activities and upregulated transcription of their respective genes. TPP and TCEP significantly decreased transcription of several genes involved in steroidogenesis regulation and testosterone production in testes (*LDL*-

*R*, *StAR*, *P450scc*, and *P450-17 $\alpha$* ), with TCEP causing a more profound effect compared to TPP at the same dose (100 mg/kg). In a separate study, male mice exposed to ToCP (100, 200, or 400 mg/kg), the ortho isomer of TCP, for 28 days resulted in hepatocellular injury and a notable increase in serum alanine aminotransferase and aspartate aminotransferase levels (Xu et al. 2016). In the liver, a significant increase in MDA and a significant decrease in GSH levels were observed along with a reduction in SOD and GTX. This reduction in antioxidant enzyme activity by ToCP was in contrast to the enhancement of these enzymes caused by TPP and TCEP in the study by Chen et al. (2015a). However, these differences could be due to the age (4 weeks vs 8 weeks) and strains of the mice (ICR vs Kunming) as well as the OPFR tested (albeit ToCP and TPP are both aryl OPFRs), and/or the study duration (35 vs 28 days) (Chen et al. 2015a; Xu et al. 2016). TBP has also been shown to adversely affect the liver. Male mice treated orally with 30 mg/kg TBP for 14 days had impaired urea synthesis and enlarged livers. Additionally, TBP activated nuclear hormone receptor constitutive androstane receptor (CAR) and induced *CYP2b10* expression, which is consistent with TBP activating CAR (Zhou et al. 2017). TDCPP, TPP, and TCP were also shown to activate CAR and PXR in mice treated daily with a mixture of the three OPFRs (1 mg/kg each, 3 mg/kg total) for 28 days (Krumm et al. 2017). Additionally, this OPFR mixture reduced body weight and energy intake in males, while increasing fasting glucose levels. Interestingly, ovariectomized females subjected to the same OPFR mixture treatment were less sensitive to the same physiological disturbances as the male mice suggesting that estrogenic signaling may partially

mediate these effects. That TPP and TCP have been shown to act as ER $\alpha$  agonists and TDCPP as an AR antagonist in reporter gene assays further supports this notion (Kojima et al. 2013).

TPP and DPP have been shown to alter metabolic profiles in adult mice following daily subcutaneous injections on postnatal days (PND) 1-10 (Wang et al. 2018). Males exposed to the low dose of TPP (2  $\mu$ g/day) had increased lipid metabolism indicated by the upregulation of lipid-related metabolites while no significant effects on females in the same treatment group were observed. The high dose (200  $\mu$ g/day) downregulated the pyruvate metabolism and TCA cycles in both sexes with females also experiencing a decrease in lipid metabolism. For both sexes and concentrations, perturbations in lipid metabolism were more pronounced in mice given DPP. Additionally, neonatal exposure to TPP and DPP did not alter estradiol levels in adult females (12 weeks) suggesting that they are either not estrogenic or their effects on estradiol, if any, do not persist into adulthood.

Several studies have investigated Firemaster 550 (FM 550)—a commercial mixture of OPFRs (TPP and a mixture of isopropylated TPP isomers) and brominated flame retardants (2-ethylhexyl-2,3,4,5-tetrabromobenzoate [TBB] and bis(2-ethylhexyl)-2,3,4,5-tetrabromophthalate [TBPH]). OPFRs and brominated flame retardants account for 62 and 38% of FM 550, respectively (McGee et al. 2013). At environmentally relevant exposure concentrations (100 and 1000  $\mu$ g/day), FM 550 was shown to increase serum thyroxine levels and reduce hepatic CES activity in dams, while accelerated female pubertal onset, male cardiac hypertrophy, weight gain, and altered exploratory behaviors in offspring (Patisaul

et al. 2013). TPP has been shown to inhibit CES activity in HEK293T lysates overexpressing these enzymes and may be responsible for the observed decrease in CES activity (Morris et al. 2014; Patisaul et al. 2013). Furthermore, since CES metabolizes the brominated components of FM 550, this could lead to an extension of their half-lives (Patisaul et al. 2013). Accumulation of FM 550 in dams and pups was observed with the brominated flame retardants, however, the authors did not quantify circulating or tissue concentrations of OPFRs citing rapid metabolism as a factor for their exclusion. Therefore, it should be noted that these outcomes cannot be attributed solely to OPFR exposure and may be a result of the brominated flame retardants or potentially a combination of the two classes of chemicals.

#### *1.5.2.2 Reproduction and Neurodevelopment*

In another study investigating the gestational and lactational transfer of FM 550 in rats, dams were orally exposed to 300 or 1000 µg of FM 550 during gestation (gestational day [GD] 9–18) or lactation (PND 3–12) (Phillips et al. 2016). TPP was not shown to undergo gestational or lactational transfer in rats as indicated by their nondetection in the whole fetus (GD 18) or pup tissue (PND 12). However, as previously mentioned, TPP, as well as other OPFRs, have been detected in human breast milk samples at concentrations below the method detection limits in Phillips et al. (2016), which may account for the lack of detection (Kim et al. 2014; Phillips et al. 2016; Sundkvist et al. 2010). Interestingly, a follow-up study using the same animals indicated that TPP, as well as the brominated flame retardants, accumulated in the placentas of dams exposed to FM 550 (300 or 1000 µg/day;

GD 9 – 18) (Baldwin et al. 2017). TPP exhibited a dose-dependent increase in male-associated placentas and was significantly higher in male placentas ( $6.5 \pm 2.02$  ng/g ww) than in the female placentas ( $1.07 \pm 0.55$  ng/g ww) in the 1000 µg/day dosing group at GD 18. Since the placenta produces hormones and neurotransmitters that are critical for fetal neurodevelopment, it is possible that perinatal exposure to FM 550 may disrupt these signals. This disruption may, in turn, alter exploratory behaviors in offspring resulting in heightened anxiety-related behaviors in males and hyperactivity in females (Baldwin et al. 2017; Patisaul et al. 2013). A recent study expanded upon this by finding that perinatal FM 550 exposure can impact multiple placental pathways including endocrine (via farnesoid X receptor), inflammation (via liver X receptor), and neurotransmitter signaling (e.g. serotonin) (Rock et al. 2018). Notably, FM 550 caused a reduction of serotonin turnover in placental tissue and fetal forebrains suggesting that serotonin signaling may be disrupted. Going forward, determining the effect of TPP apart from the brominated components of FM 550 will be beneficial to characterizing risks associated with OPFR exposure.

#### 1.5.2.3 *Neurological*

Subchronic studies with TCEP have also been performed in rats. Adult female rats administered 50-250 mg/kg/d TCEP by oral gavage for 60 days exhibited signs of neurotoxicity (Yang et al. 2018). A dose-dependent decline in spatial learning and memory functions were observed as well as apoptotic and necrotic lesions in the *Cornu Ammonis* 1 (CA1) pyramidal cells of the hippocampus in rats administered 100 and 250 mg/kg/d TCEP. These histological findings were similar those of a

16-week study in which adult female rats receiving 175 and 350 mg/kg/d TCEP presented hippocampal lesions in the CA1 region (Matthews et al. 1990). Additional pathological changes in the cortex were observed for rats receiving 250 mg/kg/d TCEP including an enhanced inflammatory response and calcified or ossified foci (Yang et al. 2018). TCEP was also shown to disrupt several physiological processes including amino acid, neurotransmitter, and energy metabolism as well as cell membrane integrity in the brain, which may account for the brain pathology and learning and memory dysfunction.

### 1.5.3 Fish

The use of zebrafish has been critical in advancing our understanding of OPFR toxicity. In fact, over the past decade studies in zebrafish have indicated that OPFRs can induce a myriad of toxic effects including endocrine disruption, reproductive toxicity, neurodevelopmental and behavioral toxicity, as well as cardiotoxicity.

#### 1.5.3.1 *Endocrine Disruption and Reproductive Toxicity*

Exposure to OPFRs has resulted in altered endocrine function. Tris(2-butoxyethyl) phosphate (TBOEP)—an OPFR frequently detected in aquatic organisms—has been shown to upregulate the expression of estrogen receptor (ER) and estrogen receptor-associated genes in zebrafish embryos and larvae at 0.5  $\mu$ M (200  $\mu$ g/L) from 3.5 to 120 hpf, suggesting that TBOEP alters the ER pathway (Ma et al. 2015). By contrast, TBOEP downregulates genes associated with the mineralocorticoid receptor pathway. In a 21-day exposure study, TBOEP was shown to increase

plasma estradiol in male (50 and 500 µg/L) and female zebrafish (500 µg/L), while elevating testosterone concentrations in males (50 and 500 µg/L) (Xu et al. 2017). In contrast, female zebrafish exposed to TDCPP (20 and 100 µg/L) significantly increased plasma estradiol and testosterone levels, whereas no change was observed in male zebrafish (Wang et al. 2015c). These findings corroborate those from a previous study that showed that TDCPP, as well as TPP and TCP, significantly increased plasma estrogen and testosterone levels in female zebrafish after a 14-day exposure while increasing estrogen and decreasing testosterone in males (Liu et al. 2012). In another study, TPP significantly increased plasma estradiol in female zebrafish exposed for 120 days, while reducing testosterone concentrations in both sexes (Liu et al. 2016b). Furthermore, TPP exposure resulted in sex-dependent changes in gene expression along the hypothalamic-pituitary-interrenal and the hypothalamic-pituitary-thyroid axes. An elevation in plasma cortisol, T3, and T4 concentrations as well as expression of mineralocorticoid receptor transcripts and the thyrotropin-releasing hormone receptor 2 gene were observed in females. In a 90 day study, TDCPP had the opposite effect on T3 and T4 levels in adult females and their progeny (Wang et al. 2015a). In salmon exposed to concentrations of 0.04, 0.2, or 1 mg/L for 7 days, TCEP had stronger effects on steroidogenesis than TBOEP (Arukwe et al. 2016). TCEP significantly altered the expression of several genes involved in neuro- and renal steroidogenesis, while TBOEP had little to no effect. Although plasma estradiol concentrations were not measured, TCEP did alter gene expression associated with estrogen biosynthesis in salmon.



OPFR exposure has been shown to disrupt zebrafish reproduction. In a study of long-term (180 days) exposure of zebrafish to low concentrations of TDCPP, hepatic vitellogenin—an egg-yolk precursor protein—was upregulated in both males and females at 20 and 100 µg/L, indicating that TDCPP may be estrogenic (Wang et al. 2015c). This is consistent with a short-term exposure study, where male and zebrafish had increased serum plasma vitellogenin levels after exposure to TDCPP and TPP for 21 days (Liu et al. 2013; Wang et al. 2015c). TBOEP was also shown to upregulate hepatic vitellogenin but only in females (Xu et al. 2017). Additionally, TBOEP and TDCPP have been shown to reduce egg production in females and delay spermiation in males (Xu et al. 2017). In fact, high levels of TDCPP and its metabolite BDCPP were detected in the gonads of male and female zebrafish exposed to 100 µg/L TDCPP from 2 hpf to 6 months (sexual maturity). (Wang et al. 2015c). Furthermore, TBOEP, TDCPP, and TPP were shown to affect transcription levels of genes along the hypothalamic-pituitary-gonadal (HPG) axis in both male and female zebrafish, which could also alter their reproductive capabilities (Liu et al. 2013; Wang et al. 2015c; Xu et al. 2017).

Recent studies have shown that OPFRs can impact the survival and development of offspring whose mothers were exposed. TDCPP limited the growth of female but not male zebrafish (1-month-old) after chronic exposure (240 days) to environmentally relevant concentrations of TDCPP (580 and 7500 ng) (Yu et al. 2017). Additionally, female zebrafish given the 7500 ng dose were shown to transfer TDCPP to their offspring via their eggs and that these offspring were marked by a significant decreased in survival at 3 dpf (13.0%) and 5 dpf (15.0%)

as well as decreased body length, and heart rate (Yu et al. 2017). The adverse effects observed in the females and their progeny may be due to the downregulation of genes involved in the hormone/insulin-like growth factor axis. Additionally, these findings corroborated those of a shorter duration of exposure study also using environmentally relevant concentrations of TDCPP in zebrafish (Yu et al. 2017; Zhu et al. 2015).

#### 1.5.3.2 *Developmental and Behavioral Toxicity*

Numerous studies in aquatic organisms have shown that the nervous system is a potential target for OPFRs. Investigating the accumulation of OPFRs in organisms may help toxicologists identify target organ toxicities. Adult female zebrafish developmentally exposed (2 hpf) to low concentrations of TDCPP (4, 20, and 100 µg/L) were found to accumulate higher levels of TDCPP—and its metabolite BDCPP, albeit to a lesser extent than TDCPP and only in the 100 µg/L exposure group—than males, with notably higher concentrations in brain tissues (Wang et al. 2015b). Moreover, dopamine (28.3-45.5%) and serotonin (32.9-34.2%) levels were decreased in a non-dose dependent manner in adult females developmentally exposed to TDCPP suggesting a possible sex-specific mechanism for TDCPP-induced neurotoxicity. In another study, developmental exposure (5 hpf to 5 dpf) to TDCPP (3 and 6 µM) was shown to limit locomotor activity in zebrafish (Oliveri et al. 2018). Additionally, TDCPP (6 µM) treatment significantly blunted the effect of dopamine antagonist induced hypoactivity in zebrafish larva challenged with dopamine D<sub>1</sub> (SCH-23390) and D<sub>2</sub> (haloperidol) receptor antagonists suggesting that TDCPP exposure may modulate dopamine

signaling. In fact, dopamine concentrations, as well as serotonin,  $\gamma$ -aminobutyric acid, and histamine concentrations were significantly decreased in larvae of zebrafish adults exposed to TDCPP for 90 days (Wang et al. 2015a). Decreased locomotor activity, as well as decreased mRNA and protein expression of factors involved in neuronal development, were also observed in these larvae. Hypoactivity was also observed in zebrafish exposed to TBP (25-3125  $\mu\text{g/L}$ ), TBOEP (50-6250  $\mu\text{g/L}$ ), and TCEP (50-6250  $\mu\text{g/L}$ ) from less than 2 hpf to 5 dpf (Sun et al. 2016). Since TDCPP can bioaccumulate in the developing brain and can modulate neurotransmitter and gene expression levels in the central nervous system, further studies investigating TDCPP's impact on cell signaling pathways in the nervous system is warranted.

Zebrafish embryos exposed to various OPFRs (including TPP, TBP, TCPP, TCEP, TCP, TBOEP, TEHP, and TDCPP) from 6 hpf to 5 dpf to a range of concentrations spanning four orders of magnitude (e.g. 6.4 nM to 64  $\mu\text{M}$ ) engendered mortality, delayed progression, and/or developmental malformations (Noyes et al. 2015). ip-PDPP treated embryos exhibited the most numerous and variable effects including yolk sac edema, axis, snout, jaw, pericardial edema, pectoral fin, swim bladder, and trunk abnormalities. TCP-treated embryos also had several malformations at concentrations 10 times higher than were elicited by ip-PDPP. Alternatively, embryos exposed to TCP were more susceptible to delayed progression and mortality than ip-PDPP exposed embryos. TEHP, ToCP, and TCEP did not cause any developmental defects, however, mortality was observed in 120 hpf embryos. TPP induced yolk sac edema at the same concentration as TCP. Additionally,

TPP-treated embryos were more susceptible to mortality at lower concentrations than those that generated deformities. TBP induced mortality in the picomolar range and pericardial edema in the nanomolar range. By comparison, TDCPP caused mortality and delayed progression of 24 hpf embryos and mortality and caudal fin malformations in the micromolar range. However, its metabolite, BDCPP was notably lethal at concentrations four orders of magnitude lower than TDCPP.

Due to the structural similarities of OPFRs to organophosphate pesticides, known acetylcholinesterase (AChE) inhibitors, researchers have investigated whether OPFRs would also induce neurotoxicity in this manner. In one study, TPP, but not TCEP or TDCPP, significantly inhibited AChE activity at high concentrations (2 mg/L) in adult Chinese rare minnows (Yuan et al. 2016). Additionally, TDCPP, but not TCEP and TPP, downregulated the expression of neurotrophic factor genes in exposed adult Chinese rare minnows. TBP, TBOEP, and TCEP were not shown to significantly affect AChE activity in zebrafish larvae (Sun et al. 2016; Wang et al. 2015a). However, TBP and TBOEP exhibited a significant downregulation of *ache* mRNA at higher concentrations (625 and 3,125 µg/L for TBP and 6.250 µg/L for TBOEP) while TCEP did not alter *ache* mRNA (Sun et al. 2016). Although OPFRs did not exhibit anticholinesterase activity, transcriptional changes in nervous system genes were observed, suggesting that OPFRs can disrupt neurodevelopment.

#### 1.5.3.3 *Cardiotoxicity*

OPFRs can induce cardiac abnormalities during zebrafish development. TPP (4  $\mu$ M) and ip-PDPP (0.5  $\mu$ M) completely blocked cardiac looping thereby inducing cardiac malformations during embryogenesis in zebrafish exposed between 5.25 and 24 hpf (McGee et al. 2013). The observed malformations were similar to those caused by TCDD, a potent AhR agonist thus the potential for AhR-mediated TPP and ip-PDPP cardiotoxicity was investigated. Despite their structural similarities, TPP and ip-PDPP induced cardiotoxicity by AhR-independent and AhR-dependent mechanisms, respectively. In another study, aryl OPFRs TPP and cresyl diphenyl phosphate were shown to be more potent developmental cardiotoxicants than alkyl OPFRs TBP, TCEP, and TDCPP in zebrafish (Du et al. 2015). Additionally, aryl OPFRs appear to induce cardiotoxicity by inhibiting the expression of key transcriptional regulators in cardiogenesis including BMP4, NKX2-5, and TBX5. Taken together, these data suggest that the heart is particularly vulnerable to aryl OPFR induced malformations during embryogenesis.

#### 1.5.3.4 *Disruption of CYP Activity*

As aforementioned, CYPs are a large family of isozymes that metabolize a diverse array of xenobiotics. TBOEP and TCEP have been shown to modulate CYP1A and CYP3A transcription and enzyme activity in salmon exposed for 7 days (Arukwe et al. 2018). In TCEP-exposed fish, *cyp1a* mRNA increased at low concentrations (0.04 mg/L) but decreased significantly at higher concentrations (0.2 and 1 mg/L). However, TBOEP treated fish exhibited a significant enhancement in *cyp1a* mRNA

for all exposure groups. For *cyp3a* mRNA, a dose-dependent reduction was observed for TCEP. Contrastingly, TBOEP significantly downregulated *cyp3a* mRNA at 0.04 and 0.2 mg/L, followed by a significant upregulation at 1 mg/L. Interestingly, TBOEP and TCEP stimulated CYP1A and CYP3A activity at low concentrations, but diminished activity at higher concentrations. By regulating CYP mRNA expression and/or CYP activity, OPFRs may potentially affect their own metabolism potentially which in turn could prolong their duration in the body and heighten the risk of adverse effects.

#### 1.5.3.5 *Distribution and Bioaccumulation*

Assessing the environmental exposure of fish to OPFRs can help identify organs that may be affected by these compounds. In a recent study, samples from river water, sediment, and crucian carp from the Nakdong River in South Korea suggested a different distribution pattern in abiotic versus biotic media for all OPFRs tested excluding TCEP, which was dominant in both media (Choo et al. 2018). TCP and TBOEP were prominently distributed in abiotic media whereas TBP, TBOEP, and triethyl phosphate (TEP) were dominant in crucian carp. Higher total OPFR concentrations were observed in the liver (6.22–18.1 ng/g ww) and the levels in muscle (4.23–7.75 ng/g ww) and gonad (3.08–7.70 ng/g ww) were similar. Additionally, TBOEP was prevalent in blood, muscle, and gonads, whereas TBP, TCEP, and TEP were equally dominant in the liver, muscle, and gonads. Interestingly, sex differences in TBP transfer from muscle to egg (female) or gonad (male) were observed such that transfer efficiencies were significantly higher in females (0.911) than in males (0.544). The results of this study emphasize the

impact of OPFR exposure and the need to further investigate the potential for maternal transfer of OPFRs.

## 1.6 Research Objective and Hypothesis

Although research on the adverse effects of OPFR exposure has increased over the past decade, there are still several gaps in our understanding of their behavior *in vivo* and their potential toxicity, especially in mammals. The central hypothesis of this dissertation is that OPFRs interact with molecular targets (AChE), metabolic enzymes (CES), and transporters (MDR1) that influence their overall disposition and potential for neurotoxicity. Three specific aims have been developed to test this hypothesis:

1. Assess the ability of OPFRs to inhibit AChE and CES activity *in vitro*.
2. Determine the distribution of OPFRs following subchronic oral exposure in adult mice and whether OPFRs undergo maternal transfer *in utero*.
3. Determine whether OPFRs act as substrates and/or inhibitors of MDR1 *in vitro* and whether MDR1 influences OPFR disposition *in vivo*.

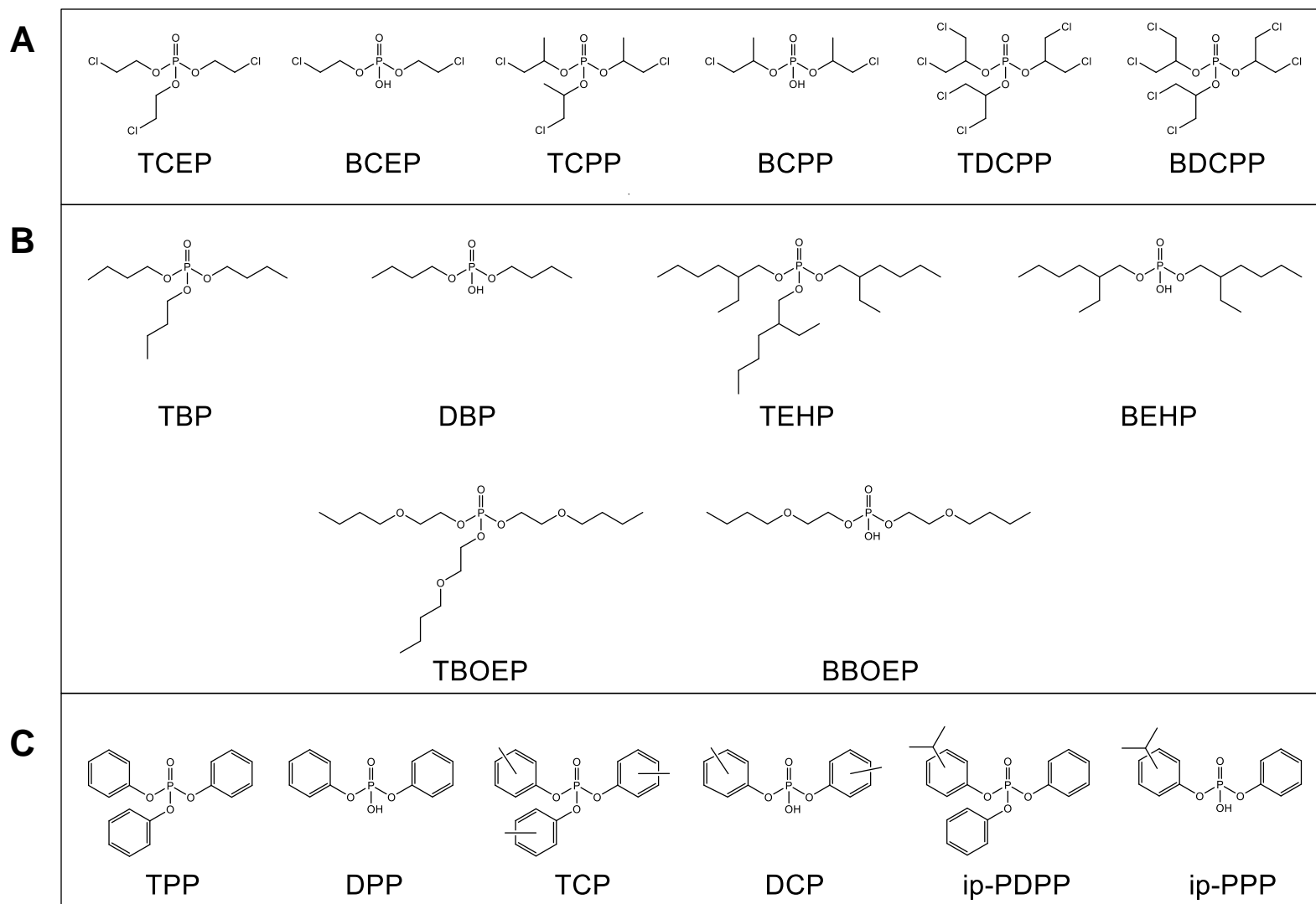
Findings from this research will elucidate the role of chemical structure and sex on OPFR distribution and accumulation and whether transporters influence OPFR disposition. Identifying OPFR storage depots will help guide future research into OPFR-induced organ-specific adverse effects. Moreover, the assessment of *in utero* exposure will help to inform future studies on potential adverse health effects on the developing fetus.

**Table 1.1.** Names and acronyms of OPFRs and metabolites reviewed

| Parent Compound                         | Acronym        | Metabolite                           | Acronym        |
|---|----------------|--------------------------------------|----------------|
| Tris(2-chloroethyl) phosphate           | TCEP           | Bis(2-chloroethyl) phosphate         | BCEP           |
| Tris(2-chloroisopropyl) phosphate       | TCPP (TCIPP)   | Bis(1-chloroisopropyl) phosphate     | BCPP (BCIPP)   |
| Tris(1,3-dichloroisopropyl) phosphate   | TDCPP (TDCIPP) | Bis(1,3-dichloroisopropyl) phosphate | BDCPP (BDCIPP) |
| Tributyl phosphate                      | TBP (TnBP)     | Dibutyl phosphate                    | DBP            |
| Tris(2-ethylhexyl) phosphate            | TEHP           | Bis(2-ethylhexyl) phosphate          | BEHP           |
| Tris(2-butoxyethyl) phosphate           | TBOEP (TBEP)   | Bis(2-butoxyethyl) phosphate         | BBOEP (BBEP)   |
| Mono-isopropylphenyl diphenyl phosphate | ip-PDPP (mITP) | Isopropylphenyl phenyl phosphate     | ip-PPP         |
| Triphenyl phosphate                     | TPP (TPhP)     | Diphenyl phosphate                   | DPP (DPhP)     |
| Tricresyl phosphate                     | TCP            | Dicresyl phosphate                   | DCP            |
| Tris(2-butoxyethyl) phosphate           | TBOEP (TBEP)   | Bis(2-butoxyethyl) phosphate         | BBOEP (BBEP)   |

Alternative abbreviations used in the literature are denoted by parenthesis.





**Figure 1.1.** Structures of OPFRs and metabolites reviewed **(A)** chlorinated, **(B)** alkyl, and **(C)** aryl-OPFRs

**Table 1.2.** OPFR metabolite concentrations in human urine (ng/mL)**Children**

| Country                | Population | BCEP    | DCP               | DPP  | BCPP  | BDCPP | DBP   | BBOEP | BEHP   | ip-PPP | Reference            |
|------------------------|------------|---------|-------------------|------|-------|-------|-------|-------|--------|--------|----------------------|
| Australia <sup>a</sup> | 0-6 yrs.   | < 0.014 | -                 | 25   | 0.85  | 2.6   | 0.18  | 0.32  | < 0.16 | -      | He et al. (2018)     |
| USA <sup>b</sup>       | 15-18 mo.  | -       | -                 | 3.37 | -     | 6.81  | -     | -     | -      | 0.43   | Thomas et al. (2017) |
|                        | 15-18 mo.  | -       | -                 | 8.15 | -     | 2.70  | -     | -     | -      | -      |                      |
| China <sup>c</sup>     | 6-14 yrs.  | 3.25    | 0.02 <sup>e</sup> | 0.40 | 0.21  | 0.12  | 0.16  | 0.06  | -      | -      | Chen et al. (2018)   |
| USA <sup>d</sup>       | 6-11 yrs.  | 0.662   | NC                | 1.69 | 0.267 | 2.25  | 0.272 | -     | -      | -      | Ospina et al. (2018) |
|                        | 12-19 yrs. | 0.602   | NC                | 1.41 | 0.190 | 1.34  | 0.207 | -     | -      | -      |                      |

**Adults**

| Country          | Population | BCEP  | DCP | DPP   | BCPP  | BDCPP | DBP   | BBOEP | BEHP | ip-PPP | Reference            |
|------------------|------------|-------|-----|-------|-------|-------|-------|-------|------|--------|----------------------|
| USA <sup>d</sup> | 20-59 yrs. | 0.394 | NC  | 0.760 | 0.188 | 0.818 | 0.169 | -     | -    | -      | Ospina et al. (2018) |
|                  | 60+ yrs.   | 0.336 | NC  | 0.640 | NC    | 0.497 | 0.205 | -     | -    | -      |                      |

**Pregnant Women**

| Country          | Population                             | BCEP | DCP | DPP  | BCPP | BDCPP | DBP | BBOEP | BEHP | ip-PPP | Reference                |
|------------------|--|------|-----|------|------|-------|-----|-------|------|--------|--------------------------|
| USA <sup>b</sup> | 18+ yrs.;<br><20 wks. gest.            | -    | -   | 0.93 | -    | 0.28  | -   | -     | -    | 0.33   | Castorina et al. (2017b) |
| USA <sup>b</sup> | ≤ 25 to ≥ 36 yrs.;<br>24-30 wks. gest. | -    | -   | 1.4  | NC   | 1.8   | -   | -     | -    | 6.8    | Hoffman et al. (2017b)   |
| USA <sup>b</sup> | 18+ yrs.;<br>≤20 wks. gest.            | 0.32 | -   | 1.40 | -    | 1.24  | -   | -     | -    | -      | Romano et al. (2017)     |

NC: Not calculated; the proportion of results below the limit of detection was too high to provide a valid result.

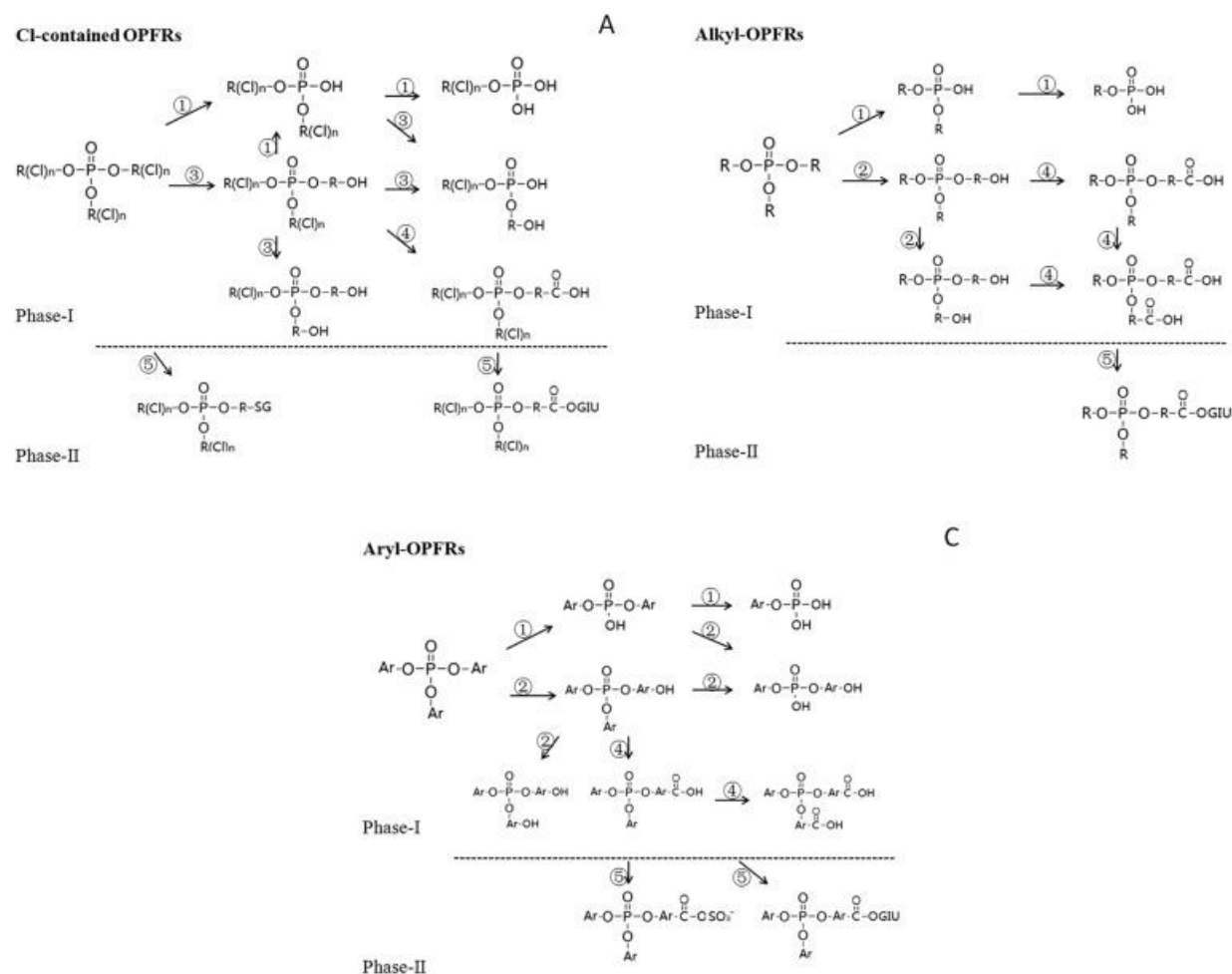
<sup>a</sup> Mean value reported; not specific gravity (SG) normalized

<sup>b</sup> Geometric mean (GM) reported; SG normalized

<sup>c</sup> Mean values reported; SG normalized

<sup>d</sup> GM values reported; not SG normalized

<sup>e</sup> Sum concentration of the ortho and para isomers of DCP



**Figure 1.2.** General metabolic pathways of the OPFRs

OPFRs (A: Chlorinated OPFRs; B: Alkyl OPFRs; C: Aryl OPFRs) in organisms from both *in vivo* and *in vitro* metabolism studies. Reactions are numbered according to the following annotation (①: O-dealkylation; ②: Hydroxylation; ③: Oxidative dechlorination; ④: Oxidation; ⑤: Conjugation). (Hou et al. 2016)

**CHAPTER 2: COMPARATIVE ASSESSMENT OF THE ORGANOPHOSPHATE  
ESTERS FOR ACETYLCHOLINESTERASE AND CARBOXYLESTERASE  
INHIBITORY ACTIVITY *IN VITRO***

Stephanie M. Marco<sup>1</sup>, Jason R. Richardson<sup>2</sup>, and Brian T. Buckley<sup>3</sup>

<sup>1</sup> Department of Pharmacology and Toxicology, Rutgers University, Piscataway,  
NJ

<sup>2</sup> Robert Stempel School of Public Health and Social Work, Florida International  
University, Miami, FL

<sup>3</sup> Environmental and Occupational Health Sciences Institute, Rutgers University,  
Piscataway, NJ

## 2.1 Abstract

The phase-out of polybrominated diphenyl ether flame retardants led to an increase in the use of alternatives including organophosphate flame retardants (OPFRs). OPFRs are structurally similar to the neurotoxic organophosphate pesticides (OPs), suggesting that OPFRs may be neurotoxic as well. The hallmark of OP-induced neurotoxicity is the inhibition of acetylcholinesterase (AChE), an enzyme critical for neuronal function. OPs are also known to inhibit carboxylesterase (CES) an important enzyme involved in endo- and xenobiotic metabolism including OPs. Whole brain and liver S9 fractions from naive male C57BL/6 mice were incubated with dichlorvos (DDVP), tris (2-chloroethyl) phosphate (TCEP), tributyl phosphate (TBP), dibutyl phosphate (DBP), triphenyl phosphate (TPP), diphenyl phosphate (DPP), tris(1,3-dichloro-2-propyl) phosphate (TDCPP), or tricresyl phosphate (TCP) to determine their effect on AChE and CES activity. AChE  $IC_{50}$  values were determined for DDVP (0.51  $\mu$ M), TCEP (14.7 mM), DPP (41.2 mM) and DBP (41.7 mM) but were not definable for TPP (max inhibition: 37% at 5 mM, solubility limit) and TCP (max inhibition: 32% at 5 mM) nor for TDCPP and TBP, which exhibited no anti-AChE activity. CES  $IC_{50}$  values for OPEs were 3 to 200 times lower than the AChE  $IC_{50}$  values: DDVP (2.9 nM), TCEP (4.3 mM), TPP (9.29  $\mu$ M), DPP (0.94 mM), DBP (13.7 mM), and TCP (41.3  $\mu$ M). Additionally, inhibitory CES activity was observed for TCP (max inhibition: 57% at 50 mM), TDCPP (max inhibition: 44% at 50 mM), and TBP (max inhibition: 14% at 5 mM). Overall, these data show that OPFRs are weak inhibitors

of AChE and CES relative to the OPs and that CES is more sensitive to perturbations by OPEs compared to AChE.

**Abbreviations**

AChE, acetylcholinesterase; ACh, acetylcholine; ATCI, acetylthiocholine iodide; CDBP, cresyl saligenin phosphate; CES, carboxylesterase; CPO, chlorpyrifos oxon; DDVP, dichlorvos; DBP, dibutyl phosphate; DPP, diphenyl phosphate; DTNB, 5,5-Dithiobis(2-nitrobenzoic acid); IC<sub>50</sub>, half maximal inhibitory concentration; NOAEL, no observed effect level; PBDE, polybrominated diphenyl ether; OPE, organophosphate ester; OPFR, organophosphate flame retardant; OP, organophosphate pesticide; PBDE, polybrominated diphenyl ether; PO, paraoxon; TBP, tributyl phosphate; TCEP, tris(2-chloroethyl) phosphate; TCP, tricresyl phosphate; TDCPP, tris(1,3-dichloro-2-propyl) phosphate; TmCP, tri-m-cresyl phosphate; ToCP, tri-o-cresyl phosphate; TpCP, tri-p-cresyl phosphate; TPP, triphenyl phosphate

## 2.2 Introduction

Organophosphate esters (OPEs) are a diverse class of compounds including pesticides (OPs), flame retardants (OPFRs), and plasticizers. OPs are a class of insecticides with agricultural, residential, and veterinary applications (Costa 2006; Roberts and Reigart 2013). OPs were one of the most widely used insecticides in the U.S. until the mid-2000s when they were phased out from residential use due to evidence that they may be hazardous to children's neurodevelopment in addition to their overall acute neurotoxic potential in humans (Roberts et al., 2013). Following the phase-out of residential OP formulations, their use nationwide has declined from 70% of total insecticide usage in 2000 to 33% in 2012 in favor of pyrethroids and neonicotinoids (Atwood and Paisley-Jones 2017). OPFRs, on the other hand, saw a substantial increase during that timeframe due to the phase-out of polybrominated diphenyl ethers (PBDEs) in the mid-2000s. OPFRs are a class of flame retardants added to plastics, construction material, textiles, furniture, and electronics. In the U.S., production of chlorinated OPFRs such as tris(2-chloroethyl) phosphate (TDCPP) and tris(2-chloroethyl) phosphate (TCEP) increased from less than 14,000 tons per year in 1986 to 38,000 tons per year in 2012 (Schreder et al. 2016).

OPEs are esters of phosphoric acid and its derivatives. The general structure of an OPE consists of (a) a central phosphorus atom (P) double bonded to an oxygen (P=O) or a sulfur atom (P=S) and (b) three alkoxy (R-O) side chains or two R-O side chains and a leaving group denoted as X, OX, or SX. OPs contain the central



P=O or P=S bond, two alkoxy side chains, and a leaving group. OPFRs contain the central P=O bond and three alkoxy substituents, making them structurally similar to the OPs, and as a result, have come under scrutiny for their potential to elicit similar toxicological effects.

OPs are acutely neurotoxic chemicals that work by inhibiting acetylcholinesterase (AChE). AChE is a critical enzyme belonging to the serine hydrolase superfamily of enzymes and is responsible for hydrolyzing the neurotransmitter acetylcholine (ACh). AChE is primarily found in brain, muscle, and erythrocytes. OPs stoichiometrically bind to AChE resulting in a phosphorylated enzyme that is more stable and has a lower rate of hydrolysis and regeneration of the active enzyme compared to the carbon-enzyme bond of ACh (Kwong 2002). Phosphorylation of AChE leads to an accumulation of ACh in cholinergic junctions hyperstimulating cholinergic receptors, which induces sweating, salivation, lacrimation, gastrointestinal hypermotility, and muscular tremors among other symptoms (Moser and Padilla 2011). Marked levels of AChE inhibition ( $\geq 70\%$ ) is lethal to mammals and insects alike (Casida 1964).

OPs also inhibit carboxylesterase (CES), a serine hydrolase found predominantly in the liver and intestine (Chanda et al. 1997). Inhibition of CES does not elicit toxicity *per se*; however, the stoichiometric binding of OPs with CES plays an important role in OP detoxification and can influence their overall disposition and potential to interact with AChE (Chanda et al. 1997; Maxwell 1992; Ross et al. 2010). CES detoxifies OPs by hydrolysis to form carboxylic acid and alcohol

metabolites (Ross et al. 2010). *In vitro* studies have suggested that liver CES is involved in increasing the effective  $IC_{50}$  of chlorpyrifos oxon (CPO, the toxic metabolite of chlorpyrifos) thereby limiting OP toxicity (Chanda et al. 1997). Additionally, OPs can act as both substrate and inhibitor of serine hydrolases (Casida and Quistad 2004). For example, CES metabolizes malathion to its toxic metabolite maloxon, which in turn inhibits detoxification via CES (Hodgson and Rose 2006). Decreased CES activity is inversely related to OPFR toxicity. In other words, reducing the number of CES molecules available for detoxification has the potential to enhance the severity of OP toxicity.

Based on the structural similarities of the OPEs, it is thought that the OPFRs may interact with AChE and CES in an analogous manner to the OPs. However, limited or conflicting data assessing these interactions and thus necessitate further analysis (EPA 2015). In one study, triphenyl phosphate (TPP), but not TCEP or TDCPP, significantly inhibited AChE activity at high concentrations (2 mg/L) in adult Chinese rare minnows (Yuan et al. 2016). An *in vitro* assessment of TPP in AChE-overexpressing HEK293T cell lysates showed that TPP did not inhibit AChE activity at 1 or 10  $\mu$ M (Morris et al. 2014). In zebrafish larvae, tributyl phosphate (TBP) and TCEP did not to significantly affect AChE activity (Sun et al., 2016; Wang et al., 2015a). However, a significant downregulation of *ache* mRNA was observed for TBP at higher concentrations (625 and 3,125  $\mu$ g/L) whereas TCEP did not alter *ache* mRNA (Sun et al., 2016). An *in vitro* study using purified human AChE indicated that the cresyl saligenin phosphate (CBDP) the toxic metabolite of tri-o-cresyl phosphate (ToCP), a component of tricresyl phosphate (TCP), inhibits

AChE at a similar rate to the potent OP paraoxon (PO,  $k_i \approx 10^6 \text{ M}^{-1} \text{ min}^{-1}$ ) (Carletti et al. 2011). Fewer studies have investigated the potential for OPFRs to interact with CES. In one *in vivo* study, TPP (100 mg/kg, IP) was shown to decrease total CES activity by 43% in mice when assayed by *p*-nitrophenyl acetate (Morris et al. 2014). Furthermore, TPP exhibited  $\text{IC}_{50}$  values of 15, 12, 5, 1100, and 2300 nM for *Ces1c*, *Ces1e*, *Ces1f*, *Ces1g*, and *Ces2a*, respectively, in recombinantly expressed HEK293T cells. Additionally, TPP (10  $\mu\text{M}$ ) completely inhibited *Ces1e*, *Ces1f*, and *Ces2a* *p*-nitrophenyl acetate hydrolytic activity in HEK293T cell lysates overexpressing those *Ces* targets. Taken together, these data indicate the need to screen OPFRs for potential AChE and CES activity.

In the present study, the ability of six OPEs to inhibit AChE and/or limit CES detoxification activity was determined: dichlorvos (DDVP), TCEP, TBP, TPP, TDCPP, TCP. Additionally, the commercially available metabolites of TBP (dibutyl phosphate, DBP) and TPP (diphenyl phosphate, DPP) were tested. It is hypothesized that the OPFRs will have less potent inhibition of AChE and CES activity than the OP, DDVP because DDVP has a slightly better leaving group. Leaving group strength is causally related to AChE binding. Additionally, it is hypothesized that the OPFR metabolites will be more potent inhibitors of the serine hydrolases than their parent compounds due to the replacement of one of the side chains with a hydroxyl group. Because the hydroxyl group should be a better leaving group than the alkoxides, the prediction is that when the active serine attacks, the hydroxide should more easily leave, and the OPFR metabolites would be more effective inhibitors.

## 2.3 Materials and Methods

### 2.3.1 Chemicals

CPO (CAS no. 5598-15-2; purity = 98.8%) and DBP (CAS no. 107-66-4; purity = 98%) were purchased from Chem Service (West Chester, PA). ATCI (CAS no. 1866-15-5; purity = 98%), DDVP (CAS no. 62-73-7; purity = 98.8%), DPP (CAS no. 838-85-7; purity = 99%), DTNB (CAS no. 69-78-3; purity = 99%), p-nitrophenyl valerate (CAS no. 1956-07-6; purity = 98%), TBP (CAS no. 126-73-8; purity = 99%) and TCEP (CAS no. 115-96-8; purity = 98%) were purchased from Sigma-Aldrich (St. Louis, MO). TCP (CAS no. 1330-78-5; purity = 99%) and TPP (CAS no. 115-86-6; purity = 99%) were purchased from Acros Organics (Fair Lawn, NJ). TDCPP (CAS no. 13674-87-8; purity = 95.6%) was purchased from TCI America (Portland, OR).

### 2.3.2 Sample Preparation

Brain AChE was prepared by homogenizing whole brain from a naïve male C57BL/6 mouse to a concentration of approximately 30 mg/mL in 50 mM Tris-HCl buffer (pH 7.4 at 37°C) using a tissue homogenizer (Tissue-Tearor Model 985-370, BioSpec Products, Bartlesville, OK). The homogenate was centrifuged at 5,000  $\times g$  for 5 min (4°C) to obtain a crude membrane pellet. The supernatant was discarded, and the pellet was resuspended in the original volume of buffer, aliquoted into multiple tubes, and stored at -80°C until analysis. This preparation was used to eliminate potential contributions from plasma butyrylcholinesterase.

Additionally, this preparation was more stable than a whole homogenate for determining AChE activity (Carr and Chambers 1996).

Liver S9 fractions from a naïve male C57BL/6 mouse was prepared by homogenizing whole liver in 1 mL of 50 mM Tris-HCl buffer per 100 mg of tissue. Homogenates were then centrifuged for 20 minutes at  $9,000 \times g$  ( $4^{\circ}\text{C}$ ). The supernatant (S9 fraction) was aliquoted into multiple tubes and stored at  $-80^{\circ}\text{C}$  until analysis. The supernatant (S9 fraction) was used to assess CES activity.

### 2.3.3 AChE Activity Assay

The AChE assay was carried out in a 96-well plate using a modified Ellman method (Ellman et al. 1961). Acetylthiocholine iodide (ATCI) was used as the reaction substrate. 5,5-dithiobis (2-nitrobenzoic) acid (DTNB) was used to measure AChE activity. OPEs were prepared in 100% ethanol (0.5%, final) and diluted in 50 mM Tris-HCl buffer to achieve the assay concentrations. Briefly, 20  $\mu\text{L}$  of brain homogenate, 20  $\mu\text{L}$  of OPE, and 140  $\mu\text{L}$  of DTNB (0.3 mM, final) were mixed and incubated for 30 min at  $37^{\circ}\text{C}$ . The reaction was initiated by the addition of 20  $\mu\text{L}$  of ATCI (1 mM, final). Hydrolysis of ATCI was measured by the formation of 5-thio-2-nitrobenzoate, the colored anion formed by the reaction of DTNB and thiocholine. Thiocholine is released by enzymatic hydrolysis of ATCI. Absorbance (mOD/min) was measured kinetically at 412 nm for 10 min using a SpectraMax M3 spectrophotometer (Molecular Devices, Sunnyvale, CA). Chlorpyrifos oxon (CPO), a potent AChE inhibitor, was used as a positive control. Absorbances were blank

corrected by subtracting the absorbance of the blank (buffer and substrate). AChE activity was calculated as nmol/min/mg protein.

#### 2.3.4 CES Activity Assay

The CES assay was performed in a 96-well plate using the continuous spectrometric methods of Ross and Borazjani with modifications (2007). OPEs were prepared in 100% ethanol (0.5%, final) and diluted in 50 mM Tris-HCl buffer to achieve the assay concentrations. Liver S9 fractions were diluted 1/5000 in Tris buffer yielding a final protein assay concentration of 8 µg/mL. 120 µL of the dilute S9 fractions were incubated with 30 µL of OPE for 30 min at 37°C. 150 µL of the CES substrate *p*-nitrophenyl valerate (500 mM, final) was added, and hydrolysis of the substrate and subsequent liberation of *p*-nitrophenol and formation of the yellow-colored *p*-nitrophenolate ion were monitored kinetically at 405 nm for 5 min using a SpectraMax M3 spectrophotometer (Molecular Devices, Sunnyvale, CA). Paraoxon (PO), a potent CES inhibitor, was used as a positive control. Absorbances were blank corrected by subtracting the absorbance of the blank (buffer and substrate). CES activity was calculated as nmol/min/mg protein.

#### 2.3.5 Protein Assay

Protein concentration was measured using the Thermo Scientific Pierce BCA Protein Assay (Garden City, NY) using bovine serum albumin as the standard. Absorbance was determined at 562 nm using a SpectraMax M3

spectrophotometer (Molecular Devices, Sunnyvale, CA). Protein concentrations were used to calculate specific activities for each enzyme preparation.

### 2.3.6 Statistical Analysis

Changes in enzyme activity were analyzed by one-way ANOVA using GraphPad Prism v6 (La Jolla, CA). Data are presented as mean  $\pm$  SEM of three independent experiments. Dunnett's test was used to determine significance between treatment and control groups. A value of  $p < 0.05$  was considered statistically significant.  $IC_{50}$  values were determined for OPEs exhibiting dose-dependent effects on AChE and CES activity using a normalized, variable hill slope, dose-dependent inhibition regression or a normalized linear regression where appropriate.

## 2.4 Results

### 2.4.1 AChE Activity

The effect of OPE treatment on AChE activity *in vitro* is shown in **Fig 2.1 A-B**. DDVP exhibited a dose-dependent inhibition of mouse brain AChE at the concentrations tested (0.01-100  $\mu$ M). Significant inhibition compared to the control was observed for 1 (55%), 10 (69%), and 100  $\mu$ M (76%). The calculated  $IC_{50}$  for DDVP was 0.51  $\mu$ M.

TBP did not impact AChE activity at 0.1, 1, or 5 mM, the observed solubility limit. Unlike its parent compound, DBP did not have any solubility limitations in our assay and was tested at concentrations that ranged between 0.1 and 100 mM. DBP significantly inhibited AChE activity at 25 (26%), 50 (59%), 75 (74%), and 100 mM (89%). The  $IC_{50}$  for DBP was determined to be 41.7 mM, 5 orders of magnitude larger than the  $IC_{50}$  for DDVP (0.51  $\mu$ M).

TPP, like TBP, could only be tested from 0.1 to 5 mM due to solubility limitations. Unlike TBP, however, 5 mM of TPP significantly inhibited AChE activity by 37%. Like DBP, DPP did not exhibit solubility limitations and was tested at concentrations ranging between 0.1 and 100 mM. DPP significantly inhibited AChE activity at 1 (8%), 5 (12%), 25 (35%), 50 (46%), 75 (71%), and 100 (89%). The calculated  $IC_{50}$  for DPP was 41.2 mM, which was comparable to the  $IC_{50}$  for DBP (41.7 mM) and 5 orders of magnitude larger than the  $IC_{50}$  for DDVP (0.51  $\mu$ M).



Mouse brain AChE treated with 0.1-100 mM of TCEP displayed a significant inhibition of activity at 5 (9%), 25 (34%), 50 (41%), 75 (44%), and 100 mM (45%). The  $IC_{50}$  was determined to be 14.7 mM, 5 orders of magnitudes larger than the  $IC_{50}$  for DDVP (0.51  $\mu$ M).

The final two OPEs tested for anti-AChE activity were TDCPP and TCP (0.1-50 mM). 50 mM was the highest concentration for which solubility was not an issue for either chemical. TDCPP had no effect on AChE activity at the concentrations tested. However, TCP significantly inhibited AChE activity at 1 (24%), 25 (26%), and 50 mM (32%). The  $IC_{50}$  could not be reliably determined for TCP.

#### 2.4.2 CES Activity

The effect of OPEs on CES activity is shown in **Fig 2.1A-B**. Liver S9 fractions from naïve mice treated with DDVP presented a dose-dependent inhibition of CES activity (0.1-1000 nM). Significant CES inhibition for DDVP occurred at 1 (24%), 5 (63%), 10 (70%), 100 (83%), and 1000 nM (89%). The observed CES  $IC_{50}$  was 2.9 nM, nearly 200 times lower than the AChE  $IC_{50}$  (0.51  $\mu$ M), indicating that CES was more sensitive to DDVP treatment than AChE.

As in the AChE assay, no inhibition was observed for 0.1 or 1 mM of TBP. However, TBP showed significant CES inhibition at 5 mM (14%). By contrast, DBP inhibited CES activity in a dose-dependent manner (0.1-100 mM). DBP significantly inhibited CES activity at 5 (13%), 10 (31%), 25 (58%), 50 (76%), 75 (89%), and 100 mM (95%). The CES  $IC_{50}$  for DBP was 13.7 mM, 3 times lower

than the AChE  $IC_{50}$  (41.7 mM), indicating that CES activity was more easily perturbed by DBP. However, the  $IC_{50}$  for DBP was 7 orders of magnitude larger than it was for DDVP (2.9 nM).

Compared to the AChE assay, in which TPP inhibited enzyme activity by 37% at 5 mM and had no effect at 0.1 or 1 mM, disruption of CES activity was more prevalent with TPP treatment. TPP significantly inhibited CES activity at all concentrations tested: 100 pM (7%), 10 nM (23%), 1  $\mu$ M (32%), 100  $\mu$ M (48%), 1 mM (55%), and 5 mM (62%; solubility limit). The  $IC_{50}$  for TPP was determined to be 9.29  $\mu$ M by normalized linear regression. By contrast, the  $IC_{50}$  for DDVP (2.9 nM) was 5 order of magnitude smaller than for TPP. DPP also showed more anti-CES activity than anti-AChE activity at the concentrations tested (0.001-50 mM). CES activity was significantly inhibited by 0.1 (17%), 1 (45%), 5 (77%), 25 (93%),  $IC_{50}$  for AChE (41.2 mM), suggesting that CES activity is more sensitive to disturbances by DPP. By contrast, CES was more sensitive to perturbations by TPP by 2 orders of magnitude over DPP. Moreover, DPP's  $IC_{50}$  was 5 orders of magnitude larger than that of DDVP (2.9 nM).

Liver S9 fractions treated with TCEP (0.1-100 mM) exhibited significant CES inhibition at 5 (27%), 25 (44%), 50 (49%), 75 (51%), and 100 mM (51%). Compared to the  $IC_{50}$  for AChE (14.7 mM), the  $IC_{50}$  for CES was 3.4 times lower, indicating the increased sensitivity of CES to TCEP treatment relative to AChE. Moreover, TCEP's  $IC_{50}$  was 6 orders of magnitude greater than DDVP's  $IC_{50}$  (2.9 nM).

TDCPP and TCP were tested at similar concentrations to the AChE assay: 0.1-50 mM (TDCPP) and 0.001-50 mM (TCP). In contrast to the results of the AChE assay—where TDCPP had no effect on enzyme activity—TDCPP significantly inhibited CES activity at 1 (26%), 5 (26%), 25 (26%), and 50 mM (44%). The  $IC_{50}$  could not be reliably determined for TDCPP. Additionally, significant CES inhibition was observed for TCP at 0.1 (40%), 1 (55%), 5 (55%), 25 (56%), and 50 mM (57%). These values were approximately 40%, 31%, 30%, and 25% higher, respectively than those obtained in the AChE assay at the same concentrations. The  $IC_{50}$  for CES was determined to be 41.3  $\mu$ M whereas the  $IC_{50}$  for AChE could not be determined. By comparison, the  $IC_{50}$  for DDVP (2.9 nM) was 4 orders of magnitude lower.

## 2.5 Discussion

In this study, the AChE and CES inhibitory potential of eight OPEs were assessed: DDVP, TCEP, TBP, DBP, TPP, DPP, TDCPP, and TCP. The goals of this study were two-fold: (1) to compare the inhibitory activity of OPs and OPRs toward AChE and CES, and (2) to determine the potency of the OPFR metabolites relative to parent compounds. Both goals test their structure-activity relationships. Overall, the OP DDVP was a more potent AChE and CES inhibitor than the OPFRs by 3-7 orders of magnitude. These results indicate that despite their structural similarities, OPFRs do not exhibit the same potential to inhibit these enzymes as the OPs do, which is likely because the OPs have functionalities that are in general better leaving groups than those of the OPFRs.

The substantial difference in anti-AChE activity between the OPs and OPFRs has also been observed in electric rays (*T. ocellata*) suggesting that AChE responds similarly to OPE exposure across species (Eldefrawi et al. 1977). In that study, 100  $\mu$ M of the OP diisopropyl fluorophosphate inhibited nearly 100% of electric ray AChE activity whereas 1 mM of TCEP and ToCP inhibited AChE activity by 26 and 18%, respectively. In the present study, 1 mM of TCEP exhibited a mere 2% inhibition suggesting that mouse AChE may be less sensitive to TCEP exposure than electric ray AChE. ToCP was not investigated in this study, however, TCP—a mixture of the ortho, meta, and para isoforms—significantly inhibited 24% of AChE activity at 1 mM. The effect of ToCP and TCP on AChE were similar in both species (electric ray: 18%, mouse: 24%) suggesting that the ortho isoform is likely

responsible for the observed anti-AChE activity. Indeed, ToCP has been shown to inhibit AChE *in vivo* (Carrington and Abou-Donia 1988; Vora et al. 1962). Although, this effect has largely been attributed to its metabolite CBDP, which has been shown to inhibit AChE at a similar rate to PO ( $k_i \approx 10^6 \text{ M}^{-1} \text{ min}^{-1}$ ) in human AChE *in vitro* (Carletti et al. 2011). In summary, DDVP was more potent than the OPFRs by at least 5 orders of magnitude and no obvious trend in potency based on OPFR structure was observed.

The two OPFR metabolites tested in this study did not exhibit greater anti-AChE potential than their parent compounds at the concentrations for which parent solubility was not an issue. In fact, TBP and DBP had the same no observed effect level (NOAEL) on AChE activity at 5 mM. By contrast, TPP had a greater effect on AChE activity than DPP at the same concentrations with a difference of 5%, 6%, and 25% at 0.1, 1, and 5 mM, respectively. The metabolites have a hydroxyl group while the parent compounds have all alkoxy substituents (TPP versus DPP and TBP versus DBP). Because hydroxide is a better leaving group than alkoxide, it could be argued that DPP and DBP should be more reactive in terms of the active site serine nucleophilic attack. However, the metabolites are not better inhibitors of AChE, so the improved leaving group of hydroxide over alkoxide does not translate to improved inhibition. This is probably because the hydroxide group is only nominally better of a leaving group than the alkoxides.

Compared to AChE, CES was more sensitive to perturbations by the OPFRs although the OPFRs were 3-7 orders of magnitude weaker than DDVP. It is

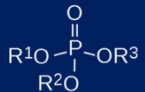

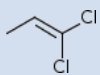
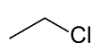

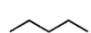
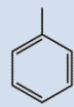
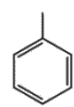
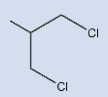
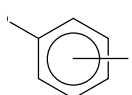
important to understand how these chemicals affect CES activity because CES plays a key role in detoxification and can impact their potential to interact with AChE. In the present study, TPP displayed the most anti-CES activity of all the OPFRs tested followed by TCP, DPP, TCEP, DBP, TDCPP, and TBP. This suggests that the aryl-phosphates (TPP, TCP, and DPP) were more active against CES than the alkyl phosphates (TCEP, DBP, TDCPP, and TBP). The effectiveness of aryl phosphates over alkyl phosphates at reducing CES activity was also observed in HEK293T cells recombinantly expressing individual mouse CES enzymes (Morris et al. 2014). In addition to TPP, the meta (TmCP) and para (TpCP) isomers of TCP, but not the ortho isomer (ToCP), inhibited *Ces1c*, *Ces1e*, *Ces1f*, *Ces1g*, and *Ces2a* at 1  $\mu$ M whereas TBP and TDCPP were ineffective at the same concentration. Interestingly, Morris et al. found that all five isozymes exhibited  $IC_{50}$  values between 5 nM and 2.3  $\mu$ M for TPP. The total CES  $IC_{50}$  for TPP in this study was just outside that range at 4.29  $\mu$ M. This could be attributed to the different methods used to assay CES activity. The percent inhibition of the different CES enzymes by TmCP and TpCP at 1  $\mu$ M was not reported by Morris et al., however, in the present study, TCP inhibited total CES activity in mouse liver by only 7% at 1  $\mu$ M. Because ToCP did not affect CES activity in the HEK293T cells, it is possible that the observed inhibition of total CES activity in mouse liver is attributed to the meta and para isomers in the mixture. In summary, the aryl phosphates, particularly TPP, exhibit greater anti-CES activity than the alkyl phosphates, indicating a good correlation between the cellular and mammalian *in vitro* studies.

The two OPFRs metabolites tested in this study differed in their anti-CES potential relative to their parent compounds at the concentrations for which parent solubility was not an issue. TBP and DBP had a similar no observed effect level on CES activity at 1 mM and a similarly modest 14% (TBP) and 13% (DBP) inhibition at 5 mM. The potency of DPP over TPP varied at 1  $\mu$ M, 100  $\mu$ M, 1 mM, and 5 mM. Both compounds had no effect on CES activity at 1  $\mu$ M. At 100  $\mu$ M, TPP was 31% more effective than DPP, but at 1 mM the difference closed to 10%. The trend reversed at 5 mM where DPP was 15% more effective than TPP. As in the AChE assay, DPP and DBP were thought to inhibit CES more readily than their parent compounds. However, this does not appear to be the case for TBP and DBP suggesting that leaving group potential does not affect inhibitory strength. Of the OPFRs tested, TBP and DBP were the weakest CES inhibitors, so it is possible that other factors such as the relatively inactive nature of the alkyl phosphates may prevail. The potential influence of leaving group strength on CES activity was even less obvious for TPP and DPP. At lower concentrations (100  $\mu$ M and 1 mM), TPP was more inhibitory than DPP, however, at higher concentrations (5 mM) DPP was more inhibitory than TPP. Thus, it is difficult to conclude whether structure played a role in the different trends observed for TPP and DPP. It is possible the presence of a stronger leaving group (relative to the alkanes) such as a hydroxyl may account for the 15% difference in CES activity between DPP and TPP at higher concentrations. However, without further studies on their specific molecular interactions with CES, it is difficult to draw a conclusion with certainty.

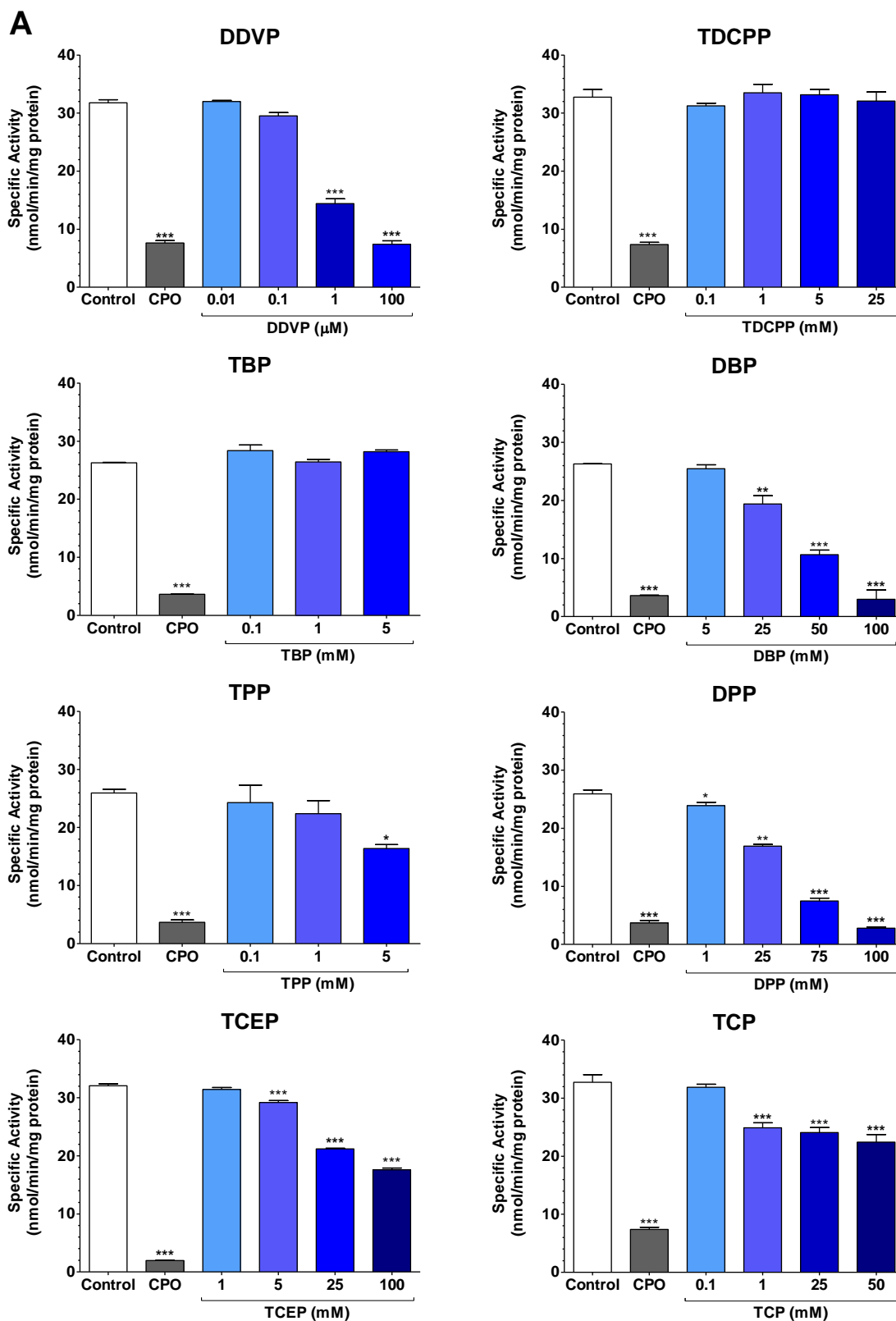
In conclusion, although some AChE and CES inhibitory activity were observed for the OPFRs, the concentrations at which the  $IC_{50}$  responses were elicited were mostly in the millimolar range. Thus, OPFRs are weak AChE and CES inhibitors relative to the OPs. Additionally, CES appeared more sensitive to perturbations by OPEs compared to AChE and that TPP and TCP were the most potent CES inhibitors of the OPFRs with an  $IC_{50}$  in the low micromolar range.

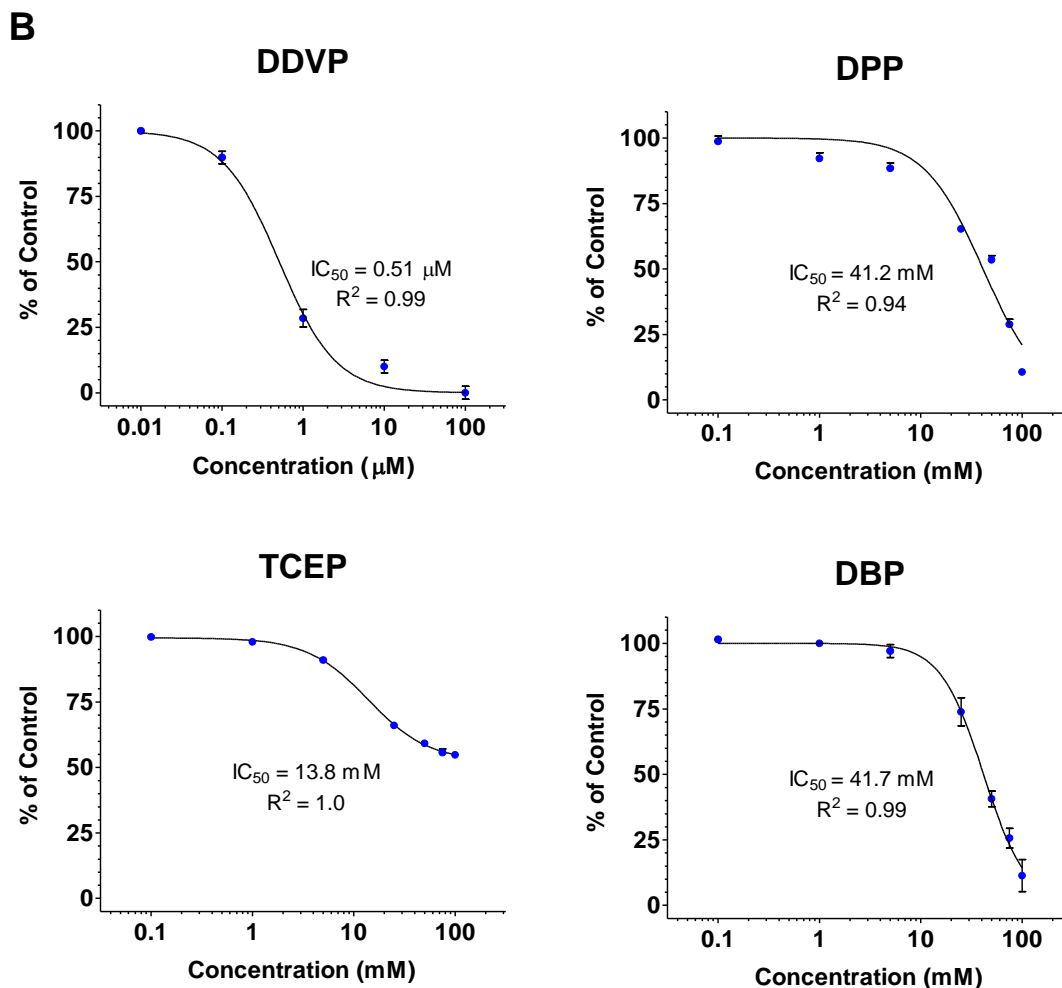


**Table 2.1.** Names, acronyms, classes, and structures of OPEs screened for inhibition of AChE and CES activity

| Name                                   | Acronym | Class                           | R Groups  |  |
|--|---------|---------------------------------|---|---|
| Dichlorvos                             | DDVP    | Pesticide                       | R <sub>1,2</sub>  R <sub>3</sub>  |   |
| Tris (2-chloroethyl) phosphate         | TCEP    | Flame retardant                 | R <sub>1,2,3</sub>   |   |
| Tributyl phosphate                     | TBP     | Plasticizer/<br>solvent         | R <sub>1,2,3</sub>   |   |
| Dibutyl phosphate                      | DBP     | TBP metabolite                  | R <sub>1,2</sub>  R <sub>3</sub> OH  |   |
| Triphenyl phosphate                    | TPP     | Flame retardant/<br>plasticizer | R <sub>1,2,3</sub>   |   |
| Diphenyl phosphate                     | DPP     | TPP metabolite                  | R <sub>1,2</sub>  R <sub>3</sub> OH   |   |
| Tris (1,3-dichloro-2-propyl) phosphate | TDCPP   | Flame retardant                 | R <sub>1,2,3</sub>   |   |
| Tricresyl phosphate                    | TCP     | Flame retardant/<br>plasticizer | R <sub>1,2,3</sub>   |   |

## Inhibition of AChE Activity by OPEs

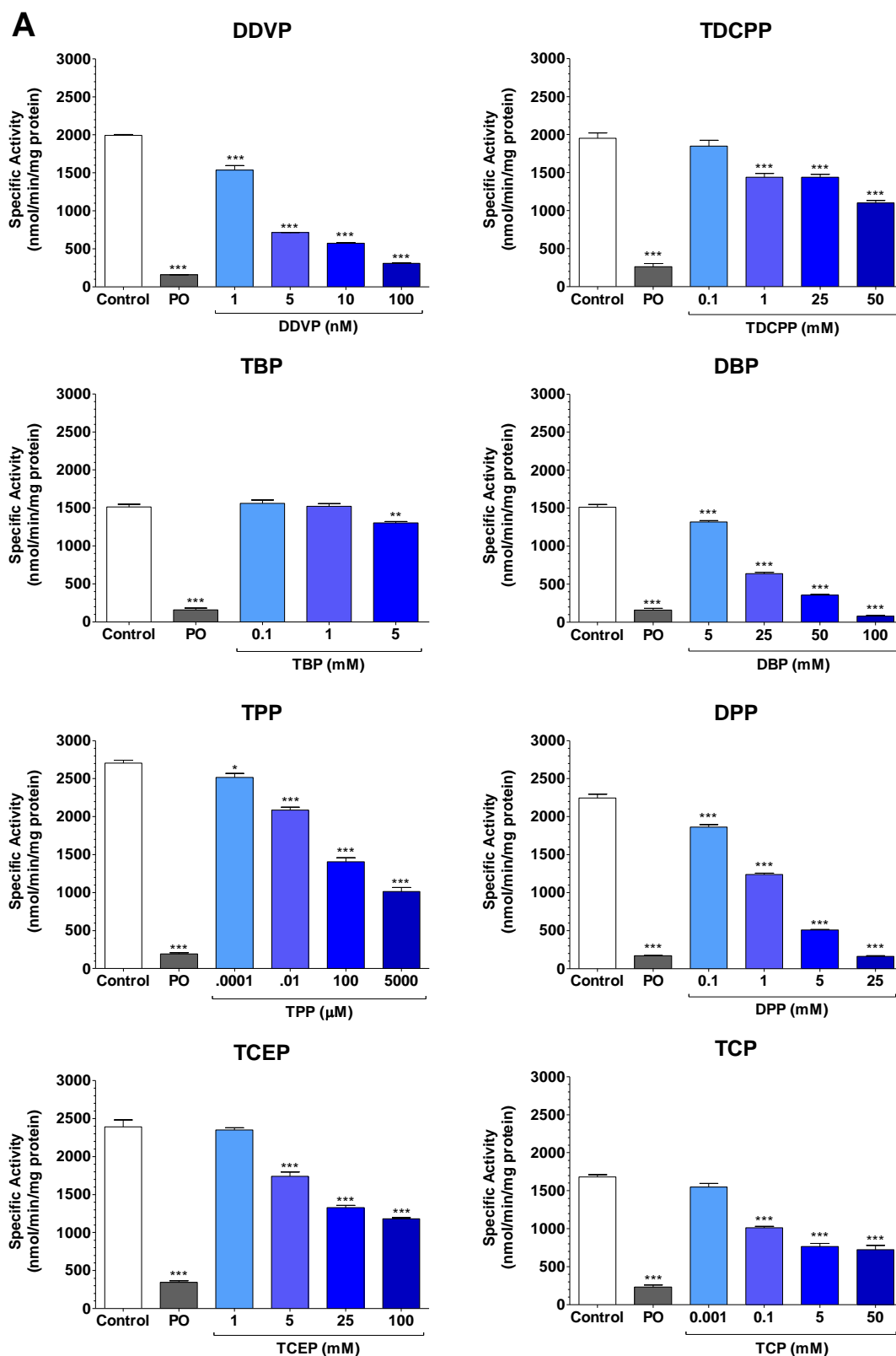


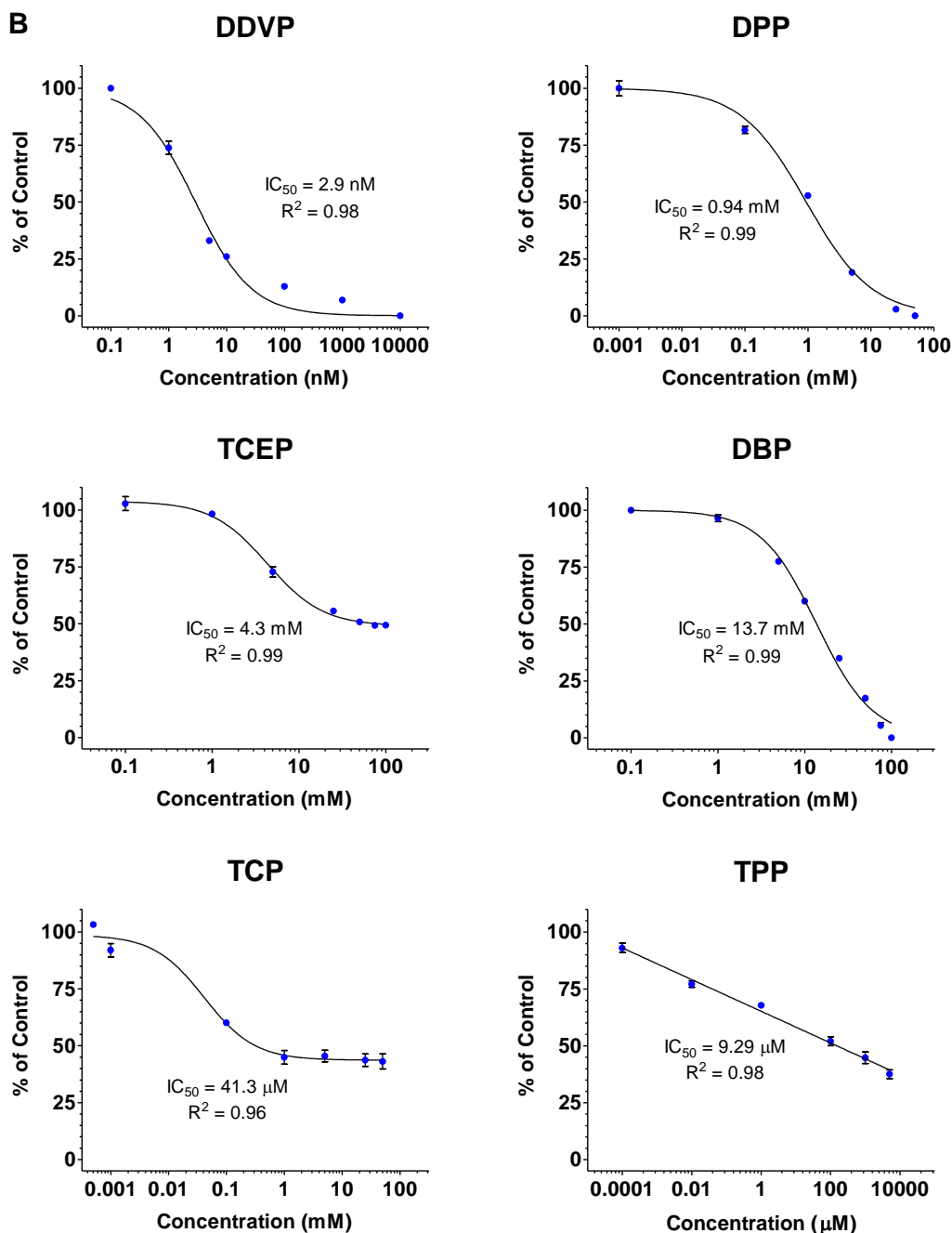


**Figure 2.1.** Inhibition of AChE activity by OPEs

AChE activity in mouse brains treated with OPEs *in vitro* was assessed. Chlorpyrifos oxon (CPO), a potent AChE inhibitor, was used as a positive control (**A**). IC<sub>50</sub> values were determined for OPEs exhibiting dose-dependent effects on AChE activity using a normalized, variable hill slope, dose-dependent inhibition regression (**B**). Error bars represent mean  $\pm$  SEM from 3 independent experiments. Data were analyzed by one-way ANOVA using Dunnett's post-test. \* $p \leq 0.05$ , \*\* $p \leq 0.01$ , and \*\*\* $p \leq 0.001$ .

## Inhibition of CES Activity by OPEs





**Figure 2.2.** Inhibition of CES activity by OPEs

CES activity in mouse live S9 fractions treated with OPEs *in vitro* was assessed. Paraoxon (PO), a potent CES inhibitor, was used as a positive control (A). IC<sub>50</sub> values were determined for OPEs exhibiting dose-dependent effects on CES activity using a normalized, variable hill slope, dose-dependent inhibition regression or a normalized linear regression (B). Error bars represent mean ± SEM from 3 independent experiments. Data were analyzed by one-way ANOVA using Dunnett's test. \*p ≤ 0.05, \*\*p ≤ 0.01, and \*\*\*p ≤ 0.001.

## **CHAPTER 3: DISPOSITION OF ORGANOPHOSPHATE FLAME RETARDANTS IN MICE**

Stephanie M. Marco<sup>1</sup>, Brittany Rickard<sup>1</sup>, Ali Yasrebi<sup>2</sup>, Ill Yang<sup>3</sup>, Jason R.  
Richardson<sup>4</sup>, Lauren M. Aleksunes<sup>1</sup>, Troy R. Roepke<sup>2</sup>, Brian T. Buckley<sup>3</sup>

<sup>1</sup> Department of Pharmacology and Toxicology, Rutgers University, Piscataway,  
NJ

<sup>2</sup> Department of Animal Sciences, Rutgers University, New Brunswick, NJ

<sup>3</sup> Environmental and Occupational Health Sciences Institute, Rutgers University,  
Piscataway, NJ

<sup>4</sup> Robert Stempel School of Public Health and Social Work, Florida International  
University, Miami, FL

### 3.1 Abstract

Organophosphate flame retardants (OPFRs) are chemicals of emerging toxicological and environmental concern due to reports of endocrine disruption, neurotoxicity, and reproductive and developmental toxicity in animals; as well as their environmental persistence and bioaccumulation. Studies on the tissue disposition and accumulation of OPFRs *in vivo* are limited. In the present study, the tissue distribution of OPFRs was quantified in adult male and female C57BL/6 mice orally administered a daily 3 mg/kg mixture of equal parts tricresyl phosphate (TCP), triphenyl phosphate (TPP), and tris(1,3-dichloro-2-propyl) phosphate (TDCPP) for four weeks using gas chromatography-ion trap mass spectrometry. Additionally, the maternal transfer of OPFRs was evaluated by gestational exposure to the 3 mg/kg OPFR mixture (GD 7-16). Greater tissue/serum ratios indicate that the liver (16.3-73.5) and kidneys (8.7-78.8) are predominant sites of OPFR disposition with the brain (9.8-19.6) being a minor site by comparison for both males and females. Modest differences in OPFR accumulation and disposition were observed between male and female mice that were tissue- and compound-specific. Serum OPFR levels were similar between the sexes for TDCPP (M:  $0.90 \pm 0.19$  ng/mL, F:  $1.04 \pm 0.13$  ng/mL), TPP (M:  $1.30 \pm 0.38$  ng/mL, F:  $0.70 \pm 0.03$  ng/mL), and TCP (M:  $3.88 \pm 0.17$  ng/mL, F:  $3.04 \pm 0.76$  ng/mL). In the liver, comparable levels of TDCPP were observed in male and female mice (M:  $15.60 \pm 3.15$  ng/g, F:  $15.18 \pm 4.30$  ng/g). Concentrations of TPP in the livers of male mice exceeded those in females (M:  $70.04 \pm 15.8$  ng/g, F:  $41.56 \pm 4.30$  ng/g) whereas female mice exhibited significantly higher levels of TCP (M:  $172.9 \pm 13.1$

ng/g, F:  $222.5 \pm 14.3$  ng/g). In the kidneys, male mice had greater accumulation of TDCPP (M:  $24.88 \pm 8.61$  ng/g, F:  $14.52 \pm 4.02$  ng/g), TPP (M:  $59.58 \pm 18.5$  ng/g, F:  $52.63 \pm 4.64$  ng/g), and TCP (M:  $33.80 \pm 2.56$  ng/g, F:  $27.36 \pm 4.48$  ng/g) than females. Concentrations of TDCPP in the brain were similar across sexes (M:  $11.88 \pm 1.89$  ng/g, F:  $10.63 \pm 1.64$  ng/g). Higher TPP concentrations were observed in the brains of male mice (M:  $15.22 \pm 3.45$  ng/g, F:  $13.60 \pm 1.06$  ng/g) whereas greater TCP accumulation was detected in the brains of female mice (M:  $36.94 \pm 7.42$  ng/g, F:  $46.76 \pm 6.09$  ng/g). In addition, TCP accumulated in placentas ( $249.7 \pm 109$  ng/g) and fetuses ( $21.90 \pm 1.19$  ng/g) following gestational exposure of dams. Overall, these data show that the liver, kidneys, and brain are preferential sites of OPFR disposition, that sex differences in OPFR disposition are largely insignificant, and that TCP likely undergoes maternal transfer.



**Abbreviations**

CYP, cytochrome P450; FM 550, Firemaster 550; IP, intraperitoneal; OPFRs, organophosphate flame retardants; PBDEs, polybrominated diphenyl ethers; TCP, tricresyl phosphate; TDCPP, tris(1,3-dichloro-2-propyl) phosphate; TpCP, tri-p-cresyl phosphate; TPP, triphenyl phosphate; TPP-D15, deuterated triphenyl phosphate; GC-MS, gas chromatography-mass spectrometry; T/S, tissue/serum ratios

### 3.2 Introduction

In the early to mid-2000s, polybrominated diphenyl ether (PBDE) flame retardants were phased out due to concerns of toxicity and persistence in the environment. This created a demand for alternative materials such as organophosphate flame retardants (OPFRs). Since the phase-out of PBDEs, the use of OPFRs has increased. In 1992, 17% of the estimated 600,000 tons of flame retardants used worldwide were OPFRs (OECD 1995) and 70% of the 300,000 tons of organophosphorus compounds consumed in 2004 were OPFRs (Wei et al. 2015). Additionally, chlorinated OPFRs represent high production chemicals with greater than 50 million pounds produced or imported into the U.S. per year (EPA 2015). OPFRs are additives in plastics, textiles, construction material, and electronics, but have also been detected in household consumables such as furniture and baby products (Patisaul et al. 2013; Stapleton et al. 2011). Like PBDEs, OPFRs are not chemically bound to materials and can easily leach into the environment via volatilization, abrasion, and dissolution.

The ubiquitous detection of OPFRs in the environment suggests that human and wildlife exposure to these chemicals are likely widespread. Several studies have reported OPFRs in sediment/soil, water, biota, indoor air, and dust (Greaves and Letcher 2016; van der Veen and de Boer 2012; Wei et al. 2015). Indoor exposures to OPFRs are often higher than outdoor exposures, suggesting that humans may be at a greater risk of adverse health effects (Dishaw et al. 2014; van der Veen and de Boer 2012).

Studies have suggested that OPFR exposure can cause adverse effects including neurotoxicity, carcinogenicity, reproductive toxicity, and endocrine disruption. OPFRs have been shown to alter sperm and hormone concentrations in humans (Meeker and Stapleton 2010), induce metabolic syndrome in rats (Patisaul et al. 2013), affect testis organization in mice (Chen et al. 2015b), and induce neurodevelopmental toxicity in zebrafish (Dishaw et al. 2014).

Profiling of OPFR tissue disposition *in vivo* would aid in identifying potential target organs for toxicity and modeling tissue exposures in humans. Few studies have investigated how OPFRs preferentially distribute across tissues post-exposure. Adult female zebrafish exposed to low concentrations of OPFRs (4, 20, and 100 µg/L) during development (2 hpf) were found to have higher levels of tris(1,3-dichloro-2-propyl) phosphate (TDCPP) than males, which was notably higher in brain tissue (Wang et al. 2015b). In wild-caught crucian carp, OPFR concentrations were highest in the liver followed by muscle and gonad (Choo et al. 2018). In rats, TDCPP concentrations were found to be highest in the liver 10 days following a 0.87 mg/kg IV dose, while tricresyl phosphate (TCP) was found to be highest in the liver and adipose 24 hours following an 89.6 mg/kg oral dose (Kurebayashi et al. 1985; Nomeir et al. 1981). Overall these data demonstrate that the OPFRs remain in the body for several days after treatment and that sex differences in OPFR disposition may occur.

Another critical area of interest is the maternal transfer of OPFRs. Several studies have demonstrated that pregnant women exhibit detectable concentrations of

OPFRs (Castorina et al. 2017b; Ding et al. 2016; Hoffman et al. 2017b; Romano et al. 2017). Furthermore, OPFRs have been detected in the maternal-embryo interface (chorionic villi and deciduae) as well as the maternal-fetal interface (placenta) of pregnant women suggesting that maternal transfer is likely (Ding et al. 2016; Zhao et al. 2017). Developmental exposure to OPFRs has been associated with adverse neurodevelopmental outcomes including decreased IQ, reduced working memory, and increased negative social behaviors in humans (Castorina et al. 2017a; Lipscomb et al. 2017). In zebrafish, females chronically exposed to an environmentally-relevant concentration of TDCPP (7500 ng, 240 days) were shown to transfer TDCPP to their offspring via their eggs resulting in decreased survival, body length, and heart rate of the offspring (Yu et al. 2017). In rats, triphenyl phosphate (TPP) has been shown to accumulate in placentas but was not detected in fetal tissue of pregnant rats exposed to 1000 µg/day of Firemaster 550 (FM 550), a flame retardant mixture, during GD 9 through 18 (Baldwin et al. 2017). These results highlight the need to further investigate the potential for maternal transfer of OPFRs.

To address these knowledge gaps, the purposes of this study were to (1) characterize the tissue distribution of TDCPP, TCP, and TPP in mice following subchronic oral exposure, (2) identify potential differences in disposition according to sex, and (3) assess whether OPFRs can undergo maternal-fetal transfer in mice.

### 3.3 Materials and Methods

#### 3.3.1 Chemicals

TPP (CAS no. 115-86-6; purity = 99%) and TDCPP (CAS no. 13674-87-8; purity = 95.6%) were purchased from Sigma-Aldrich (St. Louis, Missouri). TCP (CAS no. 1330-78-5; purity = 99%) was purchased from AccuStandard (New Haven, Connecticut). For the stock solution, 100 mg of each OPFR were dissolved in 1 mL of acetone. For the working solution, 100  $\mu$ L of the stock solution was added to 10 mL of sesame oil and mixed over a stir plate for 48 hours with venting. Ultra-residue analyzed toluene (CAS no. 108-88-3; purity = 99.7%) was purchased from Thermo Fisher Scientific (Waltham, Massachusetts). TPP-D15 (CAS no. 1173020-30-8; purity = 98%) was purchased from Cambridge Isotope Laboratories (Tewksbury, Massachusetts).

#### 3.3.2 Animal Care

All animal procedures were completed in compliance with institutional guidelines based on National Institutes of Health standards and were performed with Institutional Animal Care and Use Committee approval at Rutgers University. C57BL/6J mice (Jackson Labs, Bar Harbor, ME) were bred in-house and maintained under controlled temperature (25 °C) and 12/12-h light/dark cycle. Mice were given water and food (LabDiet PicoLab Verified 5v75 IF, <75 ppm phytoestrogens) *ad libitum*.

Two studies were run sequentially, the first examined overall tissue distribution and the second to quantified maternal-fetal transfer. In the first study, intact adult male and female C57BL/6 mice (n=5 per sex) were treated with 1 mg/kg/day of TDCPP, TPP, and TCP (3 mg/kg total OPFR) in the form of a peanut butter treat daily for 28 days. The treats were prepared by mixing 100-150 mg of peanut butter with the sesame oil/OPFR mixture at a volume determined by weight (e.g. 25  $\mu$ L for a 25 g mouse). After the final dose, mice were fasted for 1 h, sedated with ketamine (100  $\mu$ L of 100 mg/mL, IP), and decapitated. Serum was generated from trunk blood by centrifuging at 1100 x *g* for 15 min at 4°C and stored at -80°C until analysis. Brain, liver, and kidneys were collected, immediately snap frozen, and stored at -80°C until analysis.

In the second study, pregnant dams (n=4) were given 1 mg/kg/day of TDCPP, TPP, and TCP (3 mg/kg total OPFR) or vehicle in the form of a peanut butter treat from GD 7 until GD 16-18. The dams were sacrificed in the same manner as the adult mice. Serum was generated as previously described and the placentas and fetuses were collected, snap frozen, and stored at -80°C until analysis.

### 3.3.3 Sample Preparation

Brain, liver, and kidney tissues were homogenized in 50 mM Tris buffer. Placentas (n=7-10 per dam) and fetuses (n=7-10 per dam) from the maternal-fetal study were pooled for each dam and then homogenized. Tissue homogenates and serum samples were spiked with 20 ng/mL of the internal standard (TPP-D15) for recovery correction. After spiking, the samples were vortexed for 1 min followed

by the addition of toluene (25-50  $\mu$ L for serum, 100  $\mu$ L for tissue). Samples were then vortexed for 2 min and allowed to stand for 5 min. Finally, samples were centrifuged at 9000 x *g* at 4 °C for 10 min, and the organic layer was collected for analysis by gas chromatography-mass spectrometry (GC-MS).

### 3.3.4 Instrumental Analysis

Sample extracts were analyzed using an Agilent 7890B GC/240 ion trap MS. Chromatographic separation of the analytes was achieved using an Agilent DB-*XLB* microcapillary column (30 m long x 180  $\mu$ m internal diameter x 0.18  $\mu$ m film thickness; Santa Clara, California) (**Figure S3.1**). Two microliters of serum extract were injected into a septum programmable injector in splitless mode. The septum programmable injector temperature was held at 150 °C for 0.5 min, then ramped up to 280 °C at a rate of 150 °C/min and held for 12 min, before dropping to 150 °C at a rate of 8 °C/min. The GC oven temperature program was held at 90 °C for 2 min followed by a temperature ramp of 18 °C/min to 200 °C, and a final temperature ramp of 5 °C/min to 300 °C with a 4.89-min hold. Extracts were analyzed using electron impact ionization and selected ion storage of the most abundant ion: TDCPP (99 *m/z*), TPP (326 *m/z*), TPP-D15 (341 *m/z*), and TCP (366 *m/z*) (**Table S3.1**). Analyte responses (area-under-the-curve) were used to quantify each analyte against an external calibration curve in matrix matched blanks and normalized to the recovery of the internal standard.

### 3.3.5 Statistical Analysis

Statistical analysis was performed using GraphPad Prism v5 (La Jolla, CA). Significant outliers were detected using the Grubbs' test ( $\alpha = 0.05$ ) and subsequently removed from the data set. Statistical significance between males and females (adult OPFR study) or between control and treated (maternal-fetal study) was determined using the student's t-test with Welch's correction where appropriate. Data are presented as mean  $\pm$  SEM. Significance was set at  $p \leq 0.05$ .



### 3.4 Results

#### 3.4.1 OPFR disposition in adult male and female mice

##### 3.4.1.1 *Serum*

In serum, TCP was detected at higher concentrations than TPP and TDCPP (**Fig. 3.2A**). Male (n=5) and female (n=5) mice had similar serum concentrations of OPFRs. In male serum, concentrations of TCP ( $3.88 \pm 0.17$  ng/mL) were higher than TPP ( $1.30 \pm 0.38$  ng/mL) and TDCPP ( $0.90 \pm 0.19$  ng/mL) after 3 mg/kg/day dosing (1 mg/kg of each OPFR). Similarly, female serum concentrations of TCP ( $3.04 \pm 0.76$  ng/mL) were higher than TPP ( $0.70 \pm 0.03$  ng/mL) and TDCPP ( $1.04 \pm 0.13$  ng/mL) were lower in female mice. Although TCP concentrations were similar in males and female mice, it is important to note the greater inter-animal variability among female mice compared to male mice.

##### 3.4.1.2 *Liver*

As in serum, TCP was detected at higher concentrations in the liver than TPP and TDCPP (**Fig. 3.2B**). The concentrations were similar between the sexes except for TCP where female mice had significantly higher concentrations of TCP than male mice (M:  $172.9 \pm 13.11$  ng/g, F:  $222.5 \pm 14.33$  ng/g,  $p < 0.05$ ). Levels of TDCPP in males and females were  $15.60 \pm 3.15$  ng/g and  $15.18 \pm 4.30$  ng/g, respectively. Male mice tended to have higher concentrations of TPP than females, but the difference was not statistically significant (M:  $70.04 \pm 15.81$  ng/g, F:  $41.56 \pm 4.30$ ).

#### 3.4.1.3 *Kidneys*

The compound-specific disposition of OPFRs differed from the serum and liver such that TPP concentrations were highest followed by TCP and TDCPP (**Fig. 3.2C**). Additionally, no statistical differences in OPFR accumulation were discerned between the sexes. Male mice had slightly higher liver OPFR concentrations than female mice, although there was greater inter-animal variation in male kidney TPP concentrations. In both sexes, TPP concentrations (M:  $59.58 \pm 18.55$  ng/g, F:  $52.63 \pm 4.64$  ng/g) exceeded that of TCP (M:  $33.80 \pm 2.56$  ng/g, F:  $27.36 \pm 4.48$  ng/g) followed by TDCPP (M:  $24.88 \pm 8.61$  ng/g, F:  $14.52 \pm 4.02$  ng/g).

#### 3.4.1.4 *Brain*

Like serum and liver, brain concentrations of TCP were higher than TPP and TDCPP, with the latter two compounds being similar in concentration (**Fig. 3.2D**). Additionally, no statistically significant differences in OPFR concentrations were observed between males and females. Brain TCP concentrations were higher in female mice ( $46.76 \pm 6.09$  ng/g) compared to male mice ( $36.94 \pm 7.42$  ng/g). TPP levels were  $15.22 \pm 3.45$  ng/g for males and  $13.60 \pm 1.06$  ng/g for females. TDCPP concentrations were reported at  $11.88 \pm 1.89$  ng/g and  $10.63 \pm 1.64$  ng/g for males and females, respectively.

#### 3.4.1.5 *Tissue/Serum Ratios*

Tissue/serum (T/S) ratios were calculated for liver, kidney, and brain to better understand how the OPFRs partition into tissues *in vivo* (**Table 3.3**). In males treated with a mixture of OPFRs for 28 days, the T/S ratios suggest that TDCPP preferentially distributes to the kidneys (28.4), followed by the liver (17.2), and then the brain (14.0). Females had a slightly different pattern of TDCPP distribution with liver (16.3) and kidneys (15.0) being comparable followed by the brain (9.8). In males, TPP partitioning was highest in the liver (73.5), followed by the kidneys (45.7), and the brain (14.0). By contrast, TPP distributed at a higher rate in the kidney (78.8) relative to the liver (62.2) and the brain (19.6) in females. In both sexes, TCP preferentially partitioned in the liver with greater accumulation in females (69.4) than males observed (44.8). Kidney and brain TCP partitioning were comparable between the kidneys and brain within males (K: 8.7, B: 9.8) and females (K: 16.0, B: 14.3). Interestingly, T/S ratios were higher in females than in males for all three tissues.

### 3.4.2 OPFR disposition in adult male and female mice

#### 3.4.2.1 Serum

As expected, serum concentrations were higher in the treated group of dams (n=2) than in the control group (n=1) (**Fig. 3.3A**). TDCPP, TPP, and TCP concentrations for treated mice were  $4.95 \pm 0.65$  ng/mL,  $1.65 \pm 0.45$  ng/mL, and  $7.80 \pm 0.70$  ng/mL, respectively. Baseline levels of TDCPP (3.50 ng/mL), TPP (0.10 ng/mL), and TCP (3.80 ng/mL) in the vehicle control mice suggest the possibility of incidental exposure potentially via bedding or chow diet.

#### 3.4.2.2 *Placenta*

TCP concentrations in the placenta were higher in OPFR-treated mice ( $n=4$ ,  $249.7 \pm 109$  ng/g) but not statistically different relative to the vehicle-treated control group ( $n=2$ ,  $83.75 \pm 29.1$  ng/g) (**Fig. 3.3B**). TDCPP concentrations were also higher in the treated group ( $9.08 \pm 3.98$  ng/g) but not statistically different than the control group ( $2.55 \pm 0.25$  ng/g) which were below the method detection limit of 3.0 ng/g. Interestingly, placental TPP concentrations were comparable between the control group ( $13.45 \pm 0.55$  ng/g) and the treated group ( $11.25 \pm 1.42$  ng/g) suggesting that incidental exposure to TPP may have occurred.

#### 3.4.2.3 *Fetus*

Fetal TDCPP concentrations fell below the method detection limit (3.0 ng/g) for both the control ( $1.65 \pm 0.25$  ng/g) and treatment groups ( $1.15 \pm 0.48$  ng/g) (**Fig. 3.3C**). Fetal TCP, however, was significantly greater in the OPFR-treated mice ( $21.90 \pm 1.19$  ng/g) versus the vehicle-treated control mice ( $1.80 \pm 0.20$  ng/g) indicating that TCP undergoes maternal-fetal transfer. Similar to the placenta, fetal TPP were comparable between the control ( $8.00 \pm 0.20$  ng/g) and treatment groups ( $6.28 \pm 2.04$  ng/g) suggesting possible incidental exposure.

### 3.5 Discussion

The disposition of three OPFRs (TDCPP, TPP, and TCP) in adult mice and pregnant dams were assessed following administration of a mixture for 28 days. The goals were (1) to quantify organ-specific distribution of the OPFRs, (2) identify potential sex differences in OPFR disposition, and (3) to determine whether OPFRs undergo placental transfer in mice.

OPFRs accumulated at higher levels in the liver and kidneys compared to the brain and serum following 28 days of daily exposure to a 3 mg/kg mixture of TDCPP, TPP, and TCP. This finding correlates well with a previous study where the highest concentrations of TDCPP were detected in male rat liver and kidneys between 3 and 168 h after administration of a single 14 mg/kg oral dose (Minegishi et al. 1988). Likewise, the para isomer of TCP (TpCP) accumulated the highest in male rat liver and kidneys between 24 and 168 h post administration of a single 89.6 mg/kg dose (Kurebayashi et al. 1985). Although the major organs of disposition were similar, the T/S ratios in the current study are higher than in previous studies. In this study, T/S ratios were determined at 1.5-2 h after the final dose. The reported TDCPP T/S ratios for male rat liver (2.18), kidney (1.05), and brain (0.18) at 3 h post administration were much lower than male mouse liver (17.2), kidney (28.4), and brain (14.0) T/S ratios (Minegishi et al. 1988). This discrepancy could be due to several factors including species (rat vs mouse), dosing (14 vs 3 mg/kg), administration (single vs repeated), and treatment differences (single OPFR vs mixture). Likewise, previously reported TpCP T/S ratios in male rats were lower

than those observed for TCP in male mice that, in addition to the aforementioned factors, may be due to differences in sampling time (24 vs 1.5-2 h) and chemical composition (TpCP is a component of TCP) (Kurebayashi et al. 1985). Despite the differences in T/S ratios, it is clear that the liver, kidneys, and brain are sites of preferential OPFR disposition in rodents.

That the liver and kidneys are major sites of OPFR accumulation is not surprising given their role in xenobiotic metabolism and excretion. These processes are likely to have influenced the tissue concentrations observed for TDCPP, TPP, and TCP. In general, TCP was detected at higher concentrations than TPP and TDCPP in all tissues except in the kidneys where TPP was highest followed by TCP and TDCPP. OPFR toxicokinetic studies are limited, but a study in goldfish and killifish showed that chlorinated OPFRs (e.g. TDCPP) have rapid elimination rates compared to aryl OPFRs (e.g. TPP and, by extension, TCP) (Sasaki et al. 1981). The results in this study suggest that this may also be true in mice. However, slight differences in OPFR concentrations in the dosing solution may also account for the deviation. Although the dosing solution contained equal amounts of the OPFRs (1 mg/kg each, 3 mg/kg total), the molar concentrations, which are based on molecular weight, are inherently different as TDCPP (2.3 nM) is lower than TCP (2.7 nM), and TPP (3.1 nM). In addition to metabolism, it is possible that the differences in molar concentrations may contribute to the lower concentrations detected for TDCPP relative to TCP and TPP. By contrast, slight variations in the molar concentrations may not have influenced tissue TCP and TPP concentrations because TCP's molar concentration was slightly lower than TPP's. TCP

concentrations, however, were consistently higher than TPP in all tissues except for the kidney. Further studies investigating OPFR toxicokinetics in rodents would be critical to evaluating the effect of metabolism on OPFR accumulation. TPP was measured above background throughout the experiments, demonstrating its ubiquitous nature in the environment. Indeed, its environmental pervasiveness has been demonstrated in several studies (Ali et al. 2012a; Ali et al. 2012b; Cristale et al. 2018; Hoffman et al. 2015; van der Veen and de Boer 2012).

The current study is the first to investigate sex as a biological variable in the disposition of OPFRs in mice. Minor differences in OPFR accumulation and disposition were observed between male and female mice that were tissue- and compound-specific. Serum OPFR levels were similar between the sexes. In the liver, comparable levels of TDCPP were observed for males and females, however, males accumulated higher concentrations of TPP whereas females accumulated significantly higher levels of TCP. In the kidneys, males had greater OPFR accumulation than females. In the brain, TDCPP concentrations were similar for males and females, but higher TPP and TCP concentrations were observed in males and females, respectively. The observed sex differences in OPFR accumulation may be influenced by the sex-divergent expression of cytochrome P450 (CYP), a superfamily of isozymes responsible for the biotransformation of a variety of xenobiotic and endobiotic compounds. CYPs are thought to be the primary enzymes responsible for OPFR metabolism (Hou et al. 2016). In male mice, 52% of all 78 Cyp mRNA from the Cyp1-4 families were expressed in the liver followed by 10% in the kidneys and less than 4% in the brain

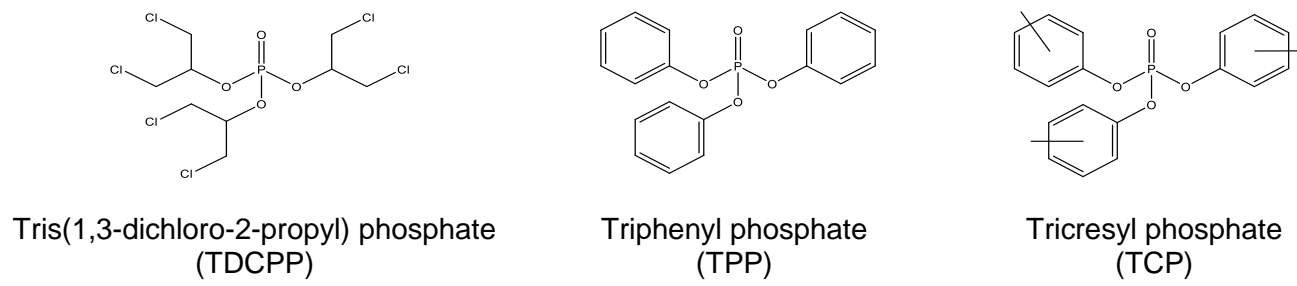
(Renaud et al. 2011). By contrast, female mice had 7% greater liver predominant Cyps, but 1% fewer kidneys predominant. Additionally, of the 29 Cyps for which sex differences were apparent, 24 were expressed higher in females than males. Of interest, female mice have significantly higher Cyp1a2 mRNA and slightly higher Cyp2e1 than male mice. Both CYP1A2 and 2E1 have been implicated in TPP metabolism. However, higher mRNA levels do not indicate greater protein concentration or increased enzymatic activity. Therefore, it is presently impossible to determine whether CYP activity is sex-divergent and could in turn influence OPFR disposition.

The final objective of this study was to determine whether OPFRs undergo placental transfer. TCP and TDCPP concentrations in the placenta were greater in the treated group but were not statistically different than the control group. In fetal tissue, TCP accumulated significantly greater concentrations in the OPFR-treated group than the vehicle-treated control group. Taken together, the data suggest that TCP crosses the placenta into the mouse fetus whereas TDCPP does not. A study in humans detected TCP, TDCPP, and TPP in 84, 44, and 86% of placentas (n=50), respectively, supports the current findings (Ding et al. 2016). TPP was detected in comparable levels in the placental and fetal tissue of control and treated mice suggesting that mice received unintended exposures through their bedding, diet, and/or cages. None of these materials were tested for TPP in this study. Additional studies in which unintended exposure to TPP is closely monitored may be necessary, but the potential for TPP to undergo placental transfer warrants further investigation. Although TPP has been detected in human and rat placentas,

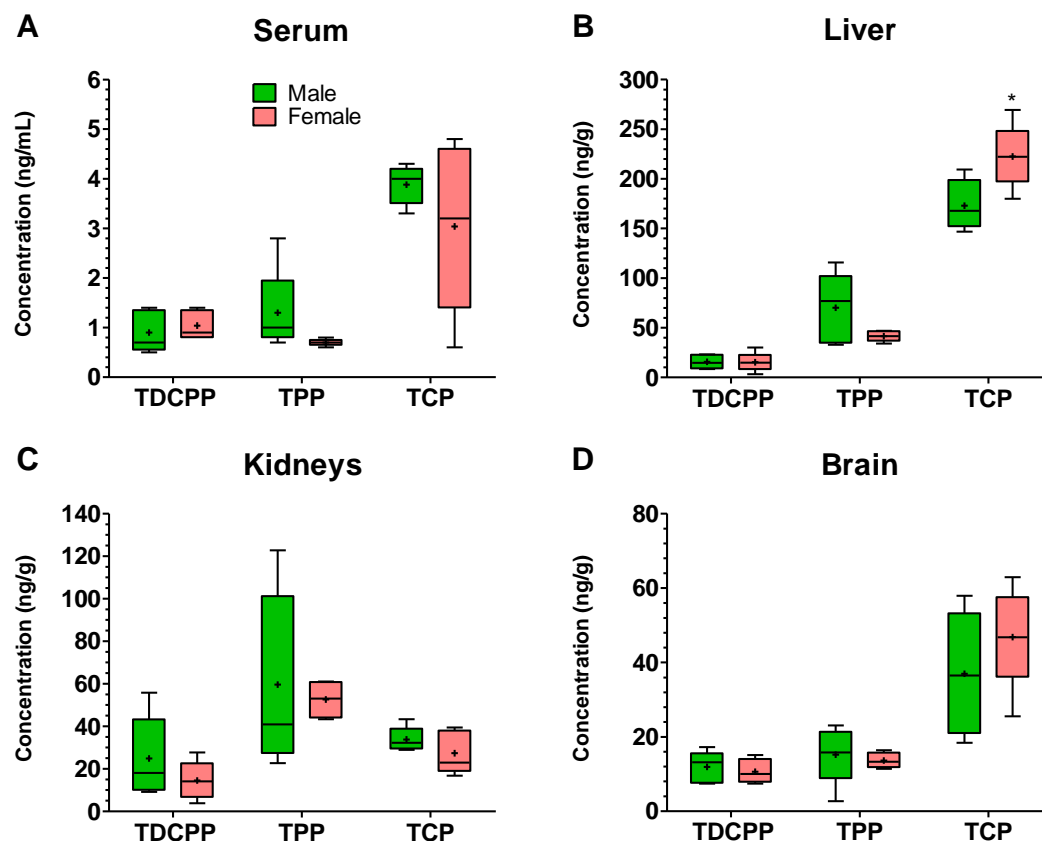


it has not previously been detected in rat fetuses (Baldwin et al. 2017; Ding et al. 2016). In the rat studies, dams were given 1000 µg (approx. 3.3 mg/kg) of FM 550 daily during GDs 9-18. Method detection limits for fetal TPP in Baldwin et al. were similar to that of the current study (3.1 vs 3.0 ng/g). However, dosing differences may account for the discrepancy. TPP makes up 19.8% of FM 550 (Phillips et al. 2017). Thus, a 3.3 mg/kg dose of FM 550 translates to approximately 0.65 mg/kg of TPP, which is less than the dose of TPP used in the current study (1 mg/kg). Alternatively, it may be possible that TPP undergoes *in utero* transfer in mice but not rats. However, further studies would be necessary to evaluate potential species differences.

In conclusion, greater T/S ratios indicate that the liver and kidneys are predominant sites of OPFR disposition with the brain being a minor site by comparison. Additionally, modest differences in OPFR accumulation between males and females were observed but were largely insignificant. Finally, the data suggest that maternal transfer of TCP, and possibly TPP, can occur and therefore may pose a risk to the developing fetus.



**Figure 3.1.** Names, acronyms, and structures of the OPFRs used in this study



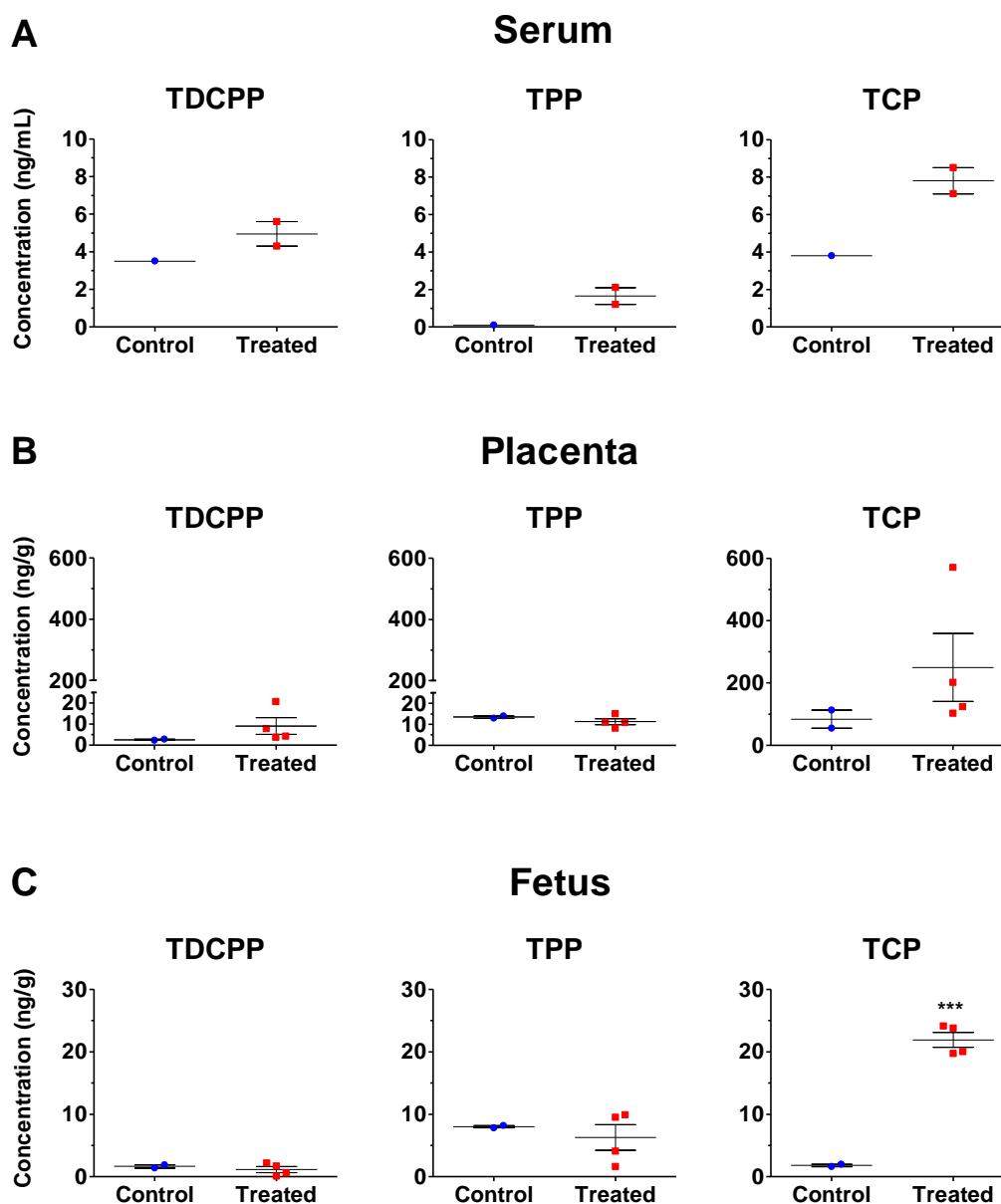
**Figure 3.2.** OPFR disposition in adult male and female mice

OPFR concentrations in serum (A), liver (B), kidneys (C) and brain (D) of male (n=5) and female (n=5) mice following a 4-week exposure to a 3 mg/kg mixture of TDCPP, TPP, and TCP. The center box is bounded by the first and third quartiles, the horizontal black line in the box depicts the median, the '+' indicates the mean, and the capped vertical line represents the range of the data. Data were analyzed by a student's t-test with Welch's correction where appropriate (\*p<0.05, \*\*p<0.01, \*\*\*p<0.001). Data are presented as mean  $\pm$  SEM (n = 4). Asterisks (\*) represent statistically significant differences (p < 0.05) compared to control cells.

**Table 3.1.** Tissue/serum partitioning of OPFRs in male and female mice

|               | Liver | Kidney | Brain |
|---------------|-------|--------|-------|
| <b>TDCPP</b>  |       |        |       |
| <i>Male</i>   | 17.2  | 28.4   | 14.0  |
| <i>Female</i> | 16.3  | 15.0   | 9.8   |
| <b>TPP</b>    |       |        |       |
| <i>Male</i>   | 73.5  | 45.7   | 14.0  |
| <i>Female</i> | 62.2  | 78.8   | 19.6  |
| <b>TCP</b>    |       |        |       |
| <i>Male</i>   | 44.8  | 8.7    | 9.8   |
| <i>Female</i> | 69.4  | 16.0   | 14.3  |

OPFR partitioning in male (n=5) and female (n=5) mice following a 4-week exposure to a 3 mg/kg mixture of TDCPP, TPP, and TCP.



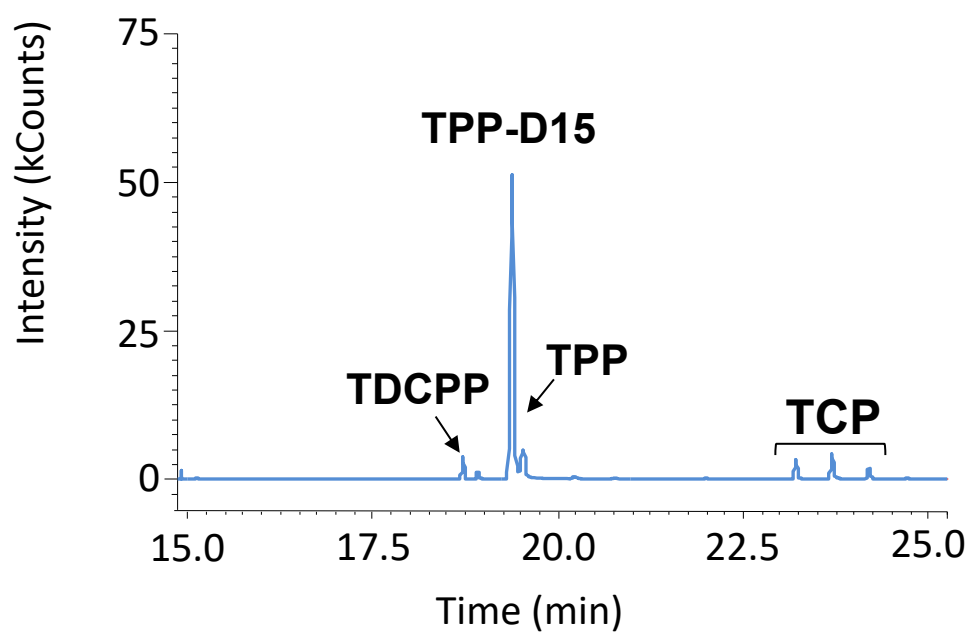
**Figure 3.3.** Maternal-fetal transfer of OPFRs *in utero*

OPFR concentrations in serum (**A**), placenta (**B**), and fetus (**C**) of dams exposed to a 3 mg/kg mixture of TDCPP, TPP, and TCP from GD 9 to GD 16-18. Each data point represents data from a single dam (n=2 for the control group, n=4 for the treatment group). One control serum sample and two treated serum samples were lost resulting in an n=1 and an n=2 for the control and treatment groups, respectively. Placentas (n=7-10 per dam) and fetuses (n=7-10 per dam) from a single dam were pooled for analysis. Data are presented as mean  $\pm$  SEM. Data were analyzed by a student's t-test (\*p<0.05, \*\*p<0.01, \*\*\*p<0.001).

**Table S3.1.** Molecular weights (MW), retention times (RT), and quantitation ions (Q) for each OPFR.

| OPFR                 | MW<br>(g/mol) | RT<br>(min) | Q ions<br>(m/z) |
|----------------------|---------------|-------------|-----------------|
| TDCPP                | 428           | 18.71       | 99              |
| TPP-D15 <sup>a</sup> | 341           | 19.38       | 341             |
| TPP                  | 326           | 19.51       | 326             |
| TCP                  | 368           | 23.20       | 368             |

<sup>a</sup> TPP-D15 was used as an internal standard.



**Figure S3.1.** Representative gas chromatogram of the OPFRs

**CHAPTER 4: ASSESSMENT OF ORGANOPHOSPHATE FLAME  
RETARDANT INTERACTIONS WITH THE MDR1 TRANSPORTER *IN VITRO*  
AND *IN VIVO***

Stephanie M. Marco<sup>1</sup>, Xia Wen<sup>1</sup>, Ill Yang<sup>2</sup>, Jason R. Richardson<sup>3</sup>, Lauren M.  
Aleksunes<sup>1</sup>, Brian T. Buckley<sup>2</sup>

<sup>1</sup> Department of Pharmacology and Toxicology, Rutgers University, Piscataway,  
NJ

<sup>2</sup> Environmental and Occupational Health Sciences Institute, Rutgers University,  
Piscataway, NJ

<sup>3</sup> Robert Stempel School of Public Health and Social Work, Florida International  
University, Miami, FL



#### 4.1 Abstract

Organophosphate flame retardants (OPFRs) are a class of chemicals applied to clothing, plastics, building materials, electronics, and furniture to reduce the flammability of commercial products. Over the past 15 years, global use of OPFRs has increased significantly, as they replace other persistent bioaccumulative compounds such as polybrominated diphenyl ethers. Biomonitoring studies in humans indicate that human exposure is widespread. The emergence of data indicating that OPFRs disrupt the reproductive, endocrine, and nervous systems *in vitro* and *in vivo* are concerning. There are several mechanisms by which tissue toxicities can be reduced including active efflux of chemicals. The multidrug resistance protein 1 (MDR1) is one such efflux transporter that can remove substrates from cells using energy generated from the hydrolysis of ATP. The purpose of this study was to test whether the OPFRs tris(1,3-dichloroisopropyl) phosphate (TDCPP), triphenyl phosphate (TPP), and tricresyl phosphate (TCP) are substrates and/or inhibitors of the MDR1 transporter. HEK293 cells expressing an empty vector or the human MDR1 gene were treated with TCP, TDCPP, and TPP for 72 h with cell viability assessed using the Alamar Blue assay. TCP, TDCPP, and TPP displayed similar concentration-dependent reductions in cell viability between empty vector- and MDR1-expressing cell lines. Additionally, none of the tested OPFRs could alter the efflux of the MDR1 substrate, rhodamine, from MDR1-expressing cells. The role of MDR1 in regulating the disposition of OPFRs was investigated in wild-type (WT) and *Mdr1a/1b*-null mice (KO). Notably, KO mice had significantly higher levels of TPP in the serum and brain (S:  $32.80 \pm 4.69$

ng/mL, WT: B:  $54.93 \pm 2.60$  ng/g) compared to WT mice (S:  $10.13 \pm 3.40$  ng/mL, B:  $25.0 \pm 3.09$  ng/g), suggesting that MDR1 may be critical to protecting the brain from TPP exposure ( $p < 0.001$ ). Taken together, these data suggest that MDR1 does not confer resistance to OPFR-induced cell death nor do these chemicals inhibit MDR1 function *in vitro*, but that MDR1 may influence TPP disposition *in vivo*.

**Abbreviations**

ABC, ATP-binding cassette; BBB, blood-brain barrier; DMSO, dimethyl sulfoxide; EV, empty vector; GC-MS, gas chromatography-mass spectrometry; IP, intraperitoneal; KO, knockout; OPFRs, organophosphate flame retardants; PBDEs, polybrominated diphenyl ethers; TBP, tributyl phosphate; TBOEP, tris(2-butoxyethyl) phosphate; TCP, tricresyl phosphate; TCEP, tris(2-chloroethyl) phosphate; TDCPP, tris(1,3-dichloro-2-propyl) phosphate; ToCP, tri-o-cresyl phosphate; TPP, triphenyl phosphate; TPP-D15, deuterated triphenyl phosphate; T/S, tissue/serum ratio; WT, wild-type

## 4.2 Introduction

Flame retardants are chemical additives that are designed to prevent or delay the spread of fire when applied to various household and industrial products including plastics, construction material, textiles, furniture, and electronics. The use of flame retardants in manufacturing began in the 1970s to meet federal and local flammability standards. Polybrominated diphenyl ethers (PBDEs) were the major class of flame retardants used up until the mid-2000s when concerns over their environmental persistence and toxicity created a demand for alternative chemicals. As a result, PBDEs were largely replaced by organophosphate flame retardants (OPFRs).

Since the phase-out of PBDEs, the use and production of OPFRs have sharply increased in the U.S. and around the world. Between 1992 and 2007, worldwide OPFR usage increased from approximately 100,000 tons per year to 341,000 tons per year (Greaves and Letcher 2016). Furthermore, global usage hit 500,000 tons in 2011 and was expected to reach 680,000 tons by 2015 (Hou et al. 2016). Because OPFRs are not chemically bound to materials, they can readily leach into the environment. Indeed, numerous studies have detected OPFRs in sediment/soil, water, biota, indoor air, and dust (Greaves and Letcher 2016; van der Veen and de Boer 2012; Wei et al. 2015). Moreover, several biomonitoring studies have indicated that humans are routinely exposed to OPFRs (Castorina et al. 2017a; Castorina et al. 2017b; Chen et al. 2018; He et al. 2018; Hoffman et al. 2017a; Hoffman et al. 2017b; Ospina et al. 2018; Thomas et al. 2017).

In the previous chapter, it was shown that the liver, kidneys, and brain are sites of preferential OPFR disposition in mice and potential targets of OPFR-induced toxicity. Studies in animals have shown that OPFR exposure can interfere with hepatic and neurological processes. Triphenyl phosphate (TPP), tri-*o*-cresyl phosphate (ToCP), and tris(2-chloroethyl) phosphate (TCEP), have been shown to affect antioxidant systems by modulating levels of malondialdehyde and activity of glutathione *S*-transferase, superoxide dismutase, catalase, and glutathione peroxidase in mice (Chen et al. 2015a; Xu et al. 2016). TDCPP, TPP, and tricresyl phosphate (TCP) were also shown to activate the CAR and PXR nuclear receptors in mice treated daily with a mixture of the three OPFRs for 28 days (Krumm et al., 2017). Furthermore, TPP has been shown to inhibit carboxylesterase activity in mouse liver S9 fractions (Chapter 2 of this Dissertation) and in HEK293T cells (Morris et al. 2014). Tris(1,3-dichloro-2-propyl) phosphate (TDCPP) has been shown to reduce dopamine and serotonin levels in adult female zebrafish exposed developmentally (2 hpf) at low concentrations (4, 20, and 100 µg/L) (Wang et al. 2015b). A study investigating neurodevelopmental outcomes in children exposed to OPFRs *in utero* showed that higher maternal exposure to TPP and total OPFR concentrations were associated with decreased IQ (-2.9 points for TPP; -3.8 points for total OPFR) and working memory (-3.9 points for DPP; -4.6 points for total OPFR) in children (n=310) for each 10-fold increase in prenatal urinary metabolite concentration (Castorina et al., 2017a). These data underscore the vulnerability of the liver and brain, in particular, to OPFR exposure because of their preferential accumulation in these organs.

The disposition of endo- and xenobiotics within the body can be influenced by transporters. One of the major transporter superfamilies in mammals is the ATP-binding cassette (ABC) transporter family. ABC transporters use primary active transport to function as efflux pumps that remove xenobiotics to limit intestinal absorption, blood-brain barrier (BBB) penetration, facilitate biliary and renal excretion, and protect against xenobiotic exposure (Klaassen and Aleksunes 2010; Mao and Unadkat 2015; Stieger and Gao 2015). The multidrug resistance protein 1 (MDR1/*ABCB1*) is one such member of the ABC family of efflux transporters and is localized on apical membranes of numerous tissues including the luminal membrane of enterocytes in the intestines, endothelial cells of brain microcapillaries, the brush border membrane of renal proximal tubules, and the canalicular membrane of hepatocytes. Studies investigating the role of transporters in OPFR disposition would help to understand how these chemicals distribute within the body.

Presently, there is only one study that has investigated the potential role of MDR1 in OPFR disposition. Adult Asian clams (*C. fluminea*) exposed to tris(2-butoxyethyl) phosphate (TBOEP) and tributyl phosphate (TBP) at 20, 299, and 2000 µg/L for 28 days displayed altered *abcb1* (gene encoding MDR1) mRNA levels (Yan et al. 2017). TBP upregulated *abcb1* mRNA levels at 20 µg/L but downregulated expression at 200 µg/L and 2000 µg/L. By contrast, TBOEP upregulated *abcb1* at all concentrations tested. These results suggest that TBP (20 µg/L) and TBOEP (20, 200, and 2000 µg/L) may activate MDR1 thereby mediating xenobiotic efflux in clams. Moreover, TBP at high concentrations (200

and 2000 µg/L) may inactivate MDR1-mediated efflux. In order to gain a better understanding of the potential interactions of OPFRs and ABC transporters, further studies must be conducted, especially in mammalian models.

The objectives of this study were to (1) determine whether TDCPP, TCP, and TPP act as substrates and/or inhibitors of MDR1 *in vitro* and (2) characterize the role of MDR1 in regulating the disposition of OPFRs *in vivo* using Mdr1a/1b knockout mice.

## 4.3 Materials and Methods

### 4.3.1 Chemicals

Dimethyl sulfoxide (DMSO), resazurin, rhodamine 123, TPP, and TDCPP were purchased from Sigma-Aldrich (St. Louis, MO). PSC833 was purchased from Xenotech (Lenexa, KS). TCP was purchased from AccuStandard (New Haven, Connecticut). Ultra-residue analyzed toluene was purchased from Thermo Fisher Scientific (Waltham, Massachusetts). TPP-D15 was purchased from Cambridge Isotope Laboratories (Tewksbury, Massachusetts).

### 4.3.2 Cell culture

Human embryonic kidney 293 cells (HEK293) were purchased from the American Type Culture Collection (Rockville, MD) and maintained in Dulbecco's Modified Eagle Media (DMEM; Invitrogen, Carlsbad, CA). Cells were stably-transfected with the human MDR1 gene or empty vector (EV) plasmids as described in (Wen et al. 2014). Cells were cultured in a humidified incubator at 37°C and 5% CO<sub>2</sub>.

### 4.3.3 Cell Viability Assay

Cell viability was assessed using an indirect approach to determine whether TDCPP, TCP, and TPP are potential substrates of the MDR1 transporter. HEK293-empty vector (EV) and MDR1-transfected (MDR1) cells were seeded at 8,000 cells/well in 96-well plates and allowed to adhere overnight. EV and MDR1 cells were incubated for 72 h with either TPP, TDCPP, or TPP (5-200 µM) or vehicle



(DMSO, 0.1%) in media. After the incubation period, cell viability was assessed using the Alamar Blue assay, which works by redox cycling. Viable cells reduce resazurin to resorufin, a fluorescent red compound that can be detected using a spectrometer. Media was aspirated from the cells and replaced with 100  $\mu$ L naïve media containing Alamar Blue (0.1 mg/mL resazurin) for 4 h. Fluorescence was then measured using Ex/Em: 535/580 nm. These values were normalized to the vehicle control group and used to calculate LC<sub>50</sub> values for each OPFR in EV and MDR1 cells.

#### 4.3.4 MDR1 Transporter Assay

HEK-EV and MDR1 cells were seeded in a 96-well round bottom plate at a density of 400,000 cells/well. The plate was centrifuged (500 x *g*, 5 min, 5°C), media was removed, and the cells were washed using ice-cold PBS. Cells were then treated with 100  $\mu$ L of treatment media containing rhodamine 123 (5  $\mu$ M), an established fluorescent MDR1 substrate, in the presence or absence of the MDR1-specific inhibitor, PSC833 (2  $\mu$ M) (Bircsak et al. 2013). The plate was incubated at 37°C for 30 min, during which rhodamine 123 was taken up into the MDR1 cells. Cells were then centrifuged and washed with ice-cold PBS. Cells were then re-suspended in substrate-free growth medium with or without PSC833 and incubated an additional 1 h at 37°C, to allow rhodamine 123 to efflux from the cells. Cells were then washed and re-suspended in 50  $\mu$ L PBS. Quantification of intracellular fluorescence was performed using a Cellometer Vision automated cell

counter (Nexcelom Bioscience, Lawrence, MA) fitted with the VB-595-502 filter cube (Ex/Em: 525/595 nm). Fluorescence was normalized for cell size.

#### 4.3.5 Animal Care

All animal procedures were completed in compliance with institutional guidelines based on National Institutes of Health standards and were performed with Institutional Animal Care and Use Committee approval (Protocol 09-037) at Rutgers University. Wild-type (WT) C57BL/6 mice were purchased from Charles River (Wilmington, MA). *Mdr1a/1b* knockout (KO) mice were purchased from Taconic Laboratories (Hudson, NY) and backcrossed to the C57BL/6 background until 99% congenic. The congenic analysis was performed by the Bionomics Research and Technology Core at Rutgers University (New Brunswick, NJ). Mice were provided with food and water *ad libitum*.

#### 4.3.6 Dosing

The *in vivo* dosing solutions were prepared as follows. For the stock solution, 100 mg of each OPFR were dissolved in 1 mL of acetone. For the working solution, 100  $\mu$ L of the stock solution was added to 10 mL of sesame oil and mixed over a stir plate for 48 h with venting. Mice were separated into four different dosing groups: vehicle (n=2), TDCPP (n=4-5 per genotype), TPP (n=4-5 per genotype), and TCP (n=4-5 per genotype). Vehicle mice were injected with 5 mL/kg of sesame oil IP. OPFR-treated mice were injected with 10 mg/kg of TDCPP, TPP, or TCP at a dosing volume of 5 mL/kg. After 4 h, mice were decapitated (no anesthesia) and

trunk blood was collected and placed on ice. Brain, liver, and kidneys were collected, weighed, and snap frozen in liquid nitrogen. Serum was generated by centrifuging blood at 2000 x *g* and 4 °C for 10 min. Tissues and serum were stored at -80 °C until analysis.

#### 4.3.7 Sample Preparation

Brain, liver, and kidney tissue were homogenized in 50 mM Tris buffer. Tissue homogenates and serum samples were spiked with 20 ng/mL of the internal standard (TPP-D15) for recovery correction. After spiking, the samples were vortexed for 1 min followed by addition of toluene (25-50 µL for serum, 100 µL for tissue). Samples were then vortexed for 2 min and allowed to stand for 5 min. Finally, samples were centrifuged at 9000 x *g* at 4 °C for 10 min, and the organic layer was collected for analysis by gas chromatography-mass spectrometry (GC-MS).

#### 4.3.8 Instrumental Analysis

Sample extracts were analyzed using an Agilent 7890B GC/240 ion trap MS. Chromatographic separation of the analytes was achieved using an Agilent DB-*XLB* microcapillary column (30 m long x 180 µm internal diameter x 0.18 µm film thickness; Santa Clara, California) (**Fig.S4.1**). Two microliters of serum extract were injected into a septum programmable injector in splitless mode. The septum programmable injector temperature was held at 150 °C for 0.5 min, then ramped up to 280 °C at a rate of 150 °C/min and held for 12 min, before dropping to 150°C

at a rate of 8 °C/min. The GC oven temperature program was held at 90 °C for 2 min followed by a temperature ramp of 18 °C/min to 200 °C, and a final temperature ramp of 5 °C/min to 300 °C with a 4.89-min hold. Extracts were analyzed using electron impact ionization and selected ion storage of the most abundant ion: TDCPP (99 m/z), TPP (326 m/z), TPP-D15 (341 m/z), and TCP (366 m/z) (**Table S4.1**). Analyte responses (area-under-the-curve) were used to quantify each analyte against an external calibration curve in matrix matched blanks and normalized to the recovery of the internal standard.

#### 4.3.9 Statistical Analysis

Statistical analysis was performed using GraphPad Prism v5 (La Jolla, CA). LC<sub>50</sub>s for the OPFRs in EV and MDR1-expressing cells were calculated using a normalized, variable hill slope, dose-dependent inhibition regression. MDR1 function data were analyzed by one-way ANOVA with Dunnett's post-test. Differences in OPFR disposition in WT and Mdr1a/1b KO mice were determined using the student's t-test with Welch's correction where appropriate. Data are presented as mean ± SEM. Significance was set at  $p \leq 0.05$ .

## 4.4 Results

### 4.4.1 Cell Viability

For the *in vitro* studies, HEK293 cells were stably-transfected with the human MDR1 gene or empty vector (EV) plasmid and the presence of MDR1 protein was previously validated (**Fig. S4.2**). Functional activity of the expressed MDR1 protein in this model was previously validated using doxorubicin, a well-known MDR1 substrate (**Fig. S4.3**). MDR1 mediated doxorubicin-induced lethality as indicated by a 4-fold increase in the concentration required for 50% cell lethality ( $LC_{50}$ ) compared to the EV control cells.

Cell viability was assessed in EV and MDR1-expressing cells treated with TDCPP, TPP, or TCP (0-200  $\mu$ M). All three OPFRs had concentration-dependent loss of cell viability after 72 h (**Fig. 4.2**). The  $LC_{50}$  values for TDCPP, TPP, and TCP were comparable in EV and MDR1-expressing cell lines. For TDCPP, the EV and MDR1  $LC_{50}$  values were 87.8  $\mu$ M and 81.4  $\mu$ M, respectively (**Fig. 4.2 A**). EV cells treated with TPP had an  $LC_{50}$  value of 63.2  $\mu$ M whereas MDR1 cells had an  $LC_{50}$  value of 66.2  $\mu$ M (**Fig. 4.2 B**). TCP-treated EV and MDR1 cells exhibited  $LC_{50}$  values of 27.5 and 27.4  $\mu$ M, respectively (**Fig. 4.2 C**).

### 4.4.2 MDR1 Function

To determine whether OPFRs inhibit MDR1 function, EV- and MDR1-expressing cell lines were treated with either the positive control MDR1 inhibitor PSC833 (PSC, 2  $\mu$ M) or one of the OPFRs (1-100  $\mu$ M) and co-incubated with the

fluorescent MDR1 substrate, rhodamine (**Fig. 4.3**). As expected, EV control cells incubated with rhodamine alone exhibited 4-6 times higher fluorescent intensity compared to the MDR1-expressing cells incubated with rhodamine. The reduced fluorescent signal in the MDR1-expressing cells indicated that active efflux of rhodamine was occurring. The co-incubation of rhodamine with PSC in MDR1-expressing cells resulted in a significant increase in rhodamine fluorescent intensity similar to the extent observed in EV cells. Following treatment of MDR1-expressing cell lines with increasing concentrations of TDCPP, TPP, or TCP, the intensity of rhodamine fluorescence was unchanged and similar to MDR1 cells incubated with rhodamine only.

#### 4.4.3 Role of MDR1 in OPFR Disposition

Male WT (n=5 per OPFR) and MDR1a/1b KO (n=4 per OPFR) mice were administered a 10 mg/kg IP dose of a single OPFR (TDCPP, TPP, or TCP) and concentrations in serum, liver, brain, and kidney determined by GC-MS after 4 h (**Fig. 4.4**).

##### 4.4.3.1 *Serum*

In serum, OPFR concentrations varied by compound and genotype (**Fig. 4.4 A**). Overall, serum TDCPP and TPP levels were greater than TCP regardless of genotype. In the KO mice, TPP serum concentrations were significantly higher than in the WT mice (KO:  $32.80 \pm 4.69$  ng/mL, WT:  $10.13 \pm 3.40$  ng/mL) at  $p < 0.001$ . TDCPP concentrations were slightly higher in the WT mice ( $27.28 \pm 4.58$

ng/mL) compared to the KOs ( $18.48 \pm 6.10$  ng/mL). Serum TCP levels were comparable between the WT ( $2.10 \pm 0.58$  ng/mL) and the KO groups ( $3.28 \pm 1.1$  ng/mL).

#### 4.4.3.2 *Liver*

TCP accumulated at greater concentrations in the liver relative to TDCPP and TPP, which were similar. Liver OPFR concentrations in the KO mice were approximately double the concentrations in the WT mice (**Fig. 4.4 B**). TCP levels in WT mice ( $340.4 \pm 57.1$  ng/g) were lower than in KO mice ( $660.3 \pm 262$  ng/g) although there was greater inter-animal variability within the KO mice group. Like TCP, greater TDCPP accumulation was observed in KO mice ( $148.8 \pm 47.9$  ng/g) compared to the WTs ( $78.24 \pm 18.5$  ng/g). Additionally, TPP concentrations in the WT mice ( $67.56 \pm 25.2$  ng/g) were approximately half of the concentrations in the KO mice ( $133.6 \pm 32.7$  ng/g).

#### 4.4.3.3 *Brain*

TCP levels were higher than TDCPP and TPP in the brain. As in the liver, the KO mice exhibited greater OPFR accumulation in the brain relative to the WT mice (**Fig. 4.4 C**). However, a significant increase in TPP accumulation was observed in the KO group ( $54.93 \pm 2.60$  ng/g) compared to the WT group ( $25.00 \pm 3.09$  ng/g). Although not statistically significant, TCP levels were also higher in KO mice than in WT mice (KO:  $94.05 \pm 9.51$  ng/g, WT:  $57.24 \pm 20.6$  ng/g). Additionally, greater variability in TCP concentrations within the WT group was observed. Like TCP,

greater TDCPP accumulation was observed in the KO mice ( $34.33 \pm 11.7$  ng/g) compared to the WT mice ( $29.20 \pm 7.32$  ng/g).

#### 4.4.3.4 Kidneys

TPP accumulated at higher concentrations than TCP and TDCPP in the kidneys. The kidneys of WT mice exhibited higher OPFR concentrations than in KO mice (**Fig. S4.4**). TDCPP levels in the WT and KO groups were  $466.0 \pm 161$  ng/g and  $328.3 \pm 131$  ng/g, respectively (**Fig. S4.4 A**). Additionally, both groups exhibited variable levels ranging from 27.4 to 884.8 ng/g for the WT mice and 35.6 to 584.2 ng/g for the KOs. Kidney TCP levels were  $96.06 \pm 10.7$  ng/g in the WT group and  $68.75 \pm 11.6$  ng/g (**Fig. S4.4 C**). TPP concentrations were comparable between the WT ( $1140 \pm 481$  ng/g) and KO groups ( $932.0 \pm 25.9$  ng/g) (**Fig. S4.4 B**). However, an uncharacteristically elevated level of TPP was observed in the vehicle control animals ( $3190 \pm 1442$  ng/g) suggesting that they were contaminated during sample collection and/or preparation for analysis. Therefore, these results should be interpreted cautiously.

#### 4.4.3.5 Tissue/Serum Ratios

Tissue/serum (T/S) ratios of OPFRs in the liver and brain were calculated for the WT and KO mice to better understand how MDR1 influences OPFR partitioning *in vivo* (**Table 4.1**). The overall trend of OPFR disposition was the same in WT and KO mice with TDCPP and TPP preferentially distributing in kidneys followed by the liver and brain and TCP preferentially distributing in the liver followed by the



kidneys and brain. In the liver, TDCPP partitioning was greater in the KO mice (8.3) compared to the WT mice (2.7). Additionally, TPP distribution rates were slightly higher in the KO mice (4.1) relative to the WT mice (3.9). Likewise, TCP partitioning was slightly greater in KO mice (271.3) than WT mice (265.0). In the brain, TDCPP distribution was comparable for WT (1.0) and KO (1.8) mice. However, the TPP T/S ratio was greater in WT mice than KO mice (WT: 3.3, KO: 1.8). Additionally, TCP partitioning was slightly higher in the WT mice (26.3) relative to the KO mice (22.8). In the kidneys, TDCPP T/S ratios were similar for the WT and KO groups at 14.6 and 15.2, respectively (**Table S4.2**). TCP disposition was higher in the WT mice (82.8) relative to the KO mice (65.3). Finally, TPP partitioning appeared to be greatest in the WT mice (WT: 72.2, KO: 30.0). However, the ratios for TPP should be interpreted cautiously due to an aberrant background level of TPP observed in the control mice.

## 4.5 Discussion

The interaction of OPFRs with MDR1 was assessed in cellular and mammalian models. The goals of this study were to (1) determine whether TDCPP, TCP, and TPP act as substrates and/or inhibitors of MDR1 *in vitro* and (2) characterize the role of MDR1 in OPFR disposition *in vivo*.

In the first study, the ability of OPFRs to alter the viability of HEK293 cells expressing EV or MDR1 was determined as an indirect method of substrate identification. Previously, doxorubicin, a well-known MDR1 substrate, has been shown to mediate doxorubicin-induced lethality as indicated by a 4-fold increase in the concentration required for 50% cell lethality ( $LC_{50}$ ) compared to the EV control cells. By contrast, MDR1 does not confer resistance to OPFR-induced lethality. The  $LC_{50}$  values for TDCPP, TPP, and TCP were relatively unchanged between the EV and MDR1-expressing cell lines suggesting that the OPFRs may not be substrates of human MDR1.

The results of the functional inhibition of MDR1 study suggested that the OPFRs do not inhibit MDR1 function. As expected, the EV control cells had elevated levels of fluorescence intensity because rhodamine easily accumulates in the cells and cannot be effluxed due to the absence of MDR1. Furthermore, in MDR1-expressing cells, fluorescent levels were decreased relative to the control because rhodamine was removed from the cells by MDR1. When PSC was co-incubated with rhodamine in the MDR1-expressing cells, the intracellular fluorescent intensity increased significantly and was comparable to EV control cells incubated with

rhodamine. This was expected because PSC blocks the MDR1-mediated efflux of rhodamine. Following treatment of MDR1-expressing cell lines with TDCPP, TPP, or TCP and co-incubation with rhodamine, fluorescent intensity levels were similar to the MDR1 cells incubated with rhodamine only. In summary, OPFRs do not inhibit MDR1 efflux of rhodamine. However, it should be noted with caution that MDR1 possesses multiple binding sites in its internal cavity. Thus, follow-up studies should assess the ability of OPFRs to inhibit the efflux of additional MDR1 substrates.

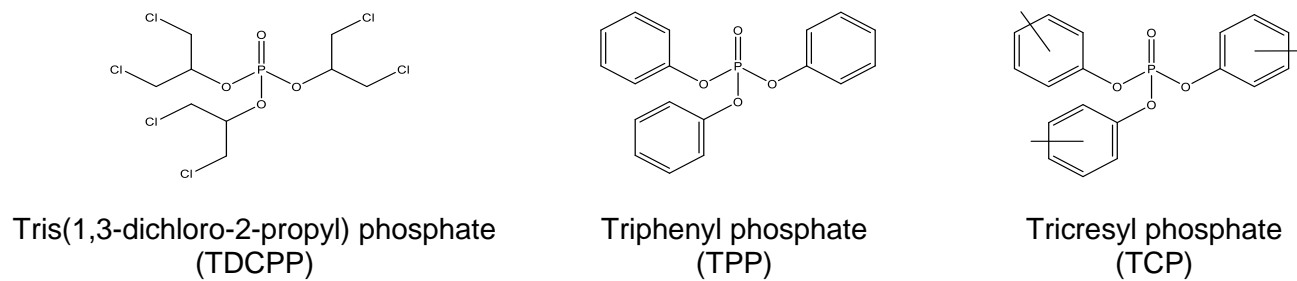
In the final study, WT and KO mice were injected with a single 10 mg/kg IP dose of TDCPP, TPP, or TCP and the disposition of OPFRs were determined 4 h later. As in Chapter 3, the liver and kidneys were shown to be the predominant sites of OPFR disposition for both WT and KO mice. This suggests that the route of OPFR administration (oral vs IP) may not affect partitioning. Although the OPFRs did not act as substrates or inhibitors of MDR1 in the *in vitro* assays, the results of the animal study indicate that MDR1 may affect OPFR partitioning in the brain *in vivo*. MDR1 is expressed in the endothelial cells of brain microcapillaries (Cui et al. 2009). Its location at the blood-brain barrier (BBB) provides protection against xenobiotic insults by decreasing the penetration of xenobiotics into the brain (Cui et al. 2009; Klaassen and Aleksunes 2010). In this study, TPP accumulation was significantly higher in the brains of KO mice compared to the WT mice ( $p < 0.001$ ) suggesting that MDR1 mediates TPP disposition in the brain. However, it should be noted that TPP concentrations in the serum of KO mice were also elevated and

thus the greater accumulation in the brain may be dependent on longer residence in the serum of KO mice.

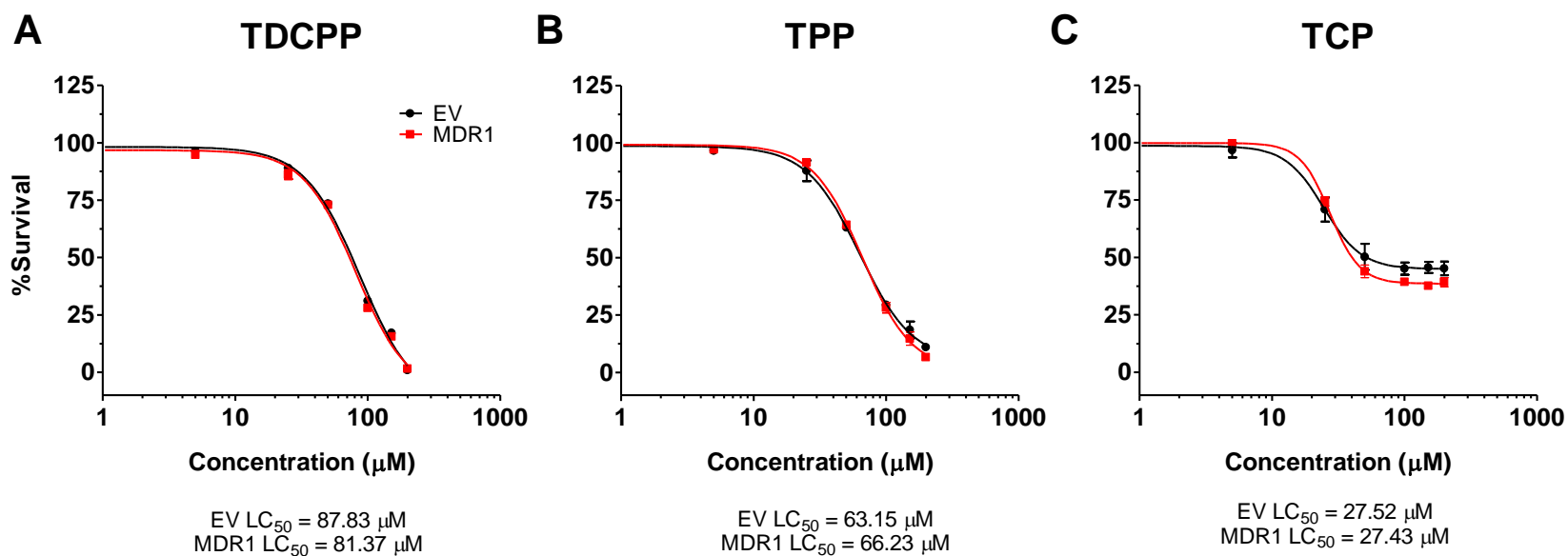
A number of genetic polymorphisms in MDR1 have been identified that have been shown to have decreased functional capacity to efflux prototypical MDR1 substrates such as vinblastine, verapamil, paclitaxel (Klaassen and Aleksunes 2010). Additionally, minimal expression of MDR1 in mice has been observed 2 days before birth up to the first 10 days after birth (Cui et al. 2009). This may result in greater exposure to chemical insults provided that the chemical undergoes maternal-fetal transfer during development or if the exposure occurs soon after birth. A critical window of increased adverse effects associated with chemical exposure may exist. Therefore, if an individual with minimal MDR1 expression or a genetic variant resulting in a defective MDR1 is exposed to TPP, it could result in the accumulation of TPP in the brain, thereby increasing the duration of chemical insult on the brain.

TPP has previously been associated with adverse neurodevelopment outcomes in children exposed to OPFRs *in utero*. Higher maternal urine diphenyl phosphate (DPP, the metabolite of TPP) was associated with decreased IQ (-2.9 points) and working memory (-3.9 points) in children (n=310) for each 10-fold increase in prenatal urinary DPP concentration (Castorina et al. 2017a). Whether TPP crosses the placental-fetal barrier is uncertain. TPP has been detected in the maternal-embryo interface (chorionic villi and deciduae) as well as the maternal-fetal interface (placenta) of pregnant women suggesting that maternal transfer is likely

(Ding et al., 2016; Zhao et al., 2017). However, it has not previously been shown to cross the placental barrier in rats and the results of Chapter 3 are inconclusive for TPP due to its pervasiveness in the vehicle control mice (Baldwin et al. 2017). Taken together, these data underscore the necessity to confirm the role of MDR1 in mediating TPP exposure using a model of the BBB *in vitro* such as the hCMEC/D3 cell line. In conclusion, while TDCPP, TPP, and TCP did not appear to be substrates of MDR1 *in vitro*, the results of the *in vivo* study suggest that TPP disposition may be mediated by MDR1, particularly in the brain. Additional time course studies are needed to definitively assess this relationship.

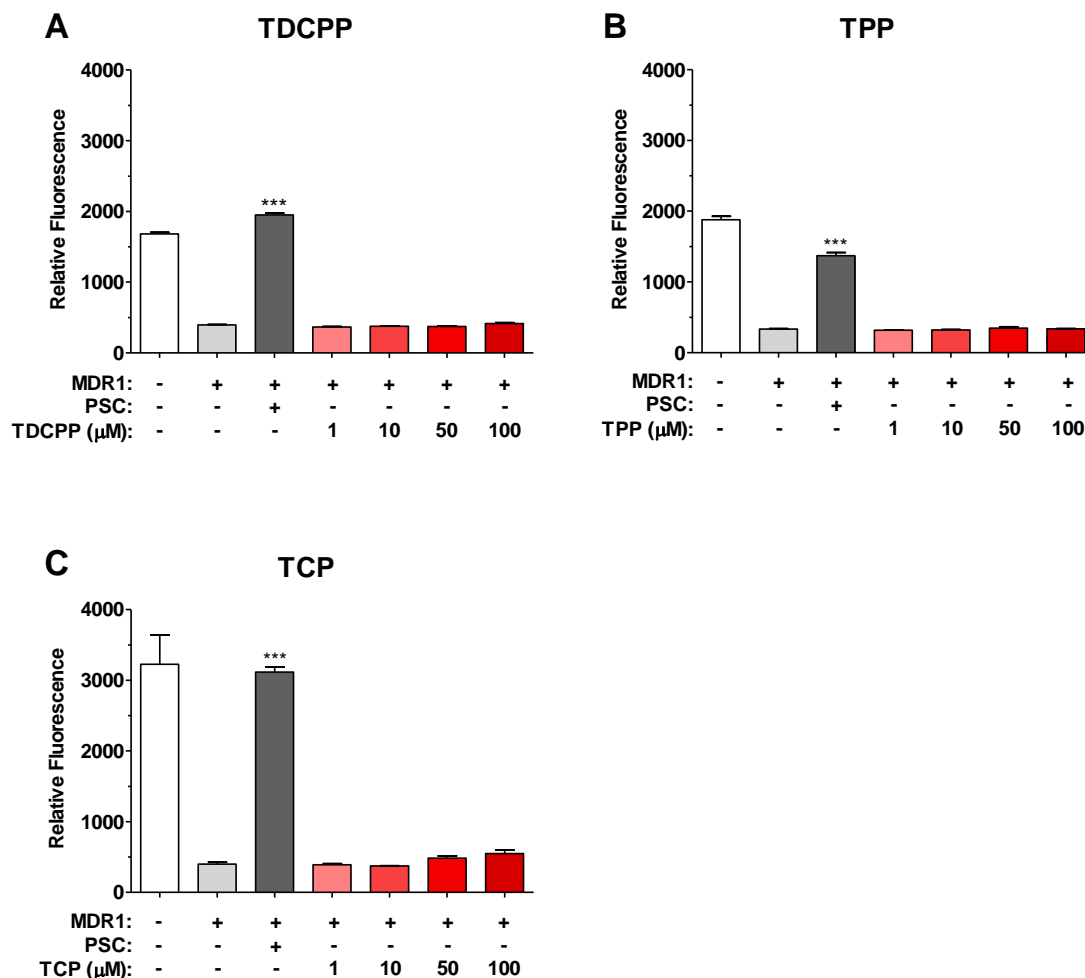


**Figure 4.1.** Names, acronyms, and structures of the OPFRs used in this study



**Figure 4.2.** OPFR-induced cell death

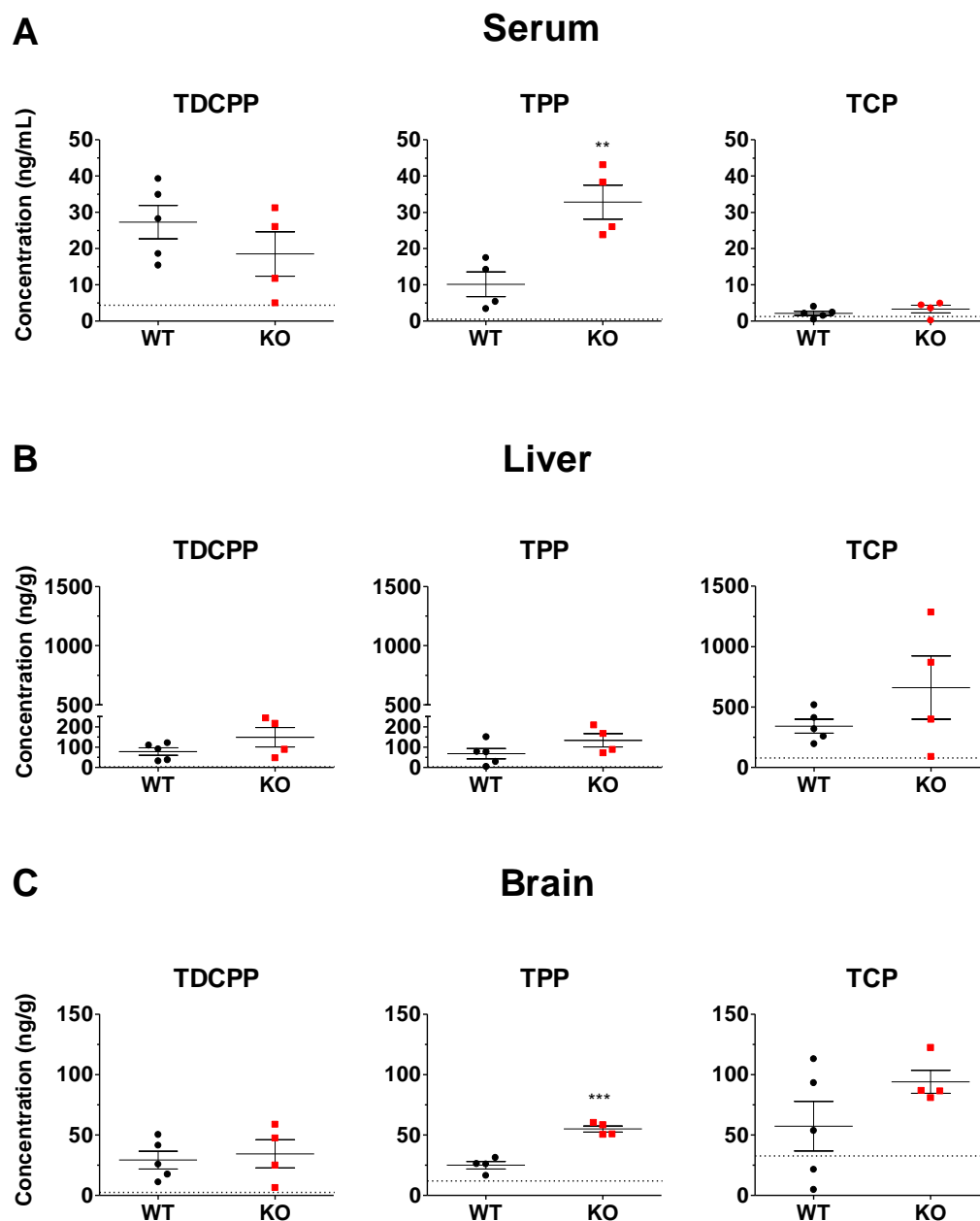
Empty vector (EV) and MDR1-expressing cells were incubated with 0-200  $\mu$ M of TDCPP, TPP, or TCP for 72 hours. Cell viability was determined using Alamar Blue. Error bars represent mean  $\pm$  SEM from 3 independent experiments. LC<sub>50</sub> values were determined using a normalized, variable hill slope, dose-dependent inhibition regression.



**Figure 4.3.** OPFR effects on MDR1 efflux function

Empty vector and MDR1-expressing cells were treated with 1-100 μM TDCPP (**A**), TPP (**B**), or TCP (**C**) and then incubated with the fluorescent MDR1 substrate, rhodamine 123. PSC833 (PSC, 2 μM), an MDR1 inhibitor, was used to block the efflux of the substrate. Data are presented as mean relative fluorescence  $\pm$  SEM normalized to cell size. Error bars represent mean  $\pm$  SEM of 4 technical replicates. Data were analyzed by one-way ANOVA with Dunnett's post-test (\* $p$ <0.05, \*\* $p$ <0.01, \*\*\* $p$ <0.001).





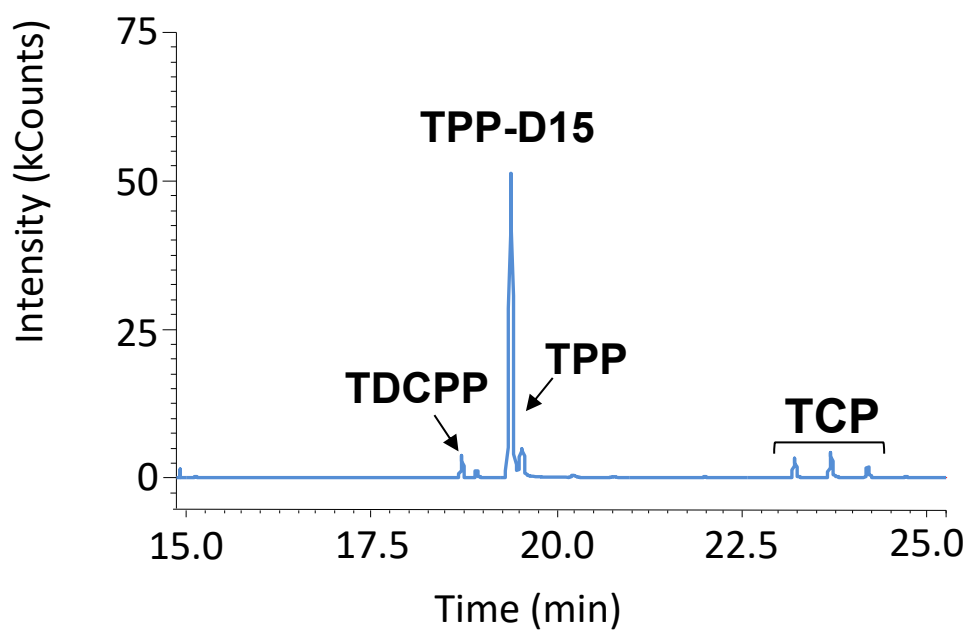
**Figure 4.4.** OPFR disposition in wild-type (WT) and Mdr1a/1b-null (KO) mice

OPFR concentrations in serum (**A**), livers (**B**), and brains (**C**) of WT and Mdr1a/1b KO male mice following a single 10 mg/kg IP dose of TDCPP, TPP, or TCP ( $n=9$  per OPFR). Data are presented as mean  $\pm$  SEM. The horizontal dotted lines indicate the background OPFR levels detected in control mice ( $n=2$  per OPFR). Data were analyzed by a student's t-test with Welch's correction where appropriate (\* $p<0.05$ , \*\* $p<0.01$ , \*\*\* $p<0.001$ ).

**Table 4.1.** Tissue/serum partitioning of OPFRs in WT and MDR1 KO mice

|              |           | <b>Liver</b> | <b>Brain</b> |
|--------------|-----------|--------------|--------------|
| <b>TDCPP</b> |           |              |              |
|              | <i>WT</i> | 2.7          | 1.0          |
|              | <i>KO</i> | 8.3          | 1.8          |
| <b>TPP</b>   |           |              |              |
|              | <i>WT</i> | 4.1          | 3.3          |
|              | <i>KO</i> | 3.9          | 1.8          |
| <b>TCP</b>   |           |              |              |
|              | <i>WT</i> | 265.0        | 26.3         |
|              | <i>KO</i> | 271.3        | 22.8         |

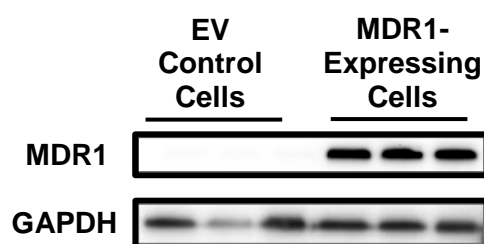
Average tissue/serum ratios of OPFRs in WT (n=5 per OPFR) and Mdr1a/1b KO (n=4 per OPFR) male mice following a single IP exposure to 10 mg/kg of TDCPP, TPP, or TCP.



**Figure S4.1.** Representative gas chromatogram of the OPFRs

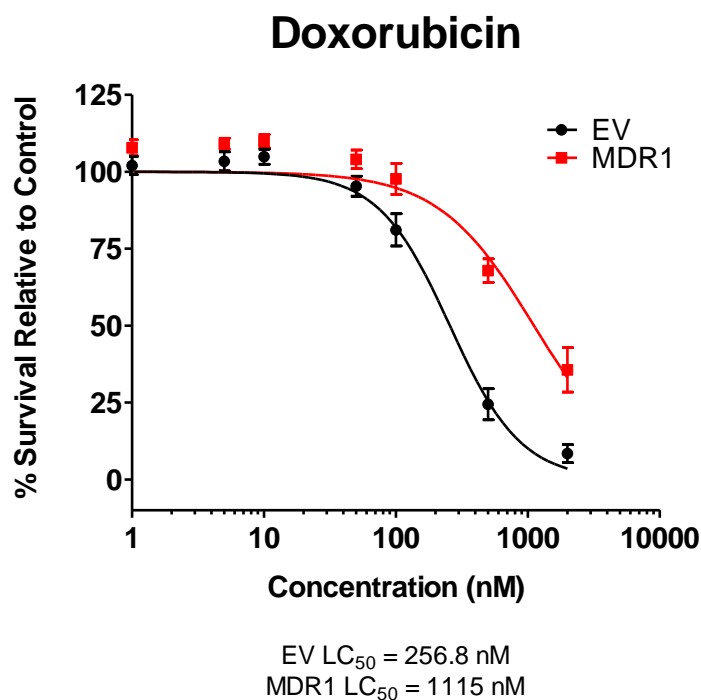
**Table S4.1.** Molecular weights (MW), retention times (RT), and quantitation ions (Q) for each OPFR. TPP-D15 was used as an internal standard.

| OPFR    | MW<br>(g/mol) | RT<br>(min) | Q ions<br>(m/z) |
|---------|---------------|-------------|-----------------|
| TDCPP   | 428           | 18.71       | 99              |
| TPP-D15 | 341           | 19.38       | 341             |
| TPP     | 326           | 19.51       | 326             |
| TCP     | 368           | 23.20       | 368             |



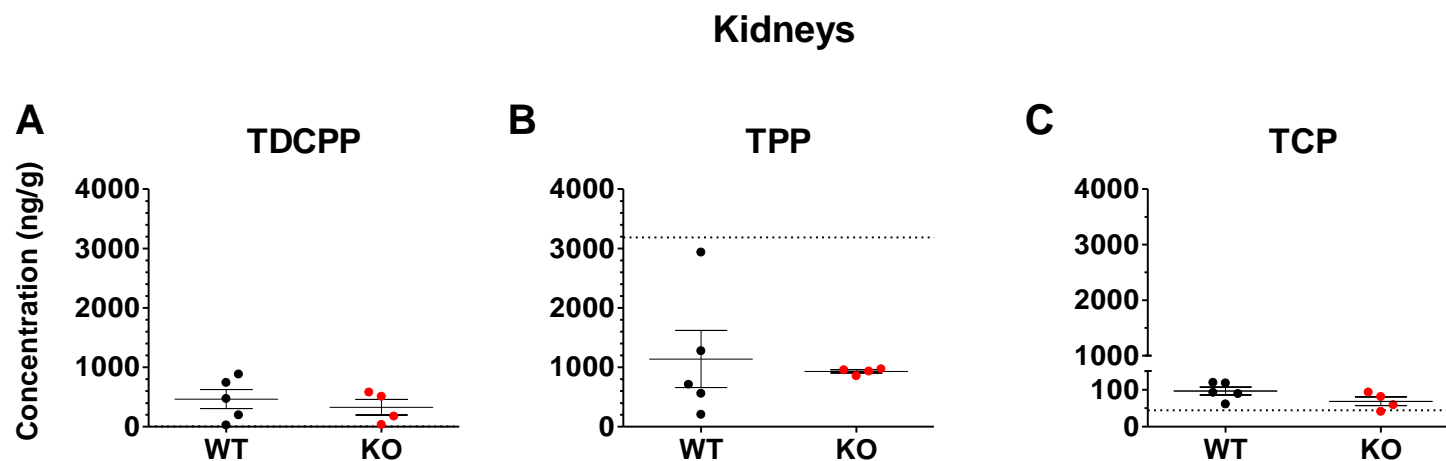
**Figure S4.2.** Confirmation of MDR1 protein expression in HEK293 cells stably-transfected with the human *MDR1* gene

Adapted from Xia et al., 2018



**Figure S4.3.** Confirmation of MDR1 function in HEK293 cells transfected with the human *MDR1* gene

Functional activity of the expressed MDR1 protein was validated using doxorubicin, an anticancer drug, and well-known MDR1 substrate. Empty vector control (EV) and MDR1-expressing cells were treated with increasing concentrations of doxorubicin for 72 hrs. A right-shift in the dose-response toxicity curve and a >4-fold increase in the concentration for 50% cell lethality (LC<sub>50</sub>) value confirms cellular protection against doxorubicin by MDR1 (adapted from Xia et al., 2018).



**Figure S4.4.** OPFR disposition in the kidneys of wild-type (WT) and Mdr1a/1b-null (KO) mice

OPFR concentrations in kidneys of WT and Mdr1a/1b KO male mice following a single 10 mg/kg IP dose of TDCPP (**A**), TPP (**B**), or TCP (**C**) (n=9 per OPFR). Data are presented as mean  $\pm$  SEM. The horizontal dotted lines indicate the background OPFR levels detected in control mice (n=2 per OPFR). An uncharacteristically high level of TPP was observed in the control animals suggesting that the tissues were contaminated during sample collection and/or preparation for analysis. Data were analyzed by a student's t-test with Welch's correction where appropriate (\*p<0.05, \*\*p<0.01, \*\*\*p<0.001).

**Table S4.2.** Kidney/serum ratios for wild-type (WT) and Mdr1a/1b-null (KO) mice

|              |           | Kidney |
|--------------|-----------|--------|
| <b>TDCPP</b> |           |        |
|              | <i>WT</i> | 14.6   |
|              | <i>KO</i> | 15.2   |
| <b>TPP</b>   |           |        |
|              | <i>WT</i> | 72.2   |
|              | <i>KO</i> | 30.0   |
| <b>TCP</b>   |           |        |
|              | <i>WT</i> | 82.8   |
|              | <i>KO</i> | 65.3   |

Average kidney/serum ratios of OPFRs in WT (n=5 per OPFR) and Mdr1a/1b KO (n=4 per OPFR) male mice following a single IP exposure to 10 mg/kg of TDCPP, TPP, or TCP. Ratios for TPP should be interpreted cautiously due to an uncharacteristically high background TPP level observed for the control mice.



## CHAPTER 5: OVERALL DISCUSSION

### 5.1 Summary

The overall objectives of this dissertation research were to: (1) assess the ability of organophosphate flame retardants (OPFRs) to affect acetylcholinesterase (AChE) and carboxylesterase (CES) activity against known inhibitors with structural similarities (organophosphate pesticides, OPs), (2) characterize the disposition of OPFRs in subchronic and gestational exposure models, and (3) to determine the extent by which the multidrug resistance protein 1 transporter (MDR1) can influence OPFR disposition. Despite the sharp increase in OPFR usage since the mid-2000s, the prevalence of human exposure to these compounds is just beginning to be appreciated. Moreover, understanding of OPFR-induced adverse effects has only recently become a focus of research due to emerging evidence of their impact on critical biological systems.

The findings presented in the previous chapters support the hypothesis that OPFRs interact with molecular targets that influence their overall disposition and potential for neurotoxicity. Three specific aims were developed to address this hypothesis: 1) Assess the ability of OPFRs to inhibit AChE and CES activity *in vitro* (**Chapter 2**); 2) Determine the disposition of OPFRs following subchronic oral exposure in adult mice and gestational exposure in dams and fetuses (**Chapter 3**); and 3) Determine whether OPFRs act as substrates and/or inhibitors of MDR1 *in vitro* and whether MDR1 influences OPFR disposition *in vivo* (**Chapter 4**).

The first aim compared the extent of OPFR-induced AChE and CES activity to that of known inhibitors with structural similarities to the OPFRs, the OPs. A suite of OPFRs was assessed alongside the OP, dichlorvos (DDVP) and the positive control, chlorpyrifos oxon. Whole brain and liver S9 fractions from naive male C57BL/6 mice were incubated with DDVP, tris (2-chloroethyl) phosphate (TCEP), tributyl phosphate (TBP), dibutyl phosphate (DBP), triphenyl phosphate (TPP), diphenyl phosphate (DPP), tris(1,3-dichloro-2-propyl) phosphate (TDCPP), or tricresyl phosphate (TCP) to determine their effect on AChE and CES activity. The concentration at which 50% of enzyme activity was inhibited ( $IC_{50}$ ) indicated that DDVP was a much more potent AChE inhibitor than the OPFRs by at least 5 orders of magnitude (**Fig. 2.1**). Additionally, TPP and TCP inhibited AChE activity up to their solubility limit (5 mM) exhibited anti-AChE activity whereas TDCPP and TBP did not. CES  $IC_{50}$  values showed that TCEP, TPP, DPP, DBP, and TCP were 3-7 magnitudes of order weaker than DDVP (**Fig. 2.2**). CES inhibition was observed for TDCPP and TBP up to their solubility limit of 50 and 5 mM, respectively. Overall, these data indicated that OPFRs are weak inhibitors of AChE and CES relative to the OPs but that CES is more sensitive than AChE to perturbations by OPEs. Furthermore, these data suggest that despite evidence of rising human exposure to OPFRs, the risk of acute AChE toxicity is minimal.

The second aim investigated the partitioning of OPFRs in mice with the goal of identifying target organs of OPFR toxicity, sex differences in disposition, and maternal-fetal transfer of OPFRs. In the first part of this study, the tissue distribution of OPFRs was quantified in adult male and female C57BL/6 mice orally

administered a daily 3 mg/kg mixture of equal TDCPP, TPP, and TCP for 28 days using gas chromatography-ion trap mass spectrometry (**Fig. 3.2**). High tissue/serum ratios indicated that the liver and kidneys are predominant sites of OPFR disposition with the brain being a minor site by comparison. (**Table 3.1**). Modest differences in OPFR accumulation were observed between male and female mice that were tissue- and compound-specific. Serum OPFR levels were similar between the sexes for TDCPP, TPP, and TCP. In the liver, comparable levels of TDCPP were observed in male and female mice. Concentrations of TPP in the livers of male mice exceeded those in females whereas female mice exhibited significantly higher levels of TCP compared to male mice. In the kidneys, male mice had a greater accumulation of all three OPFRs than the female mice. Concentrations of TDCPP in the brain were similar across sexes. Higher TPP concentrations were observed in the brains of male mice whereas greater TCP accumulation was detected in the brains of female mice. In the second part of the study, dams were given a 3 mg/kg dose of total OPFR or vehicle in the form of a peanut butter treat from GD 7 through 16-18. Following gestational exposure, TCP was shown to accumulate in placentas and fetuses (**Fig. 3.3**). Overall, these data indicate that the liver, kidneys, and brain are preferential sites of OPFR disposition, that sex does not significantly affect OPFR disposition, and that TCP likely undergoes maternal transfer.

The final aim identified whether OPFRs are substrates and/or inhibitors of the MDR1 transporter *in vitro* and whether MDR1 influences OPFR disposition *in vivo*. In the first study, the cell viability of HEK293 cells expressing an empty vector (EV)

or the human MDR1 gene treated with TCP, TDCPP, and TPP for 72 h was assessed using the Alamar Blue assay. All three OPFRs displayed similar concentration-dependent reductions in cell viability between EV- and MDR1-expressing cell lines (**Fig. 4.2**). In the second study, none of the OPFRs altered the efflux of the MDR1 substrate, rhodamine, from MDR1-expressing cells (**Fig. 4.3**). In the final study, the potential for MDR1 to influence OPFR disposition was investigated in wild-type (WT) and Mdr1a/1b-null mice (KO). KO mice had significantly higher levels of TPP in the serum and brain compared to WT mice, suggesting that MDR1 may protect the brain from the accumulation of TPP (**Fig. 4.4**). Overall, these data suggest that MDR1 does not confer resistance to OPFR-induced cellular lethality nor do these chemicals inhibit MDR1 function *in vitro*, but that MDR1 may influence TPP disposition *in vivo*.

## 5.2 Discussion

### 5.2.1 AChE and CES Activity

In Chapter 2 it was determined that OPFRs are poor inhibitors of AChE and CES activity. However, TPP and TCP did exhibit anti-CES activity in the low micromolar range, may warrant further investigation. Young children have been historically considered as a vulnerable population to OPFR exposure due to their frequent hand-to-mouth contact, increased time spent indoors, and lower body weights compared to adults (EPA 2015). Dust ingestion is a common route of OPFR exposure, especially in children. Toddlers consume an average of 50 mg/day with a high ingestion rate of 200 mg/day of dust (Jones-Otazo et al. 2005; Van den

Eede et al. 2011). Based on a previous study in which TPP was reported at concentrations up to 1.8 mg/g in household dust, and assuming that the average household contains 1 g of dust, Morris et al. estimated that ingesting 0.33 mg of TPP in dust would translate to a 1  $\mu\text{M}$  blood concentration in children (12-13 kg, 1 L blood volume) (Morris et al. 2014; Stapleton et al. 2009). Using this logic, a child would need to consume 3.33 mg of TPP in dust to yield a 10  $\mu\text{M}$  blood level, which is just above the CES  $\text{IC}_{50}$  observed in Chapter 2 (9.29  $\mu\text{M}$ ). Additionally, the highest reported TCP concentration in household dust was 10.0  $\mu\text{g/g}$  (Dodson et al. 2012). Therefore, the maximum TCP blood level due to dust ingestion would be 27  $\mu\text{M}$ , which is below the CES  $\text{IC}_{50}$  determined in this study (41.3  $\mu\text{M}$ ). Data from Chapters 3 and 4 suggest that TCP actively accumulates in the liver, and therefore could more readily target CES localized in the liver hepatocytes. In summary, although CES inhibition was observed for TPP and TCP, the concentrations for which the  $\text{IC}_{50}$  responses were elicited are unlikely to occur as an acute exposure.

Although acute effects of OPFRs on AChE and CES activity are unlikely it is important to consider the effect chronic OPFR exposure may have on these enzymes. The ubiquitous detection of OPFR metabolites in humans justify cause for concern (Castorina et al. 2017a; Castorina et al. 2017b; Chen et al. 2018; He et al. 2018; Hoffman et al. 2017a; Hoffman et al. 2017b; Ospina et al. 2018; Thomas et al. 2017). The upper estimate of cumulative exposure to  $\Sigma\text{OPFRs}$  in dust for toddlers in the U.S. (1680 ng/d), Belgium (128 ng/kg bw/d), Germany (22.4 ng/kg bw/d), and New Zealand (69.8 ng/kg bw/d), among others, will likely increase proportionately as the use and environmental persistence of OPFRs increases

worldwide (Wei et al. 2015). This may warrant further investigation in which studies better representing typical exposures conditions (i.e. exposure to multiple OPFRs over a longer period of time) are conducted to understand the effects of chronic OPFR exposure on CES activity, in particular. Moreover, it is not known whether OPFRs could have a combined effect in regulating not only CES function but also its transcription and translation leading to changes in the expression of CES in hepatocytes.

### 5.2.2 OPFR Disposition

In Chapter 3, the liver, kidneys, and brain were identified as target organs for OPFR disposition. Additionally, sex did not appear to significantly influence OPFR disposition although modest differences in accumulation were observed. The most provocative result of this study was that TCP was shown to undergo maternal-fetal transfer in mice, which heretofore had not been identified.

Interestingly, TPP was found in placental and fetal tissues of treated and vehicle-control dams. This suggests that mice may have received unintended exposures through their bedding, diet, and/or cages. Indeed, the pervasiveness of TPP has been demonstrated in a number of environmental and human biomonitoring studies (Ali et al. 2012a; Castorina et al. 2017a; Castorina et al. 2017b; Ding et al. 2016; Dodson et al. 2012; He et al. 2018; van der Veen and de Boer 2012). Notably, indoor exposures to OPFRs are often higher than outdoor exposures because OPFRs are not chemically bound in the fire-proofed material and can easily leach via volatilization, abrasion, and dissolution (van der Veen and de Boer

2012). In addition to its application as a flame retardant, TPP in paint and lacquer applications and as a plasticizer (van der Veen and de Boer 2012; Wei et al. 2015). Thus, it is possible that incidental exposure may have occurred. Although none of the cage materials were tested for TPP in this study, results were blank corrected for toluene background (toluene was used as the extracting solvent during sample preparation). In the future, additional precautions may be necessary to limit unintended exposure to TPP. Baldwin et al. (2017) used housing conditions specifically designed to minimize unintended exposure to endocrine disrupting chemicals (TPP has been implicated as one). These housing conditions include the use of glass water bottles, soy-free diet (albeit the chow used in this study contained <75 ppm phytoestrogens and should therefore not be a contributor), woodchip bedding, and thoroughly washed polysulfone caging.

### 5.2.3 Molecular Interactions of OPFRs with MDR1

In Chapter 4, OPFRs were not shown to be likely substrates and/or inhibitors of MDR1 *in vitro*, but Mdr1a/1b was shown to influence TPP disposition in serum and brain *in vivo*. To confirm the role of MDR1 as a protective mechanism against TPP accumulation in the brain, human capillary endothelial brain (hCMEC/D3) cells can be utilized. The hCMEC/D3 cell line is a model of the blood-brain barrier. Because MDR1 is an apical efflux transporter, basolateral-to-apical transport experiments should be conducted to validate the results of the *in vivo* study.

Additionally, levels of serum and liver TPP and liver and brain TCP were greater in Mdr1a/b-null mice (KO) were higher than the wild-type (WT) MDR1 mice. This

may suggest that the disposition of TPP and TCP in the liver and brain, respectively, may be influenced by additional transporters such as the breast cancer resistance protein (BCRP). Like MDR1, BCRP is a member of the ATP-binding cassette (ABC) family of transporters, which are localized on apical membranes of numerous tissues including the luminal membrane of enterocytes and endothelial cells of brain microcapillaries, the brush border membrane of renal proximal tubules, and the canalicular membrane of hepatocytes (Klaassen and Aleksunes 2010; Mao and Unadkat 2015; Stieger and Gao 2015). BCRP has a broad range of substrate and inhibitor specificity that substantially overlaps but is also distinct from that of MDR1 (Mao and Unadkat 2015). Interestingly, a synergistic effect between MDR1 and BCRP in the BBB has been observed where brain exposure of an MDR1/BCRP dual substrate in MDR1/BCRP double-knockout mice is markedly increased than exposure in MDR1 and BCRP single-knockout mice (Polli et al. 2009). Despite their co-localization in the luminal side of brain endothelial cells, the synergistic effect is indicative of MDR1 and BCRP1 transport as the primary clearance pathways of xenobiotics from the brain rather than direct interaction of the two transporters (Kodaira et al. 2010; Mao and Unadkat 2015). Thus, it may be of interest to investigate BCRP as a potential contributor to OPFR disposition *in vivo*.

### **5.3 Overall Conclusions and Implications**

The findings in this dissertation demonstrate that OPFRs do not behave like the structurally similar OPs in terms of inhibiting brain AChE and liver CES activity.



Although, the OPFRs did not demonstrate adverse effects on serine hydrolase activity, the brain and liver, as well as the kidneys, placenta, and fetus were identified as target organs of toxicity due to their preferential accumulation of OPFRs. Identifying these OPFR storage depots will help guide future research into OPFR-induced organ-specific adverse effects. Moreover, the assessment of *in utero* exposure will help to inform future studies on potential adverse health effects on the developing fetus. Finally, MDR1 was shown to potentially influence the disposition of TPP in the brain *in vivo* suggesting that MDR1 protects the brain from potential TPP-induced chemical insults. Future studies investigating the various mechanisms by which TPP can cause neurotoxicity will be key to assessing the risk of exposure during critical periods of development and in young children.

**APPENDIX 1: Organophosphate flame-retardants alter adult mouse  
homeostasis and gene expression in a sex-dependent manner potentially  
through interactions with ERalpha**

Elizabeth A. Krumm<sup>\*,†,#</sup>, Vipra J. Patel<sup>\*,#,,</sup>, Taylor S. Tillery<sup>\*</sup>, Ali Yasrebi<sup>\*,†</sup>,  
Jianliang Shen<sup>‡</sup>, Grace L. Guo<sup>‡</sup>, Stephanie M. Marco<sup>§</sup>, Brian T. Buckley<sup>¶¶</sup>, and  
Troy A. Roepke<sup>\*,†,§</sup>

<sup>\*</sup>Department of Animal Sciences, School of Environmental & Biological Sciences,  
Rutgers, The State University of New Jersey, New Brunswick, NJ. USA

<sup>†</sup>Graduate Program in Endocrinology and Animal Biosciences, Rutgers, The State  
University of New Jersey, New Brunswick, NJ. USA

<sup>‡</sup>Department of Pharmacology and Toxicology, School of Pharmacy, Rutgers  
University, Piscataway, NJ 08854, USA.

<sup>§</sup>Joint Graduate Program in Toxicology, Rutgers, The State University of New  
Jersey, New Brunswick, NJ. USA

<sup>¶¶</sup>Environmental and Occupational Health Institute, Rutgers, The State University  
of New Jersey, New Brunswick, NJ. USA

### A-1.1 Abstract

Flame retardants (FRs) such as polybrominated diphenyl ethers and organophosphate FR (OPFR) persist in the environment and interact with multiple nuclear receptors involved in homeostasis, including estrogen receptors (ERs). However, little is known about the effects of FR, especially OPFR, on mammalian neuroendocrine functions. Therefore, we investigated if exposure to FR alters hypothalamic gene expression and whole-animal physiology in adult wild-type (WT) and ER $\alpha$  KO mice. Intact WT and KO males and ovariectomized WT and KO females were orally dosed daily with vehicle (oil), 17 $\alpha$ -ethynylestradiol (2.5  $\mu$ g/kg), 2,2', 4,4-tetrabromodiphenyl ether (BDE-47, 1 or 10 mg/kg), or an OPFR mixture {1 or 10 mg/kg of tris(1, 3-dichloro-2-propyl)phosphate, triphenyl phosphate, and tricresyl phosphate each} for 28 days. Body weight, food intake, body composition, glucose and insulin tolerance, plasma hormone levels, and hypothalamic and liver gene expression were measured. Expression of neuropeptides, receptors, and cation channels was differentially altered between WT males and females. OPFR suppressed body weight and energy intake in males. FR increased fasting glucose levels in males, and BDE-47 augmented glucose clearance in females. Liver gene expression indicated FXR activation by BDE-47 and PXR and CAR activation by OPFR. In males, OPFR increased ghrelin but decreased leptin and insulin independent of body weight. The loss of ER $\alpha$  reduced the effects of both FR on hypothalamic and liver gene expression and plasma hormone levels. The physiological implications are that males are more sensitive than ovariectomized females to OPFR exposure and that these effects are mediated, in part, by ER $\alpha$ .

## A-1.2 Introduction

Because polybrominated diphenyl ethers (PBDE) have been phased out of use in the United States since 2004 and subsequently concentrations in humans have declined (Zota et al., 2013), many products now employ nonbrominated flame retardants (FRs) such as organophosphate FRs (OPFRs) (Hoffman et al. 2017a; van der Veen and de Boer 2012). Therefore, environmental concentrations of OPFR are increasing and are detectable in significant concentrations in women's breast milk and urine (Cequier et al. 2014; Hoffman et al. 2017a; Hoffman et al. 2014; Kim et al. 2014; Sundkvist et al. 2010). A primary source of OPFR is dust in the home and work environments. Indeed, OPFR are found in low  $\mu\text{g/g}$  concentration in house dust (3-month geometric mean for Tris (1,3-dichloro-2-propyl)phosphate (TDCPP) =  $1.58 \mu\text{g/g}$  and for TPP =  $6.8 \mu\text{g/g}$ ) (Meeker et al. 2013b) and in dust from offices ( $6.06 \mu\text{g/g}$ ) and vehicles ( $12.5 \mu\text{g/g}$ ) (Carignan et al. 2013) as well as drinking water (Li et al. 2014), and air in offices and aircrafts (Yang et al. 2014). OPFR are known to interact with a range of nuclear receptors *in vitro*. Indeed, triphenyl phosphate (TPP) and tricresyl phosphate (TCP) activate human estrogen receptor (ER) $\alpha/\beta$  transactivation assays, although with lower potency than  $17\beta$ -estradiol (E2) (Kojima et al. 2013; Liu et al. 2012; Pillai et al. 2014). TDCPP is a potential ER antagonist (Liu et al., 2012) and also upregulates ER $\alpha$  target genes (Liu et al. 2013; Lu et al. 2014).

Little is known about the effects of adult OPFR exposure on the neuroendocrine control of energy homeostasis in mammalian models. In chicks, TDCPP-induced

cholestatic liver and biliary fibrosis, decreased plasma cholesterol, disrupted lipid and steroid metabolism, induced CYP3A37 and CYP2H1 expression, and altered ApoE, hepatocyte nuclear factor 4 $\alpha$ , and peroxisome proliferator activated receptor (PPAR $\alpha$ ) expression (Farhat et al. 2014). In zebrafish, TDCPP and TPP decreased fecundity, increased plasma E2, and upregulated steroid hormone receptors and reproductive genes in the hypothalamus and pituitary in a sex-dependent manner (Liu et al. 2013; Lu et al. 2014). These studies demonstrate that selected OPFR can interact with nuclear receptors to elicit complex interactions impacting neural growth, steroidogenesis, lipid and glucose homeostasis, and hypothalamic functions.

Although a number of brain regions play a role in body weight homeostasis (Berthoud 2002), the hypothalamus is regarded as the key regulator of energy homeostasis, especially the arcuate nucleus (ARC) (Saper et al. 2002). The ARC is a heterogeneous nucleus containing neurons involved in energy homeostasis, growth, and reproduction including proopiomelanocortin (POMC), neuropeptide Y (NPY)/agouti-related peptide (AgRP), growth hormone-releasing hormone (GHRH), and kisspeptin-neurokinin B (Tac2)-dynorphin (KNDy) neurons (Bosch et al. 2012; Gottsch et al. 2011; Proudant et al. 2015). These neurons are in a unique position because of their proximity to a “leaky” region of blood-brain barrier and subsequently receive information reflecting the body’s energy status (Schwartz et al. 2000).

A wide range of hormones produced by the gonads, fat, pancreas, gastrointestinal tract, and liver modulate ARC neurons (Woods 2009). E2 modulates energy intake and expenditure and controls glucose homeostasis through actions of ER $\alpha$  in the hypothalamus (Mauvais-Jarvis et al. 2013). ER $\alpha$  knockout (KO) females are phenotypically obese, glucose intolerant, and resistant to the effects of E2 as full-grown adults (Geary et al. 2001; Yasrebi et al. 2017). Leptin and insulin, peripheral hormones from fat and pancreas, differentially depolarize and hyperpolarize POMC and NPY neurons (Baquero et al. 2014; Elias et al. 1999; Mirshamsi et al. 2004; Qiu et al. 2010; Qiu et al. 2014). These hormones activate TRPC channels (TRPC5) to excite POMC neurons and activate KATP channels to suppress NPY neurons through their respective receptors, LepR and InsR (Baquero et al., 2014; Elias et al., 1999; Mirshamsi et al., 2004; Qiu et al., 2010, 2014). Ghrelin is secreted by the stomach to drive hunger and increase feeding through the growth hormone secretagogue receptor (GHSR). GHSR is expressed in NPY/AgRP neurons and increases NPY neuronal excitability (Andrews 2011; Nogueiras et al. 2010). GHSR is also highly expressed in KNDy neurons and is upregulated by estradiol through ER $\alpha$  (Yang et al. 2016a; Yang et al. 2016b). GHSR stimulation activates a Gq-coupled signaling pathway that inhibits KCNQ channel activity to increase neuronal excitability (Shi et al. 2013; Yasrebi et al. 2016). The KCNQ family of potassium channels produces the neuronal M-current, a noninactivating outward potassium current under the control of E2 in the ARC (Roepke et al. 2011).

As ER $\alpha$  is highly expressed in the ARC (Roepke et al. 2011), there is potential for FR to disrupt ER $\alpha$ -mediated pathways involved in energy homeostasis in the ARC.

Although PBDE have been phased out in the United States and Europe, it is crucial to identify the impacts of their replacement compounds, OPFR, to determine if these compounds are also harmful. We chose to use TPP, TCP, and TDCPP as a mixture due to their potential interactions with steroid receptors and their detection in human samples. Furthermore, these OPFR disrupt neural, reproductive, and homeostatic gene expression and function in a sex-dependent manner in nonmammalian models. Therefore, we hypothesized that OPFR treatment will differentially impinge on homeostatic ARC genes between male and female mice. Because FRs may interact with nuclear steroid receptors, in particular ER $\alpha$ , we also hypothesize that their effects would be reduced in mice lacking the functional expression of ER $\alpha$  (ER $\alpha$  KOs)

### **A-1.3 Materials and Methods**

#### *Animal care*

All animal procedures were completed in compliance with institutional guidelines based on National Institutes of Health standards and were performed with Institutional Animal Care and Use Committee approval at Rutgers University. Wild-type (WT) C57/BL6J mice and Ex3a ER $\alpha$  KO transgenic mice (provided by Dr Ken Korach, NIEHS) (Hewitt et al. 2010) were bred in-house and maintained under controlled temperature (25 °C) and 12/12-h light/dark cycle. Mice were fed ad libitum a chow diet (LabDiet PicoLab Verified 5v75 IF, <75 ppm phytoestrogens) and given free access to water. To eliminate the need to track and characterize the estrous cycle before sample collection and reduce the impact of estrogens on ER-mediated transcription, all adult females were bilaterally ovariectomized (OVX) under isoflurane anesthesia using sterile no-touch technique according to the NIH Guidelines for Survival Rodent Surgery. Animals were given a dose of analgesia (4 mg/kg carprofen [Rimadyl]) 1 day following surgery for pain management. Animals typically lost 1–2 g of weight within 24 h after surgery.

#### *Chemicals*

17 $\alpha$ -ethynylestradiol (EE2), TPP (CAS no. 115-86-6; purity = 99%), and TDCPP (CAS no. 13674-87-8; purity = 95.6%) were purchased from Sigma-Aldrich (St. Louis, Missouri). 2,2', 4,4'-tetrabromodiphenyl ether (BDE-47) was purchased from Matrix Scientific (CAS no. 5436-43-1; purity = 95+%; Elgin, South Carolina), and



TCP (CAS no. 1330-78-5; purity = 99%) was purchased from AccuStandard (New Haven, Connecticut). For the stock solution, 100 mg of the BDE-47 or 100 mg of each OPFR were dissolved in 1 ml of acetone. For the working stock, 100  $\mu$ l of the acetone: FR mixture was added to 10 ml of sesame oil and mixed over a stir plate for 48 h with venting. Ultra residue-analyzed toluene (CAS no. 108-88-3; purity = 99.7%) was purchased from ThermoFisher Scientific (Waltham, Massachusetts). TPP D15 (CAS no. 1173020-30-8; purity = 98%) was purchased from Cambridge Isotope Laboratories (Tewksbury, Massachusetts).  $^{13}\text{C}_{12}$  BDE-47 (IUPAC no. 47 L; purity = 99%) was purchased from Wellington Laboratories (Guelph, Ontario, Canada). 1  $\mu$ g/ml TPP D15 and 1  $\mu$ g/ml  $^{13}\text{C}_{12}$  BDE-47 stock solutions were made in toluene.

*Experiment no. 1: WT brain and liver tissue collection*

Intact male and OVX female WT mice were divided into 6 endocrine disrupting compound (EDC) treatment groups ( $n = 8/\text{treatment}/\text{sex}$ ): Oil (negative control), EE2 (positive estrogenic control; 2.5  $\mu$ g/kg/d), 2 doses of BDE-47 (1 or 10 mg/kg/d), and 2 doses of OPFR mixture (TCP, TPP, and TDCPP at 1 or 10 mg/kg/d of each OPFR). BDE-47 was included in these experiments to compare effects between the groups of FR and because BDE-47 and its metabolites potentially have estrogenic activity (Lu et al. 2014). Age range at the start of dosing for males was 12–16 weeks, and date of ovariectomy for females was 12–16 weeks. Animals were dosed orally using peanut butter as the carrier. Untreated peanut butter was given to the mice to acclimate the mice for 4 days before FR dosing. For females,

acclimation occurred 3 days before surgery and FR dosing began immediately after surgery. Dosing consisted of mixing 100–150 mg of all-natural peanut butter with the respective sesame oil mixture (blank [oil], EE2, BDE-47, and OPFR) at a volume determined by weight (25  $\mu$ l for a 25-g mouse). Dosing continued every morning (1000 h) for 4 weeks. After the dosing periods, all mice were fasted for 1 h and decapitated after sedation with ketamine (100  $\mu$ l of 100 mg/ml, IP; Henry Schein [Melville, New York]) at 1000 h.

The brain was immediately extracted from the skull and rinsed in ice-cold Sorensen's buffer for 30 s. The brain was cut using a brain matrix (Ted Pella, Redding, California) into 1-mm thick coronal rostral and caudal blocks corresponding to plates 42–53, respectively, from *The Mouse Brain in Stereotaxic Coordinates* (Paxinos and Franklin 2008). Blocks of the basal hypothalamus (BH) were transferred to RNALater (Life Technologies, Grand Island, New York) and stored overnight at 4 °C. The rostral and caudal parts of the ARC were dissected from slices using a dissecting microscope. Dissected tissue was stored in RNALater at –80 °C. The abdominal cavity was dissected for liver tissue (secondary lobe). Liver tissue was fixed in RNALater and stored at –80 °C. Liver RNA was extracted using a standard TRIzol extraction (Life Technologies) coupled with Macherey-Nagel NucleoSpin RNA extraction kit with rDNase digestion (Bethlehem, Pennsylvania). Total ARC RNA was extracted from the combined rostral and caudal ARC using Ambion RNAqueous-Micro Kits (Life Technologies) as per the manufacturer's protocol. Total RNA was treated with DNase I using the extraction kit protocol at 37 °C for 30 min to minimize any genomic DNA

contamination. Liver and arcuate RNA quantity and quality were determined using a NanoDrop ND-2000 spectrophotometer (ThermoFisher, Waltham, Massachusetts) and an Agilent 2100 Bioanalyzer and RNA Nano Chips (Agilent Technologies, Santa Clara, California). Only samples with RNA Integrity Number (RIN) > 8 were used.

*Experiment no. 2: WT energy and glucose homeostasis*

A second group of WT intact male and OVX female mice (n = 8 per group) were separated into 4 groups (Oil, EE2, 1 mg/kg BDE-47, and 1 mg/kg of OPFR mixture) and dosed for 4 weeks. Because we found similar effects on gene expression between the 2 doses of OPFR, we eliminated the 10 mg/kg dose for experiment nos. 2 and 3. Age ranges at the start of dosing for males was 10–12 weeks, and date of ovariectomy for females was 10–12 weeks. At the end of the 4 weeks, a small rodent MRI (EchoMRI, Houston, Texas) was used to determine body composition. For a glucose tolerance test (GTT), each mouse was IP-injected with a bolus of glucose (2 g/kg) after a 5 h fast. Glucose was measured in tail blood using an AlphaTrak glucometer (Zoetis, Parsippany, NJ). Glucose measurements were taken every 0, 15, 30, 60, 90, and 120 min after injection. For the insulin tolerance test (ITT), mice were IP-injected with insulin (0.75 U/kg body weight in sterile saline) after a 4 h fast. Glucose measurements were taken at 0, 15, 30, 60, 90, and 120 min after insulin injection.

After sufficient recovery from the ITT (approximately 1 week) during which dosing continued, all mice were fasted for 1 h and decapitated after sedation with

ketamine at 1000 h. Trunk blood was collected in a K<sup>+</sup> EDTA collection tube. Plasma was prepared for peptide hormone analysis by adding a protease inhibitor, 4-(2-aminoethyl) benzenesulfonyl fluoride hydrochloride (1 mg/ml, Sigma-Aldrich), to each collection tube. Samples were maintained on ice until centrifugation at 1,100 rcf for 15 min at 4 °C. Plasma was stored at –80 °C until analysis. Plasma insulin, leptin, and ghrelin levels were determined by multiplex assay (MMHMAG-44 K, EMD Millipore, Billerica, Massachusetts).

### *Experiment no. 3: ER $\alpha$ KO exposure and tissue collection*

Intact male and OVX female ER $\alpha$  KO mice were divided into 4 treatment groups (n = 6/treatment/sex): Oil, EE2, BDE-47 (1 mg/kg), and the OPFR mixture (1 mg/kg). Age ranges at the start of dosing for males was 10–12 weeks, and date of ovariectomy for females was 10–12 weeks. KOs were dosed for 4 weeks. After dosing, all mice were sedated, decapitated, and prepared for brain, liver, and plasma collection as described above. ARC and liver RNA was prepared for analysis of gene expression, and plasma was prepared and stored for analysis of peptide hormone levels.

### *Reverse transcription and quantitative real-time PCR*

Analysis of gene expression used standard protocols for quantitative real-time PCR (qPCR) as previously published (Mamounis et al. 2014). Briefly, for both ARC and liver RNA, complementary DNA (cDNA) was synthesized using a standard Superscript III reverse transcriptase (Life Technologies) protocol: 5 min at 25 °C,

60 min at 50 °C, and 15 min at 70 °C. All primers were designed to span exon-exon junctions and synthesized by Life Technologies, using Clone Manager 5 software (Sci Ed Software, Cary, North Carolina). See Supplementary Table 1 for a list of all primer sequences. qPCR amplification followed standard protocols for either PowerSYBR Green (Life Technologies) or Sso Advanced SYBR Green (BioRad, Hercules, CA) master mixes on CFX-Connect Real-time PCR instrument (BioRad). All efficiencies were between 90% and 110%. The relative mRNA expression was calculated using the  $\Delta\Delta CT$  method and a calibrator of diluted (1:20) cDNA from liver or medioBH of an untreated male. The geometric mean of the reference genes  $\beta$ -actin (Actb), hypoxanthine guanine phosphoribosyl transferase 1 (Hprt), and glyceraldehyde 3-phosphate (Gapdh) was used to calculate  $\delta Cq$  values. Quantification values were generated only from samples showing a single product at the expected melting point. All gene expression data were expressed as an n-fold difference relative to the calibrator (Schmittgen and Livak 2008).

#### *Dosing and serum sample analytical methods*

Serum samples from mice treated with either 10 mg/kg/d of BDE-47 or the OPFR mixture were spiked with 1  $\mu$ g/ml of the internal standard ( $^{13}C_{12}$  BDE-47 and TPP D15, respectively) for recovery calculations, having a final concentration of 50 ng/ml. After spiking, the samples were vortexed for 1 min followed by the addition of toluene. Samples were then vortexed for 2 min and allowed to stand for 5 min. Finally, samples were centrifuged at 6500 rpm at 4 °C for 5 min, and the organic layer was collected for gas chromatography-mass spectrometry (GC-MS) analysis.

Serum sample extracts were analyzed using an Agilent 7890B GC/240 ion trap MS. Chromatographic separation of the analytes was achieved using an Agilent DB-XLB microcapillary column (30 m  $\times$  180  $\mu$ m i.d.  $\times$  0.18  $\mu$ m film thickness; Santa Clara, California). Two microliter of serum extract were injected into a septum programmable injector in splitless mode. The septum programmable injector temperature program was held at 150 °C for 0.5 min, then ramped up to 280 °C at a rate of 150 °C/min and held for 12 min, before dropping to 150 °C at a rate of 8 °C/min. The GC oven temperature program was held at 90 °C for 2 min followed by a temperature ramp of 18 °C/min to 200 °C, and a final temperature ramp of 5 °C/min to 300 °C with a 4.89-min hold. Serum extracts were analyzed under electron impact ionization using selected ion storage of the most abundant ion. These ions were used for quantitation of each compound: TDCPP (99 m/z), TPP (326 m/z), TPP D15 (341 m/z), BDE-47 (487 m/z), 13C12 BDE-47 (498 m/z), and TCP (366 m/z). Analyte responses were used to quantify each analyte against an external calibration curve in serum and recovery of internal standards (TPP D15 for TDCPP, TPP, and TCP; 13C12 BDE-47 for BDE-47) was calculated. The BDE-47 dosing solution (1 mg/ml dose) had a concentration of  $0.98 \pm 0.22$  mg/ml, and the OPFR dosing solution (1 mg/ml dose) had a concentration of  $0.99 \pm 0.18$  mg/ml (TDCPP),  $0.98 \pm 0.33$  mg/ml (TPP), and  $1.0 \pm 0.24$  mg/ml (TCP). The limits of detection for TDCPP, TPP, TCP, and PBDE-47 were 0.09, 0.02, 0.03, and 0.01 ng/ml, respectively.

#### *Data analysis*

All RNA extractions, reverse transcriptions, and qPCR analyses were conducted as a group for the experiment 1 ARC and liver samples. All the KO gene expression studies in experiment 3 were prepared and analyzed together. All WT physiology data were from experiment 2, except for the addition of the body weight data from experiment 1. All metabolic hormone data from WT (experiment 2) and KO (experiment 3) mice were analyzed in the same batch of multiplex plates.

All the data are expressed as mean  $\pm$  SEM. All physiology data were analyzed using GraphPad Prism software (GraphPad Software, La Jolla, California) by a 2-way ANOVA (EDC and genotype) with a post hoc Bonferroni's multiple comparisons test except for the GTT and ITT, which were analyzed by a repeated-measures ANOVA (EDC and time). All gene expression data were analyzed by a 1-way ANOVA within sex. All GC-MS data were analyzed by a 1-way ANOVA with a post hoc Tukey's multiple comparison test. We did not analyze for sex differences because sexes were not of similar condition (intact vs gonadectomized). In all experiments, effects were considered significant at an  $\alpha \leq 0.05$ .

## A-1.4 Results

### *Concentrations of BDE-47 and OPFR in Serum Samples*

Quantitative analysis of the serum extracts from WT mice treated with BDE-47 (10 mg/kg/d, n = 8 for each sex) or OPFR mixture (TPP, TCP, and TDCPP; 10 mg/kg/d of each OPFR, n = 8 for each sex) were performed using GC-MS (Figure 1) . Serum extracts were injected and analyzed in triplicate. Within intact WT males, the serum concentration of BDE-47 ( $70 \pm 11$  ng/ml) was significantly higher ( $p < .05$ ) than that of TPP ( $2.8 \pm 0.63$  ng/ml), TCP ( $5.6 \pm 0.89$  ng/ml), and TDCPP ( $3.7 \pm 0.61$  ng/ml). Similarly, within OVX WT females, the serum concentration of BDE-47 ( $103 \pm 12.4$  ng/ml) was also significantly higher ( $p < .05$ ) than that of TPP ( $1.0 \pm 0.23$  ng/ml), TCP ( $4.7 \pm 0.91$  ng/ml), and TDCPP ( $3.9 \pm 0.86$  ng/ml).

### *Effects of the FR on Body Weight, Energy Intake, and Glucose Homeostasis*

Body weight gain was determined by calculating percent body weight gain ( $[(\text{week 4 body weight} \div \text{week 0 body weight}) \times 100]$ ; Figs. 2A and B). Data from experiments 1 and 2 were combined for oil, EE2, BDE-1, and OP-1 for the WT and presented with data from experiment 3 (KO). Within intact WT males, there was an effect of EDC ( $F[5, 74] = 5.361$ ,  $p < .001$ ). Within KO males, there was no effect of EDC on percent body weight gain. However, when comparing oil, EE2, BDE-1, and OP-1 doses between WT and KO, body weight gain was determined by both genotype ( $F[1, 81] = 60.85$ ,  $p < .0001$ ) and EDC ( $F[3, 81] = 4.128$ ,  $p < .01$ ). Specifically, EE2 ( $p < .01$ ), OP-1 ( $p < .05$ ), and OP-10 ( $p < .05$ ) reduced WT male



body weights, and KO males in all treatment groups gained more weight than their WT counterparts. In OVX WT females, body weight gain was augmented by EE2 ( $p < .001$ ), BDE-10 ( $p < .05$ ), and OP-10 ( $p < .05$ ) compared with oil-treated females ( $F[5, 73] = 8.513$ ,  $p < .0001$ ). When comparing treatment groups between WT and KO females, only EDC affected body weight gain ( $F[3, 79] = 5.384$ ,  $p < .01$ ), not genotype, unlike in males. There was no effect of EDC on body composition, ie, fat and lean mass, in intact males (Figure 2C) or OVX females (Figure 2D). Because we only measured body composition at week 4, we cannot state with any certainty that the changes in body weight involved changes in adiposity.

In addition to gaining less mass, OP-1-treated WT males consumed less ( $p < .05$ ) than oil-treated WT males ( $F[3, 12] = 3.757$ ,  $p < .05$ ; Figure 3A). Feeding efficiency in intact WT males was reduced by EE2 compared with oil-treated males ( $p < .05$ ;  $F[3, 12] = 2.983$ ,  $p < .05$ ; Figure 3B). There was no effect of EDC on energy intake or feeding efficiency in OVX WT females. Both BDE-1 and OP-1 induced hyperglycemia in fasted (5 h) WT males (BDE-1:  $p < .01$ ; OP-1:  $p < .01$ ;  $F[3, 28] = 5.191$ ,  $p < .01$ ; Figure 3C). There was no effect of EDC on fasting glucose levels in OVX WT females.

EDC had no effect on glucose clearance or insulin tolerance in males (Figs. 4A–C). Conversely, EDC increased glucose clearance in OVX WT females ( $F[3, 27] = 3.753$ ,  $p < .05$ ; Figure 4D). Specifically, EE2 and BDE-1 increased glucose clearance at 30 min ( $p < .05$  and  $p < .05$ , respectively) and 60 min ( $p < .01$  and  $p < .01$ , respectively).

.01, respectively). There was no effect of EDC on insulin tolerance in OVX WT females, although EE2 at 30 min ( $p < .05$ ) reduced glucose clearance, indicating a slower glucose uptake compared with oil-treated females (Figure 4E). Analysis of area under the curve illustrated the increase in glucose clearance by EE2 ( $p < .01$ ) and BDE-1 ( $p < .05$ ) (EDC:  $F[3, 27] = 4.137$ ,  $p < .05$ ; Figure 4F).

Plasma peptide hormone levels were measured in males and females from experiment 2 (WT) and experiment 3 (KO). In males, ghrelin was impacted by EDC ( $F[3, 48] = 3.662$ ,  $p < .05$ ), but not by genotype. Specifically, EE2 ( $p < .05$ ) and OP-1 ( $p < .01$ ) induced hyperghrelinemia in WT males, increasing plasma ghrelin by 4-fold (Figure 5A). Plasma leptin in males was differentially expressed between the genotypes ( $F[1, 48] = 10.92$ ,  $p < .01$ ) and EDC ( $F[3, 48] = 3.557$ ,  $p < .05$ ; Figure 5B). Leptin was reduced by EE2 ( $p < .05$ ) and OP-1 ( $p < .05$ ) in WT ( $F[3, 48] = 3.557$ ,  $p < .5$ ) and increased by OP-1 ( $p < .05$ ) in KO. The differential effect of OP-1 on insulin between WT and KO was significant ( $p < .01$ ). Plasma insulin levels were also affected by genotype ( $F[1, 48] = 18.09$ ,  $p < .0001$ ) and EDC ( $F[3, 48] = 6.405$ ,  $p < .001$ ; Figure 5C). EE2 ( $p < .001$ ) and OP-1 ( $p < .05$ ) reduced plasma insulin levels in WT. Although there was no effect of EDC in KO males, KO males treated with EE2 ( $p < .01$ ) and OP-1 ( $p < .05$ ) expressed higher insulin levels than WT counterparts.

In OVX WT and KO females, there was no effect of EDC or genotype on plasma ghrelin, although OP-1 reduced ghrelin in WT females compared with oil-treated WT ( $p < .05$ ; Figure 5D). Plasma leptin levels were not altered by EDC but were

differentially expressed between the genotypes (KO  $\gg$  WT) ( $F[1, 47] = 46.04$ ,  $p < .0001$ ; Figure 5E). Plasma insulin levels were affected by EDC ( $F[3, 47] = 3.475$ ,  $p < .05$ ) and genotype ( $F[1, 47] = 32.67$ ,  $p < .0001$ ) with a significant interaction between the 2 factors ( $F[3, 47] = 4.075$ ,  $p < .05$ ; Figure 5F). BDE-1 increased plasma insulin only in KO females ( $p < .01$ ) producing a difference between WT and KO treated with BDE-1 ( $p < .0001$ ).

E2 replacement is known to induce uterine hypertrophy through an ER $\alpha$ -mediated mechanism (Mamounis et al. 2014). In our study, only EE2 increased uterine weight ( $2.2 \pm 0.5$  g,  $p < .01$ ) compared with oil ( $0.6 \pm 0.5$  g) in WT females. There were no significant effects of FR treatment on uterine weight at any dose in WT or KO (data not shown).

#### *ARC Gene Expression in WT and ERKO Mice*

We selected E2-responsive ARC genes primarily involved in reproduction, energy homeostasis, and neuronal excitability (Qiu et al. 2006; Roepke et al. 2007; Yang et al. 2016a; Yang et al. 2016b; Yasrebi et al. 2016). Genes were grouped based on function as neuropeptides, hormone and nuclear receptors, and cation channels. Differential ARC gene expression by FR in intact male and OVX female WT and KO mice is reported in Tables 1 and 2. The first set of ARC genes are the neuropeptides involved in energy homeostasis including POMC, cocaine- and amphetamine-regulated transcript (CART), NPY, and AgRP. These neuropeptides were differentially regulated by FR in males. *Pomc* expression was affected by EDC ( $F[5, 40] = 4.92$ ,  $p < .01$ ) and was increased approximately 2-fold by OP-1 ( $p$

< .001) and OP-10 ( $p < .001$ ). In females, OP-10 reduced *Pomc* expression by approximately 30% ( $p < .05$ ). In males, all EDC reduced *Cart* expression by approximately 50%–70% (all:  $p < .0001$ ;  $F[5, 40] = 16.79$ ,  $p < .0001$ ), and in females, BDE-1 ( $p < .05$ ) and OP-10 ( $p < .05$ ) treatment reduced *Cart* expression by approximately 30% ( $F[5, 40] = 2.67$ ,  $p < .05$ ). *Npy* expression was affected by EDC only in males ( $F[5, 40] = 32.16$ ,  $p < .0001$ ), in which all EDC reduced *Npy* expression by approximately 30%–70% (all:  $P < 0.001$ ). *Agrp* expression was increased approximately 2-fold after OP-10 treatment ( $p < .001$ ) in males ( $F[5, 40] = 6.24$ ,  $p < .001$ ) while no EDC had any affect in OVX females. Another ARC neuropeptide under the control of E2 is kisspeptin. *Kiss1* expression was increased approximately 2-fold by both FR in males ( $F[5, 40] = 2.54$ ,  $p < .05$ ) and females ( $F[5, 42] = 4.26$ ,  $p < .01$ ). In KO mice, there were no effects of any EDC on *Pomc*, *Npy*, and *Agrp* expression. *Cart* was reduced by OP-1 treatment ( $p < .05$ ;  $F[5, 20] = 3.94$ ,  $p < .05$ ), and *Kiss1* was reduced by EE2 ( $p < .05$ ) and BDE-47 ( $p < .05$ ;  $F[5, 20] = 3.66$ ,  $p < .05$ ) in males.

Hormone and nuclear receptors for E2 (*ERα*/*Esr1*), ghrelin (*GHSR*), insulin (*InsR*), leptin (*LepR*), and fatty acids (*PPARγ*) modulate energy balance through actions in the ARC (Long et al. 2014; Qiu et al. 2010; Qiu et al. 2014; Yasrebi et al. 2016; Yasrebi et al. 2017). *Esr1* expression was reduced by approximately 50%–60% by all EDC in males ( $F[5, 40] = 31.87$ ,  $p < .0001$ ) but not in females. *Insr* expression was increased by all EDC 6- to 8-fold in males (all:  $p < .0001$  except BDE-10:  $p < .001$ ;  $F[5, 40] = 11.88$ ,  $p < .0001$ ) and 2- to 3-fold in females (all:  $p < .0001$  except EE2:  $p < .05$ ;  $F[5, 42] = 11.22$ ,  $p < .0001$ ). *LepR* expression was increased

approximately 4-fold by all EDC in males (all:  $p < .0001$  except BDE-10:  $p < .001$ ;  $F[5, 40] = 11.31$ ,  $p < .0001$ ) but not in females. *Ghsr* expression was also augmented 4- to 6-fold by EDC in males ( $F[5, 40] = 25.2$ ,  $p < .0001$ ; all:  $p < .0001$ ) but reduced approximately 10%–20% in females ( $F[5, 42] = 4.24$ ,  $p < .01$ ; BDE-10:  $p < .01$ ; OP-1 and OP-10:  $p < .05$ ). *Ppar $\gamma$*  expression in males was augmented 2- to 3-fold by all EDC except for OP-1 (EE2:  $p < .0001$ ; BDE-1:  $p < .01$ ; BDE-10:  $p < .05$ ; OP-10:  $p < .05$ ;  $F[5, 40] = 2.63$ ,  $p < .05$ ), and *Ppar $\gamma$*  expression in females was augmented approximately 2-fold by EE2 ( $p < .05$ ) and OP-1 ( $p < .05$ ;  $F[5, 42] = 3.39$ ,  $p < .05$ ). In KO mice, *Ghsr* and *Insr* expression was not altered by EDC in males or females. Conversely, *Lepr* expression was decreased by EE2 ( $p < .05$ ), BDE-1 ( $p < .01$ ), and OP-1 ( $p < .001$ ) in males ( $F[3, 18] = 41.80$ ,  $p < .0001$ ). As in the WT, *Ppar $\gamma$*  expression was augmented by OP-1 ( $p < .05$ ) in KO females ( $F[3, 18] = 7.816$ ,  $p < .01$ ).

We also examined cation channel subunits that are involved in neuroendocrine functions including the potassium channel KCNQ subunits (KCNQ2, -3, -5) (Roepke et al. 2011; Roepke et al. 2012), T-type calcium channel subunits (Cav3.1, Cav3.2, Cav3.3) (Bosch et al. 2009; Qiu et al. 2006), and nonselective cation current canonical transient receptor potential 5 (TRPC5) (Qiu et al. 2010; Qiu et al. 2014) (see Table 2). *Kcnq2* expression was not changed by FR in WT females but was increased by EE2 ( $p < .0001$ ;  $F[5, 42] = 5.64$ ,  $p < .001$ ). In WT males, EE2 ( $p < .0001$ ), BDE-10 ( $p < .01$ ), OP-1 ( $p < .0001$ ), and OP-10 ( $p < .0001$ ) increased *Kcnq2* expression 2- to 3-fold ( $F[5, 40] = 11.9$ ,  $p < .0001$ ). As with *Kcnq2*, *Kcnq3* expression in females was not altered by EDC except for EE2 ( $p < .001$ ;

$F[5, 42] = 12.04$ ,  $p < .0001$ ). *Kcnq3* expression in males was increased approximately 2- to 3-fold by EE2 ( $p < .0001$ ), BDE-1 ( $p < .05$ ), BDE-10 ( $p < .0001$ ), OP-1 ( $p < .0001$ ), and OP-10 ( $p < .0001$ ;  $F[5, 40] = 13.15$ ,  $p < .0001$ ). *Kcnq5* expression in females was also not changed by EDC except for EE2 ( $p < .0001$ ;  $F[5, 42] = 12.29$ ,  $p < .0001$ ) and was increased 2- to 3-fold in males by EE2 ( $p < .001$ ), BDE-10 ( $p < .01$ ), OP-1 ( $p < .0001$ ) and OP-10 ( $p < .001$ ;  $F[5, 40] = 8.42$ ,  $p < .0001$ ). In KO mice, *Kcnq2* and *Kcnq5* expression was not altered by EDC in males or females. However, *Kcnq3* expression was decreased by OP-1 ( $p < .05$ ) only in females ( $F[3, 18] = 4.34$ ,  $p < .05$ ).

ARC expression of the T-type calcium channel subunits was also regulated by EDC exposure. *Cav3.1* (*Cacna1g*) expression was increased 3- to 5-fold by EDC in males (EE2:  $p < .0001$ ; BDE-1:  $p < .05$ ; BDE-10:  $p < .01$ ; OP-1:  $p < .01$ ; OP-10:  $p < .01$ ;  $F[5, 40] = 6.25$ ,  $p < .001$ ) and females (all:  $p < .0001$ ;  $F[5, 42] = 25.06$ ,  $p < .0001$ ). *Cav3.2* (*Cacna1h*) expression was increased 2- to 3-fold by all EDC, except BDE-1 in males ( $F[5, 40] = 8.23$ ,  $p < .0001$ ), and only by EE2 ( $p < .05$ ) in females ( $F[5, 42] = 4.9$ ,  $p < .01$ ). Similarly, *Cav3.3* (*Cacna1i*) expression was increased 2- to 3-fold by all EDC in males ( $F[5, 40] = 11.53$ ,  $p < .0001$ ) except for BDE-1 and only by EE2 in females ( $p < .01$ ;  $F[5, 42] = 4.75$ ,  $p < .01$ ). All EDC exposures increased *Trpc5* expression in males 3- to 5-fold ( $F[5, 40] = 17.71$ ,  $p < .0001$ ; all:  $p < .0001$  except BDE-1:  $p < .001$ ) with no effect in females except a reduction by EE2 ( $p < .05$ ;  $F[5, 42] = 2.97$ ,  $p < .05$ ). In KO mice, *Cav3.2* expression was reduced by EDC in males ( $F[3, 18] = 5.52$ ,  $p < .01$ ; EE2:  $p < .05$ , BDE-1:  $p < .05$ ; OP-1:  $p < .01$ ). EDC had no effect on *Cav3.1*, *Cav3.3*, or *Trpc5* in the KO.

*Regulation of Xenobiotic Receptor Target Genes in Livers from WT and ERKO Mice*

PBDE are known to activate xenobiotic receptors (pregnane X receptor [PXR], PPAR $\alpha$ , constitutive androstane receptor [CAR]) in the liver and subsequently modulate receptor target genes (Pacyniak et al. 2007; Sueyoshi et al. 2014). In WT males, the target genes regulated by EDC were Abcb11 (Bsep) ( $F[5, 40] = 84.16$ ,  $p < .0001$ ), Cd36 ( $F[5, 40] = 4.93$ ,  $p < .01$ ), Cyp2b10 ( $F[5, 40] = 10.89$ ,  $p < .0001$ ), Cyp3a11 ( $F[5, 40] = 19.27$ ,  $p < .0001$ ), Cyp4a10 ( $F[5, 40] = 2.66$ ,  $p < .05$ ), Slc51b (Ost $\beta$ ) ( $F[5, 40] = 6.49$ ,  $p < .001$ ), and Nr0b2 (Shp) ( $F[5, 40] = 6.66$ ,  $p < .001$ ) (see Table 3). In WT females, the target genes regulated by EDC were Bsep ( $F[5, 41] = 65.91$ ,  $p < .0001$ ), Cd36 ( $F[5, 41] = 7.90$ ,  $p < .0001$ ), Cyp2b10 ( $F[5, 41] = 17.89$ ,  $p < .0001$ ), Cyp3a11 ( $F[5, 41] = 15.0$ ,  $p < .0001$ ), Cyp4a10 ( $F[5, 41] = 3.37$ ,  $p < .05$ ), Cyp7a1 ( $F[5, 41] = 5.64$ ,  $p < .001$ ), Ost $\beta$  ( $F[5, 41] = 6.43$ ,  $p < .001$ ), and Shp ( $F[5, 41] = 17.91$ ,  $p < .0001$ ). PBDE treatment increased expression of Bsep, Ost $\beta$ , Cyp3a11, and Cyp2b10 in males and females. OPFR treatment only increased expression of Cyp3a11 and Cyp2b10 in males. PBDE and OPFR suppressed Cd36 in both males and females, and OPFR suppressed Shp in males and females. In KO mice, the only target gene in the liver increased by FR (BDE-1) was Cd36 ( $p < .05$ ) in males ( $F[3, 19] = 3.81$ ,  $p < .05$ ).

### A-1.5 Discussion

Our characterization of the effects of adult FR exposure on the neuroendocrine control of energy homeostasis began with measurements of the FR in mouse serum. These serum concentrations (low ng/ml) correlate to the concentrations found in human serum, hair, nail, and urine samples and supports the environmental relevance of our dosing concentrations. In human serum collected in the United States, TDCPP and TPP were not detected in serum, although BDE-47 was detected in 94% of the samples with a geomean concentration of 17 ng/g lipid (Liu et al. 2016a). However, in the same study, both TPP and TDCPP were detected in hair, fingernail, and toenail samples at concentrations ranging from 280 to 1980 ng/g for TPP and 230–390 ng/g TDCPP. In another study from China, TPP was measured at concentrations of 30–40 ng/g lipid in human serum with TPP consisting of approximately 5% of the total OPFR concentration (Ma et al. 2017). The metabolites for TDCPP (bis[1, 3-dichloro-2-propyl] phosphate), and TPP (diphenyl phosphate [DPP]) are detectable in urine samples from adults and children in the range of 0.1–1000 ng/ml, but most commonly between 1 and 10 ng/ml (Butt et al. 2014; Hoffman et al. 2017a; Meeker et al. 2013b). Interestingly, TPP was not detected in serum from rat dams dosed to 1 mg/kg TPP for 10 days, while DPP was detected at approximately 700 ng/ml in the urine (Phillips et al. 2016). The differences in the serum concentrations between the OPFR compounds and PBDE-47 were likely due to the detoxification and clearance rates of each compound. Indeed, the whole-body half-life ( $t_{1/2\alpha}$ ) of BDE-47 is 1.5 days and 1.1 days in blood, while the terminal half-life ( $t_{1/2\beta}$ ) is 23 and 13 days,



respectively (Staskal et al. 2005). The half-life of the OPFR range from 0.63 h ( $t_{1/2\alpha}$ ) and 13.9 days ( $t_{1/2\beta}$ ) for TPP (Carrington and Abou-Donia 1988) to 46 h ( $t_{1/2\beta}$ ) for TCP (Abou-Donia et al. 1990) and <5 days for TDCPP in rats (Lynn et al. 1980). Despite the higher clearance rates, these 3 OPFR, or their metabolites, may accumulate with repeated dosing sufficiently to impact to the neuroendocrine axis. Further investigation into the partition and deposition of these 3 OPFR in the adult mouse model especially in the hypothalamus and whole brain is warranted.

There are few in vivo studies examining the effects of OPFR treatment on the hypothalamic control of energy balance in adult male or female rodents. Due to the ability of BDE-47, TDCPP, TPP, and TCP (or their metabolites) to interact with ER, our objective was to determine if the selected FR alter ARC gene expression of known E2-regulated genes in a sex-dependent manner using the mouse (Kojima et al. 2013; Liu et al. 2012). We demonstrated that FR, especially OPFR, differentially regulate the expression of ARC genes in adult, intact males and OVX females. In WT males, OPFR increased *Pomc* and decreased *Npy*, producing an anorectic neuropeptide gene profile. Consequently, OPFR-exposed WT males consumed less chow (a decrease in energy intake) than the oil-treated WT males, which reduced weight gain over the 4 weeks of dosing. As expected, KO males weighed more than their WT counterparts, regardless of EDC treatment, and were not susceptible to the effects of EE2 and OPFR on weight gain. Conversely, WT females exposed to the high-dose of OPFR gained more weight than the oil-treated females, which correlated with a reduction in anorexigenic (*Pomc/Cart*) gene expression. As expected, OVX KO females did not gain more weight than their WT

counterparts and were not susceptible to EDC treatment like KO males. These novel findings indicate that the effects of adulthood OPFR exposure are potentially dependent on the differential actions of ER $\alpha$  within each sex, although we cannot state this with certainty since the female mice were OVX. Alternatively, OPFR exposure may sensitize females to an obesogenic diet while reducing sensitivity in males, especially during a longer duration of oral dosing.

These effects on neuropeptide gene expression may be partially dependent on ER $\alpha$ , as only *Cart* was downregulated in KO males similar to WT males. Furthermore, FR (and EE2) treatment suppressed male ARC *Esr1* gene expression, which is a similar response to ligand exposure (E2 treatment) in female mice (Yang et al. 2016a; Yang et al. 2016b). However, female *Esr1* gene expression was unaffected. It is well established that ovariectomy promotes hyperphagia and body weight gain, which can be prevented by E2 replacement acting through ER $\alpha$  (Asarian and Geary 2002). Therefore, OPFR may not be acting directly on ER $\alpha$  but via regulation of the *Esr1* gene. FR also interact with multiple steroid and nuclear receptors in vitro such as PXR, thyroid receptors, PPAR $\alpha/\gamma$ , androgen receptors (ARs), and mineralocorticoid and glucocorticoid receptors (Belcher et al. 2014; Hu et al. 2014; Kojima et al. 2013). Interestingly, PPAR $\gamma$  expression is elevated by FR in males and females and may mediate, in part, the effects of these compounds on ARC gene expression. PPAR $\gamma$  is a known modulator of POMC neuronal activity and mediates the impact of high-fat diets on the hypothalamus (Long et al. 2014). However, hypothalamic PPAR $\gamma$  activation augments *Npy* and *Agrp* expression in the ARC (Garretson et al. 2015), but these

findings do not align with our results. Further investigation is required to determine which nuclear or steroid receptors are interacting with FR either directly or indirectly to control ARC gene expression; those studies should utilize global or brain-specific ER $\alpha$ / $\beta$ , PPAR $\gamma$ , or other nuclear receptor KO models.

Whether interacting with ER $\alpha$  or PPAR $\gamma$ , FR upregulated ARC expression of peptide hormone receptors Ghnr, Insr, and Lepr in males and Insr in females. Insr is a tyrosine kinase receptor activated by insulin to control glucose metabolism and suppress appetite (Hill et al. 2010). ARC insulin signaling activates POMC neurons and inhibits NPY neurons (Qiu et al. 2014). The adipokine leptin also activates POMC neurons and inhibits NPY neurons through its receptor (Qiu et al. 2010). Both insulin and leptin receptor activation targets nonselective canonical transient receptor potential (TRPC5) channels in POMC and KNDy neurons (Qiu et al., 2010, 2014). Activation of these channels causes depolarization in the neurosecretory neurons, leading to suppressed food intake and other physiological outcomes. Therefore, an increase in Insr or Lepr expression in POMC neurons or an increase of Trpc5 expression would increase their sensitivity to insulin and leptin, leading to decreased food intake.

OPFR also affected leptin and insulin plasma levels. Leptin production from adipose tissue and insulin production from the pancreas were reduced by OPFR in WT males but were augmented in KO males. The differences between the genotypes indicate that the peripheral actions of OPFR may not be mediated by ER $\alpha$  but rather by other nuclear receptors including PPAR $\gamma$  (Kim et al. 2013;

Kubota et al. 1999; Tung et al. 2017). Consequently, the increase in leptin and insulin receptor expression in the ARC may be offset by the OPFR-induced hypoinsulinemia and hypoleptinemia in WT males. Furthermore, the increase in receptor may be due to the decrease in ligand as many hormone receptors are downregulated or undergo desensitization when ligand concentrations are elevated (Zabeau et al. 2003). In females, leptin production was not modulated by FR. However, leptin production in KO females was higher compared with WT females. The elevated leptin in KO has been previously reported and is indicative of greater adiposity in KO females (Yasrebi et al. 2017). Interestingly, insulin was elevated by BDE-47 (1 mg/kg) in KO females compared with both oil-treated KO and BDE-47-treated WT females. This unexpected finding suggests that ER $\alpha$  protects against BDE-47-induced insulin production in OVX females or that the lack of ER $\alpha$  disrupts the interactions of FR with the pancreatic  $\beta$ -cells.

GHSR is a G-protein-coupled receptor that is activated by ghrelin, a hormone secreted by the stomach to promote hunger (Andrews 2011). In the ARC, GHSR is primarily found in NPY/AgRP, KNDy, and GHRH neurons (Yang et al. 2016a; Yang et al. 2016b; Yasrebi et al. 2016). In our study, GHSR expression was upregulated by FR in males but not in females. Interestingly, E2 upregulates Ghsr in the ARC through ER $\alpha$  (Yang et al. 2016a; Yang et al. 2016b) primarily in KNDy neurons (Yang et al. 2016a; Yang et al. 2016b) and not in NPY/AgRP neurons (Yasrebi et al. 2016). Considering the fact that males consumed less energy with OPFR, we hypothesize that the increase in GHSR expression is occurring in KNDy neurons from WT males and potentially impacts the effects of ghrelin on the

negative feedback of gonadal steroids on luteinizing hormone pulse frequency. This may be especially true in WT males due to OPFR-induced hyperghrelinemia, which is potentially mediated by ER $\alpha$ .

Activation of the GHSR in NPY neurons suppresses the KCNQ-mediated M-current (Yasrebi et al. 2016). When stimulated by depolarization, KCNQ (Kv.7) channels facilitate an outward potassium current (M-current) to stabilize membrane potential and reduce action potential frequency (Roepke et al. 2011). KCNQ channel subunits Kcnq2, Kcnq3, and Kcnq5 are highly expressed in the ARC POMC and NPY neurons (Roepke et al. 2007), and expression of these subunits are controlled in NPY neurons by fasting in males and females (Roepke et al. 2011). In our study, KCNQ expression was increased in males by FR but only by EE2 in females, which is similar to the effects of E2 in females (Roepke et al. 2011). An increase in KCNQ expression and subsequent M-current activity would lead to a suppression of neuronal excitability. We hypothesize that these effects are occurring primarily in NPY neurons because such an increase in M-current activity would lead to a decrease in food intake.

T-type calcium channels associated with the Cav3.1 (Cacna1g), Cav3.2 (Cacna1h), and Cav3.3 (Cacna1i) subunits are highly expressed in ARC POMC and KNDy neurons and produce the low-voltage-activated calcium currents responsible for neuronal burst firing and neurotransmitter release (Bosch et al. 2013; Qiu et al. 2006). In female mice, E2 increases Cacna1g in the ARC through an ERE-dependent mechanism (Bosch et al. 2009; Yang et al. 2016a; Yang et al.

2016b), increases *Cacna1h* expression by both ER $\alpha$  and ER $\beta$  activation (Bosch et al. 2009), and increases *Cacna1i* in ARC KNDy neurons (Gottsch et al. 2011). It is unknown whether E2 or androgens control Cav3.x channels in the ARC of males. In our study, FR, along with EE2, increased expression of all 3 subunits in males, but only Cav3.1 in females. Potentially, an increase in Cav 3.x channel expression results in more burst firing in neurosecretory neurons, leading to more frequent secretion of their respective neuropeptides ( $\alpha$ -melanocyte-stimulating hormone (MSH),  $\beta$ -endorphin, kisspeptin, neurokinin B, etc.) and controlling downstream homeostatic functions.

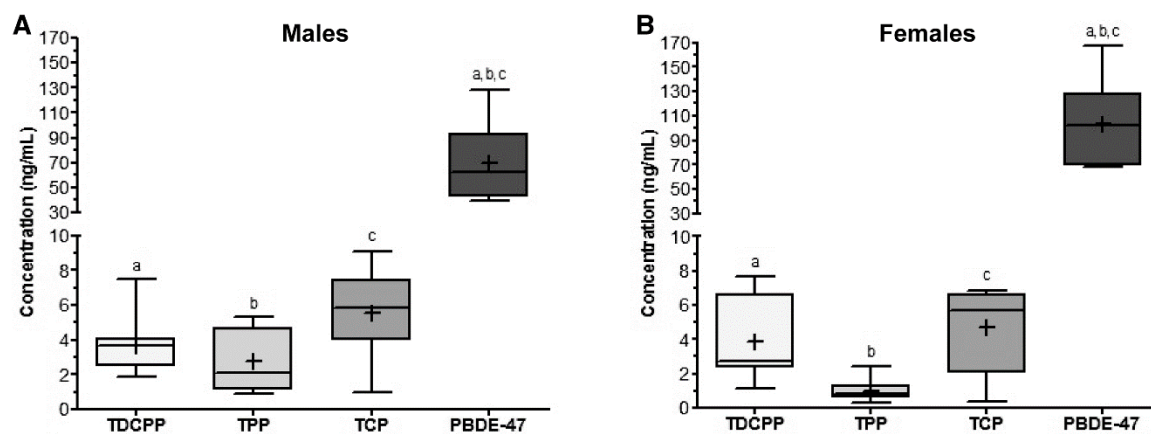
One of these downstream homeostatic functions is glucose homeostasis and, in particular, hepatic glucose production (Lin et al. 2010). Both BDE-47 and OPFR elevated fasting glucose levels in males, indicating an increase in hepatic glucose production either directly by altering liver glucose metabolism or indirectly by altering the neuroendocrine control of glucose production. FR did not have an effect in females, most likely due to the disruptive effects of ovariectomy (loss of E2) on glucose metabolism. Indeed, glucose clearance was augmented by EE2 and BDE-47 in females, recapitulating the effects of E2 replacement in OVX female rodents (Yasrebi et al. 2017). The activation of ER $\alpha$  increases glucose tolerance by regulating the glucose transporter type 4 (GLUT4) expression and activity in skeletal muscle (Gorres et al. 2011). Thus, ER $\alpha$  KO females exhibit impairments to glucose clearance (Yasrebi et al. 2017) and were not examined in this study.

FR, especially PBDE, can induce xenobiotic receptor signaling in the liver. In our in vivo study, BDE-47 activated farnesoid X receptor (FXR), PXR, and CAR target genes in males and females and OPFR activated PXR and CAR only in males. In human hepatic cells, BDE-47 enhances PXR and CAR activation (Hu et al. 2014; Sueyoshi et al. 2014). In fact, in vivo, PBDE (BDE-47, -09, and -209) induce Cyp3a11 and Cyp2b10 gene expression by activating PXR in rat livers (Pacyniak et al. 2007). Whether BDE-47 is a FXR modulator needs detailed study in the future. Little is known about the impacts of in vivo OPFR exposure on xenobiotics receptors and their targets genes in the liver. In transfected human liver cells, TPP activates mouse and human PXR and CAR (Honkakoski et al. 2004). Surprisingly, in the ER $\alpha$  KO, there were no significant effects on target gene expression except for an increase in Cd36 by BDE-47, indicating activation of PPAR $\alpha$  (Gao et al. 2013). The lack of target gene regulation in the KO suggests that these mechanisms are dependent on interaction with ER $\alpha$  or that the loss of ER $\alpha$  in the liver disrupts normal xenobiotic receptor activity or expression.

In summary, FR, or their metabolites, alter hypothalamic and liver gene expression of intact male and OVX female mice and impact food intake and glucose homeostasis in a sex-dependent manner. If ARC neurons, especially POMC and NPY (which express ER $\alpha$  and PPAR $\gamma$ ) are found to be more sensitive to ghrelin, insulin, or leptin after FR exposure, then the downstream control of energy homeostasis (feeding behavior, energy expenditure) could be altered (see Figure 6). Furthermore, if these neurons exhibit elevated cation channel activation, their intrinsic activity and response to these hormones or other neurotransmitters would

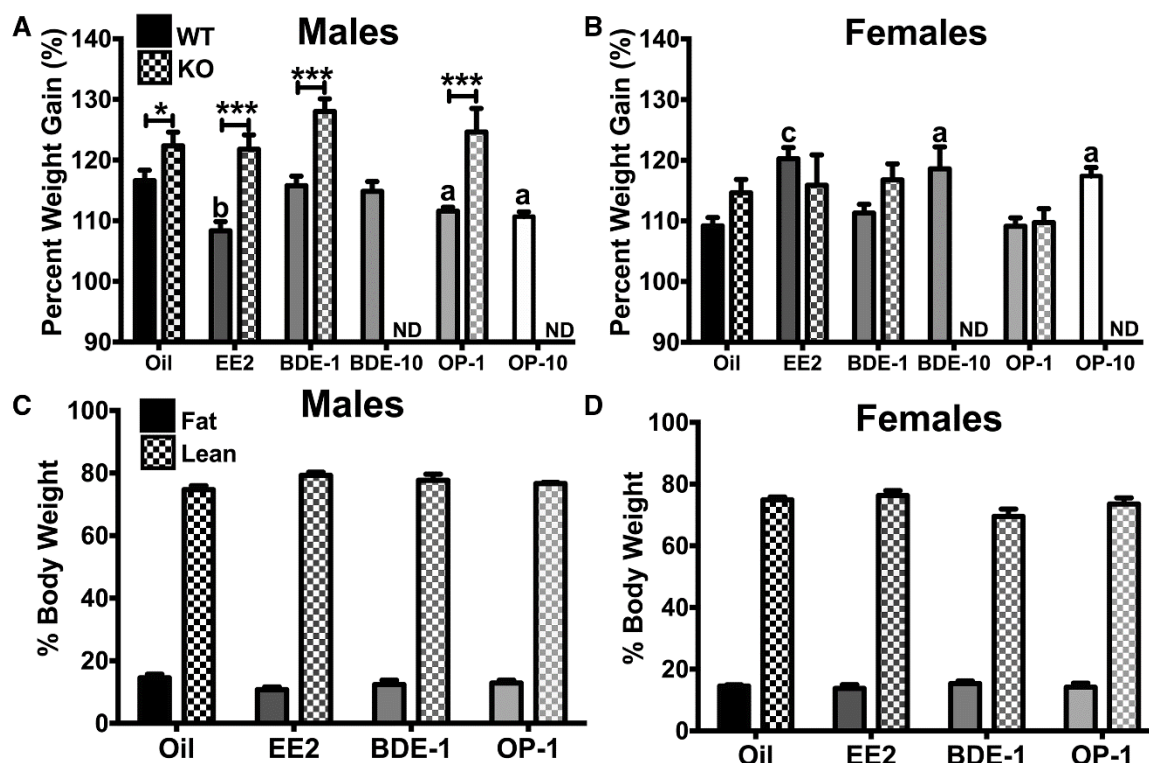
be changed. Because FR augment both hormone receptors and cation channel subunits in the heterogeneous ARC, future experiments will characterize cell type-specific gene expression using standard whole-cell patch clamp electrophysiology coupled with single-cell qPCR after FR treatment. Results from the current study provide insight into the effects of adult exposure to FR in a part of the rodent brain that controls energy homeostasis. Although not “obesogens”, FR, especially OPFR, do disrupt energy homeostasis and may sensitize the animal to further assaults through either diet or concurrent EDC exposure.





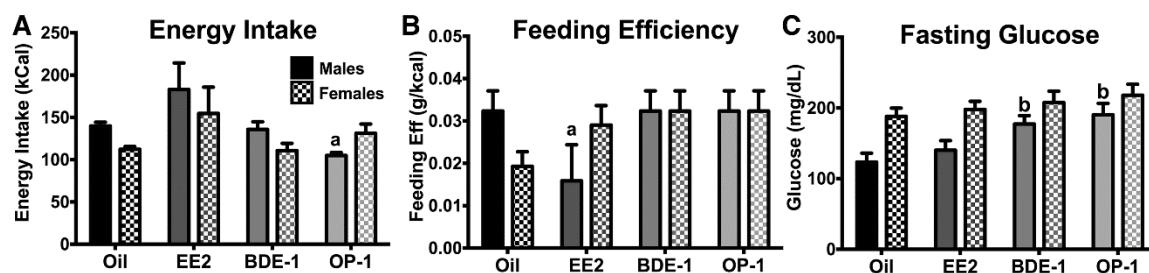
**Figure A-1.1. Serum concentrations of TDCPP, TPP, TCP, and PBDE-47**

(A) Intact WT males and (B) OVX WT females dosed with 10 mg/kg/d of PBDE-47 (BDE-10) or of the OPFR (OP-10) mixture ( $n = 8$  for each group [sex + FR]). Data were analyzed by a 1-way ANOVA with post hoc Tukey's multiple comparison test. Letters denote comparison between analytes where  $a-c$  are  $p < .05$ . Data are presented as mean  $\pm$  SE.



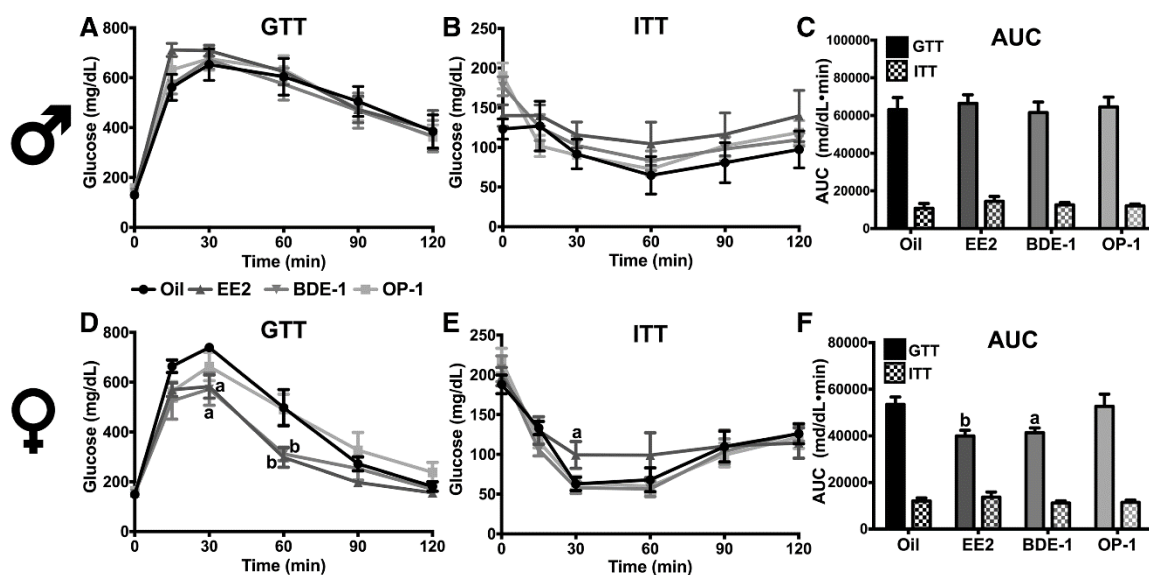
**Figure A-1.2. Percent weight gain and body weight in mice.**

(A) Body weight gain of intact WT (oil, EE2, BDE-1, OP-1:  $n = 16$ ; BDE-10, OP-10:  $n = 8$ ) and ER $\alpha$  KO ( $n = 6$ ) males. (B) Body weight gain of OVX WT (oil, EE2, BDE-1, OP-1:  $n = 16$ ; BDE-10, OP-10:  $n = 8$ ) and ER $\alpha$  KO ( $n = 6$ ) females. (C) Percent fat mass and percent lean mass in intact WT males. (D) Percent fat mass and percent lean mass in OVX WT females. Data were analyzed by a 2-way ANOVA with post hoc Bonferroni's multiple comparisons test. ND, no data. Letters denote comparison to oil and asterisks denote comparison between genotypes: \* $a = p < .05$ ; \*\* $b = p < .01$ ; \*\*\* $c = p < .001$ . Data are presented as mean  $\pm$  SE.



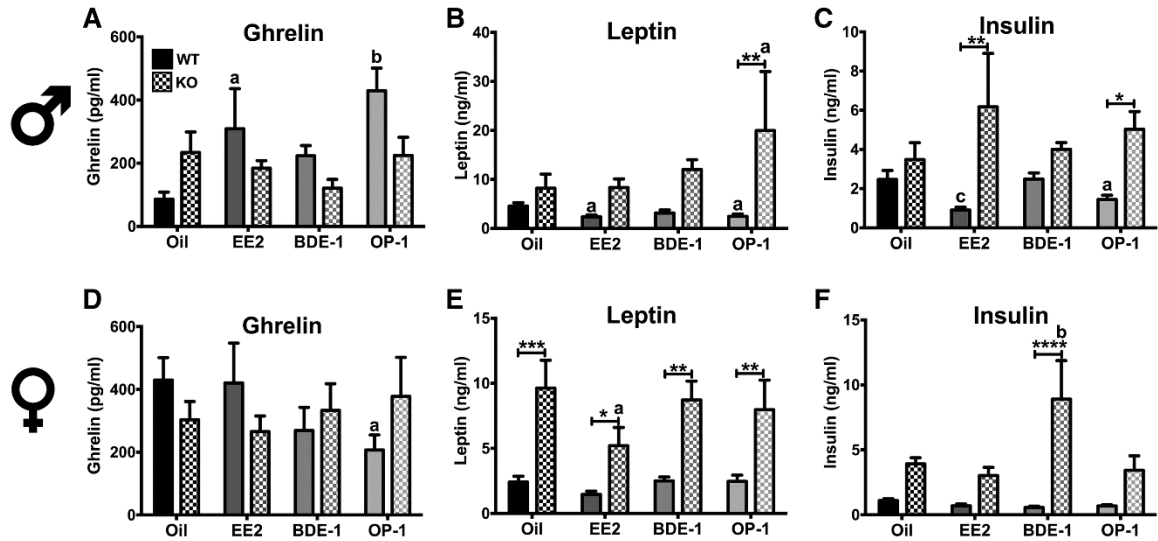
**Figure A-1.3. Weekly energy intake, feeding efficiency, and fasting glucose in mice**

(**A**) Weekly energy intake, (**B**) weekly feeding efficiency, and (**C**) Fasting (5 h) glucose levels in WT males and females. Data ( $n = 4$  for A and B,  $n = 8$  for C) were analyzed by a 2-way ANOVA with post hoc Bonferroni's multiple comparisons test. Letters denote comparison to oil:  $a = p < .05$ ;  $b = p < 0.01$ . Data are presented as mean  $\pm$  SE.



**Figure A-1.4. Glucose and insulin tolerance in mice.**

Glucose tolerance of WT males (**A**) and females (**D**). Insulin tolerance of WT males (**B**) and females (**E**). (**C**) AUC analysis of (A and B). (**F**) AUC analysis of (D) and (E). Data were analyzed by a 2-way ANOVA with post hoc Bonferroni's multiple comparisons test. Letters denote comparison to oil: \*a =  $p < .05$ ; \*\*b =  $p < .01$ . Data ( $n = 8$ ) are presented as mean  $\pm$  SE.



**Figure A-1.5. Plasma levels of peptide hormone ghrelin, leptin, and insulin**

Plasma levels of peptide hormone ghrelin (A, D), leptin (B, E), and insulin (C, F), in male and female WT and KO mice. Data (n = 8 for WT, n = 6 for KO) were analyzed by a 2-way ANOVA with post hoc Bonferroni's multiple comparisons test. Letters denote comparison to oil and asterisks denote comparison between genotypes: \*a =  $p < .05$ ; \*\*b =  $p < .01$ ; \*\*\*c =  $p < .001$ . Data are presented as mean  $\pm$  SE.

**Table A-1.1.** Arcuate expression of neuropeptides and hormone receptors from WT and ERKO male and females

| Gene         | Geno-type | Males      |            |            |            |            | Females    |            |            |            |            |
|--------------|-----------|------------|------------|------------|------------|------------|------------|------------|------------|------------|------------|
|              |           | EE2        | BDE-1      | BDE-10     | OP-1       | OP-10      | EE2        | BDE-1      | BDE-10     | OP-1       | OP-10      |
| <i>Agrp</i>  | WT        | n.s.       | 1.5 ± 0.2a | 1.2 ± 0.2  | n.s.       | 1.9 ± 0.2d | n.s.       | n.s.       | n.s.       | n.s.       | n.s.       |
|              | KO        | n.s.       | n.s.       | NA         | n.s.       | NA         | n.s.       | n.s.       | NA         | n.s.       | NA         |
| <i>Cart</i>  | WT        | 0.5 ± 0.1d | 0.4 ± 0.0d | 0.3 ± 0.0d | 0.4 ± 0.0d | 0.5 ± 0.1d | n.s.       | 0.7 ± 0.1a | n.s.       | n.s.       | 0.7 ± 0.1a |
|              | KO        | n.s.       | n.s.       | NA         | 0.7 ± 0.1a | NA         | n.s.       | n.s.       | NA         | n.s.       | NA         |
| <i>Esr1</i>  | WT        | 0.4 ± 0.0d | 0.4 ± 0.0d | 0.3 ± 0.0d | 0.4 ± 0.0d | 0.4 ± 0.0d | n.s.       | n.s.       | n.s.       | n.s.       | n.s.       |
|              | KO        | NA         | NA         | NA         | NA         | NA         | NA         | NA         | NA         | NA         | NA         |
| <i>Ghsr</i>  | WT        | 6.5 ± 0.4d | 5.5 ± 0.5d | 4.6 ± 0.2d | 4.9 ± 0.1d | 5.4 ± 0.5d | n.s.       | n.s.       | 0.8 ± 0.0b | 0.8 ± 0.0a | 0.8 ± 0.0a |
|              | KO        | n.s.       | n.s.       | NA         | n.s.       | NA         | n.s.       | n.s.       | NA         | n.s.       | NA         |
| <i>Insr</i>  | WT        | 8.1 ± 0.6d | 7.2 ± 1.4c | 5.9 ± 0.5d | 7.3 ± 0.4d | 7.2 ± 0.6d | 1.9 ± 0.1a | 2.7 ± 0.2d | 2.6 ± 0.1d | 2.6 ± 0.2d | 2.5 ± 0.2d |
|              | KO        | n.s.       | n.s.       | NA         | n.s.       | NA         | n.s.       | n.s.       | NA         | n.s.       | NA         |
| <i>Kiss1</i> | WT        | n.s.       | n.s.       | 2.0 ± 0.2a | n.s.       | 2.4 ± 0.5a | n.s.       | n.s.       | 2.6 ± 0.4b | 2.1 ± 0.3a | 2.0 ± 0.2a |
|              | KO        | n.s.       | 0.6 ± 0.1a | NA         | n.s.       | NA         | n.s.       | n.s.       | NA         | n.s.       | NA         |
| <i>Lepr</i>  | WT        | 4.4 ± 0.4d | 4.5 ± 0.6d | 3.3 ± 0.2c | 3.9 ± 0.3d | 4.1 ± 0.2d | n.s.       | n.s.       | n.s.       | n.s.       | n.s.       |
|              | KO        | 0.5 ± 0.1d | 0.4 ± 0.0d | NA         | 0.3 ± 0.1d | NA         | n.s.       | n.s.       | NA         | n.s.       | NA         |
| <i>Npy</i>   | WT        | 0.6 ± 0.0d | 0.4 ± 0.0d | 0.3 ± 0.0d | 0.3 ± 0.0d | 0.5 ± 0.0d | n.s.       | n.s.       | n.s.       | n.s.       | n.s.       |
|              | KO        | n.s.       | n.s.       | NA         | n.s.       | NA         | n.s.       | n.s.       | NA         | n.s.       | NA         |
| <i>Pomc</i>  | WT        | n.s.       | n.s.       | n.s.       | n.s.       | 2.4 ± 0.4c | n.s.       | n.s.       | n.s.       | n.s.       | 0.7 ± 0.1a |
|              | KO        | n.s.       | n.s.       | NA         | n.s.       | NA         | n.s.       | n.s.       | NA         | n.s.       | NA         |
| <i>Pparγ</i> | WT        | 3.4 ± 0.6d | 2.8 ± 0.7b | 2.6 ± 0.5a | n.s.       | 2.4 ± 0.3a | 2.1 ± 0.3a | n.s.       | n.s.       | 2.1 ± 0.4a | n.s.       |
|              | KO        | n.s.       | n.s.       | NA         | n.s.       | NA         | n.s.       | n.s.       | NA         | 2.9 ± 0.4b | NA         |

All data were normalized to oil-treated within each sex: a = P < .05; b = P < .01; c = P < .001; d = P < .0001. n = 7-8 for WT and 5-6 for KO. NA = not applicable and n.s. = not significant.

**Table A-1.2.** Arcuate expression of cation channels from WT and ERKO male and females.

| Gene           | Geno-<br>type | Males              |                    |                    |                    |                    | Females            |                    |                    |                    |                    |
|----------------|---------------|--------------------|--------------------|--------------------|--------------------|--------------------|--------------------|--------------------|--------------------|--------------------|--------------------|
|                |               | EE2                | BDE-1              | BDE-10             | OP-1               | OP-10              | EE2                | BDE-1              | BDE-10             | OP-1               | OP-10              |
| <i>Cacna1g</i> | WT            | 5.0 ± 0.5 <b>d</b> | 3.2 ± 0.5 <b>a</b> | 3.5 ± 0.3 <b>b</b> | 4.1 ± 0.6 <b>b</b> | 4.0 ± 0.6 <b>b</b> | 1.9 ± 0.2          | 4.0 ± 0.3 <b>d</b> | 4.6 ± 0.4 <b>d</b> | 5.4 ± 0.4 <b>d</b> | 4.3 ± 0.8 <b>d</b> |
|                | KO            | n.s.               | 0.9 ± 0.1          | NA                 | n.s.               | NA                 | n.s.               | n.s.               | NA                 | n.s.               | NA                 |
| <i>Cacna1h</i> | WT            | 4.0 ± 0.3 <b>d</b> | 2.4 ± 0.2          | 3.1 ± 0.3 <b>b</b> | 3.2 ± 0.3 <b>b</b> | 3.8 ± 0.6 <b>d</b> | 1.4 ± 0.1 <b>a</b> | n.s.               | n.s.               | 0.9 ± 0.1          | n.s.               |
|                | KO            | 0.7 ± 0.1 <b>a</b> | 0.7 ± 0.1 <b>a</b> | NA                 | 0.6 ± 0.1 <b>b</b> | NA                 | n.s.               | n.s.               | NA                 | 1.5 ± 0.2          | NA                 |
| <i>Cacna1i</i> | WT            | 2.5 ± 0.2 <b>d</b> | 1.8 ± 0.2          | 2.7 ± 0.2 <b>d</b> | 2.9 ± 0.2 <b>d</b> | 2.8 ± 0.3 <b>d</b> | 1.7 ± 0.1 <b>a</b> | n.s.               | n.s.               | n.s.               | n.s.               |
|                | KO            | 1.8 ± 0.2 <b>a</b> | n.s.               | NA                 | n.s.               | NA                 | n.s.               | n.s.               | NA                 | n.s.               | NA                 |
| <i>Kcnq2</i>   | WT            | 2.7 ± 0.1 <b>d</b> | 1.8 ± 0.2          | 2.0 ± 0.1 <b>b</b> | 2.8 ± 0.2 <b>d</b> | 2.8 ± 0.4 <b>d</b> | 1.8 ± 0.1 <b>d</b> | n.s.               | n.s.               | n.s.               | n.s.               |
|                | KO            | n.s.               | n.s.               | NA                 | n.s.               | NA                 | n.s.               | n.s.               | NA                 | n.s.               | NA                 |
| <i>Kcnq3</i>   | WT            | 2.6 ± 0.1 <b>d</b> | 1.8 ± 0.1 <b>a</b> | 2.3 ± 0.2 <b>d</b> | 2.8 ± 0.2 <b>d</b> | 2.7 ± 0.2 <b>d</b> | 1.8 ± 0.1 <b>c</b> | n.s.               | n.s.               | n.s.               | n.s.               |
|                | KO            | 1.8 ± 0.4          | 1.9 ± 0.3          | NA                 | n.s.               | NA                 | n.s.               | n.s.               | NA                 | 0.4 ± 0.1 <b>a</b> | NA                 |
| <i>Kcnq5</i>   | WT            | 2.3 ± 0.1 <b>d</b> | n.s.               | 2.1 ± 0.2 <b>b</b> | 2.5 ± 0.2 <b>d</b> | 2.3 ± 0.3 <b>d</b> | 2.4 ± 0.2 <b>d</b> | n.s.               | n.s.               | n.s.               | n.s.               |
|                | KO            | n.s.               | n.s.               | NA                 | n.s.               | NA                 | n.s.               | n.s.               | NA                 | n.s.               | NA                 |
| <i>Trpc5</i>   | WT            | 5.0 ± 0.3 <b>d</b> | 3.1 ± 0.3 <b>c</b> | 3.5 ± 0.2 <b>d</b> | 3.7 ± 0.3 <b>d</b> | 4.0 ± 0.4 <b>d</b> | 0.7 ± 0.1 <b>d</b> | n.s.               | n.s.               | n.s.               | n.s.               |
|                | KO            | n.s.               | n.s.               | NA                 | n.s.               | NA                 | 2.1 ± 0.3 <b>a</b> | n.s.               | NA                 | n.s.               | NA                 |

All data were normalized to oil-treated within each sex: a =  $P < .05$ ; b =  $P < .01$ ; c =  $P < .001$ ; d =  $P < .0001$ .  $n = 7-8$  for WT and 5-6 for KO. NA = not applicable and n.s. = not significant.

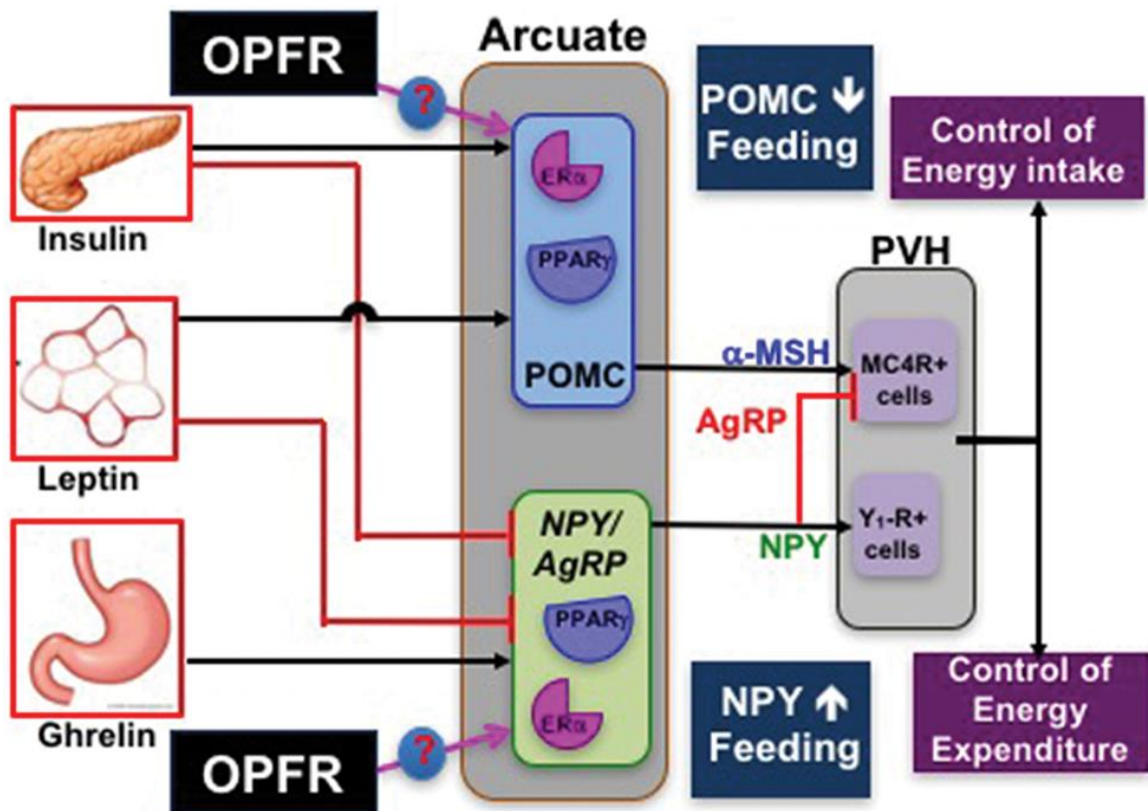
**Table A-1.3.** Liver expression of xenobiotic receptor target genes from WT and ERKO male and females.

| Gene           | Geno-type | Males      |            |            |            |            | Females     |            |            |            |       |
|----------------|-----------|------------|------------|------------|------------|------------|-------------|------------|------------|------------|-------|
|                |           | EE2        | BDE-1      | BDE-10     | OP-1       | OP-10      | EE2         | BDE-1      | BDE-10     | OP-1       | OP-10 |
| <i>Bsep</i>    | WT        | 6.6 ± 0.5d | 7.4 ± 0.5d | 6.5 ± 0.3d | n.s.       | n.s.       | 11.5 ± 0.8d | 8.1 ± 0.9d | 9.7 ± 0.8d | n.s.       | n.s.  |
|                | KO        | n.s.       | n.s.       | NA         | n.s.       | NA         | n.s.        | n.s.       | NA         | n.s.       | NA    |
| <i>Cd36</i>    | WT        | n.s.       | n.s.       | 0.6 ± 0.1a | n.s.       | n.s.       | 0.4 ± 0.0c  | 0.4 ± 0.1c | n.s.       | 0.5 ± 0.1b | n.s.  |
|                | KO        | n.s.       | 3.2 ± 0.8a | NA         | n.s.       | NA         | n.s.        | n.s.       | NA         | n.s.       | NA    |
| <i>Cyp2b10</i> | WT        | n.s.       | 5.2 ± 1.0d | 3.5 ± 0.6b | n.s.       | 3.7 ± 0.4b | n.s.        | n.s.       | 5.0 ± 0.8d | n.s.       | n.s.  |
|                | KO        | n.s.       | 2.1 ± 0.6d | NA         | v          | NA         | n.s.        | n.s.       | NA         | n.s.       | NA    |
| <i>Cyp3a11</i> | WT        | 3.7 ± 0.5d | 4.8 ± 0.5d | 2.8 ± 0.2c | n.s.       | 2.8 ± 0.2c | 1.9 ± 0.2a  | n.s.       | 2.8 ± 0.4d | n.s.       | n.s.  |
|                | KO        | n.s.       | n.s.       | NA         | n.s.       | NA         | n.s.        | n.s.       | NA         | n.s.       | NA    |
| <i>Cyp4a10</i> | WT        | n.s.       | n.s.       | n.s.       | n.s.       | n.s.       | n.s.        | n.s.       | n.s.       | 0.6 ± 0.1b | n.s.  |
|                | KO        | n.s.       | n.s.       | NA         | n.s.       | NA         | v           | n.s.       | NA         | n.s.       | NA    |
| <i>Cyp7a1</i>  | WT        | n.s.       | n.s.       | n.s.       | n.s.       | n.s.       | 0.2 ± 0.0b  | n.s.       | n.s.       | n.s.       | n.s.  |
|                | KO        | n.s.       | n.s.       | NA         | n.s.       | NA         | n.s.        | n.s.       | NA         | n.s.       | NA    |
| <i>Ostβ</i>    | WT        | n.s.       | 3.3 ± 0.8b | 2.1 ± 0.3a | n.s.       | n.s.       | n.s.        | 2.7 ± 0.4a | 2.9 ± 0.4a | n.s.       | n.s.  |
|                | KO        | n.s.       | n.s.       | NA         | n.s.       | NA         | n.s.        | n.s.       | NA         | n.s.       | NA    |
| <i>Shp</i>     | WT        | n.s.       | n.s.       | n.s.       | 0.4 ± 0.1a | n.s.       | 5.3 ± 0.7d  | n.s.       | n.s.       | n.s.       | n.s.  |
|                | KO        | n.s.       | n.s.       | NA         | n.s.       | NA         | n.s.        | n.s.       | NA         | n.s.       | NA    |

All qPCR data is normalized to oil-treated within sex: a =  $P < .05$ ; b =  $P < .01$ ; c =  $P < .001$ ; d =  $P < .0001$ .  $n = 7-8$  for WT and 5-6 for KO. NA = not applicable and n.s. = not significant.



Figure A-1.6. Illustration of our hypothesis



An illustration of our hypothesis that OPFR interact with  $ER\alpha$  and/or  $PPAR\gamma$  in arcuate POMC and NPY/AgRP neurons to control expression of hormone receptors and cation channels to alter release of  $\alpha$ -MSH, NPY, and AgRP on downstream targets in the paraventricular hypothalamus, leading to a decrease in food intake or an increase in energy expenditure.

## REFERENCES

- Abou-Donia MB, Nomeir AA, Bower JH, Makkawy HA. 1990. Absorption, distribution, excretion and metabolism of a single oral dose of [<sup>14</sup>C]tri-o-cresyl phosphate (tocp) in the male rat. *Toxicology*. 65(1-2):61-74.
- Agarwala S, Chen W, Cook TJ. 2004. Effect of chlorpyrifos on efflux transporter gene expression and function in caco-2 cells. *Toxicology in Vitro*. 18(4):403-409.
- Ali N, Dirtu AC, Van den Eede N, Goosey E, Harrad S, Neels H, t Mannetje A, Coakley J, Douwes J, Covaci A. 2012a. Occurrence of alternative flame retardants in indoor dust from new zealand: Indoor sources and human exposure assessment. *Chemosphere*. 88(11):1276-1282.
- Ali N, Van den Eede N, Dirtu AC, Neels H, Covaci A. 2012b. Assessment of human exposure to indoor organic contaminants via dust ingestion in pakistan. *Indoor Air*. 22(3):200-211.
- Andrews ZB. 2011. Central mechanisms involved in the orexigenic actions of ghrelin. *Peptides*. 32(11):2248-2255.
- Arukwe A, Carteny CC, Eggen T, Möder M. 2018. Novel aspects of uptake patterns, metabolite formation and toxicological responses in salmon exposed to the organophosphate esters—tris(2-butoxyethyl)- and tris(2-chloroethyl) phosphate. *Aquatic Toxicology*. 196:146-153.
- Arukwe A, Carteny CC, Möder M, Bonini A, Maubach MA, Eggen T. 2016. Differential modulation of neuro- and interrenal steroidogenesis of juvenile salmon by the organophosphates - tris(2-butoxyethyl)- and tris(2-cloroethyl) phosphate. *Environmental Research*. 148:63-71.
- Asarian L, Geary N. 2002. Cyclic estradiol treatment normalizes body weight and restores physiological patterns of spontaneous feeding and sexual receptivity in ovariectomized rats. *Horm Behav*. 42(4):461-471.
- ASTDR. 2012. Toxicological profile for phosphate ester flame retardants. Atlanta, GA: Agency for Toxic Substances and Disease Registry, U.S. Dept. of Health and Human Services, Public Health Service. <https://www.atsdr.cdc.gov/toxprofiles/tp202.pdf>.
- Atwood D, Paisley-Jones C. 2017. Pesticides industry sales and usage: 2008–2012 market estimates. United States Environmental Protection Agency: Washington, DC, USA.
- Bain LJ, LeBlanc GA. 1996. Interaction of structurally diverse pesticides with the human *mdr1* gene product p-glycoprotein. *Toxicol Appl Pharmacol*. 141(1):288-298.
- Baldwin KR, Phillips AL, Horman B, Arambula SE, Rebuli ME, Stapleton HM, Patisaul HB. 2017. Sex specific placental accumulation and behavioral effects of developmental firemaster 550 exposure in wistar rats. *Sci Rep*. 7(1):7118.

- Baquero AF, de Solis AJ, Lindsley SR, Kirigiti MA, Smith MS, Cowley MA, Zeltser LM, Grove KL. 2014. Developmental switch of leptin signaling in arcuate nucleus neurons. *J Neurosci.* 34(30):9982-9994.
- Belcher SM, Cookman CJ, Patisaul HB, Stapleton HM. 2014. In vitro assessment of human nuclear hormone receptor activity and cytotoxicity of the flame retardant mixture fm 550 and its triarylphosphate and brominated components. *Toxicol Lett.* 228(2):93-102.
- Berthoud HR. 2002. Multiple neural systems controlling food intake and body weight. *Neurosci Biobehav Rev.* 26(4):393-428.
- Bircsak KM, Gibson CJ, Robey RW, Aleksunes LM. 2013. Assessment of drug transporter function using fluorescent cell imaging. *Curr Protoc Toxicol.* 57:Unit 23 26.
- Bosch MA, Hou J, Fang Y, Kelly MJ, Ronnekleiv OK. 2009. 17beta-estradiol regulation of the mrna expression of t-type calcium channel subunits: Role of estrogen receptor alpha and estrogen receptor beta. *J Comp Neurol.* 512(3):347-358.
- Bosch MA, Tonsfeldt KJ, Ronnekleiv OK. 2013. Mrna expression of ion channels in gnRH neurons: Subtype-specific regulation by 17beta-estradiol. *Mol Cell Endocrinol.* 367(1-2):85-97.
- Bosch MA, Xue C, Ronnekleiv OK. 2012. Kisspeptin expression in guinea pig hypothalamus: Effects of 17beta-estradiol. *J Comp Neurol.* 520(10):2143-2162.
- Burka LT, Sanders JM, Herr DW, Matthews HB. 1991. Metabolism of tris(2-chloroethyl) phosphate in rats and mice. *Drug Metab Dispos.* 19(2):443-447.
- Butt CM, Congleton J, Hoffman K, Fang M, Stapleton HM. 2014. Metabolites of organophosphate flame retardants and 2-ethylhexyl tetrabromobenzoate in urine from paired mothers and toddlers. *Environ Sci Technol.* 48(17):10432-10438.
- Butt CM, Hoffman K, Chen A, Lorenzo A, Congleton J, Stapleton HM. 2016. Regional comparison of organophosphate flame retardant (pfr) urinary metabolites and tetrabromobenzoic acid (tbba) in mother-toddler pairs from california and new jersey. *Environ Int.* 94:627-634.
- Carignan CC, McClean MD, Cooper EM, Watkins DJ, Fraser AJ, Heiger-Bernays W, Stapleton HM, Webster TF. 2013. Predictors of tris(1,3-dichloro-2-propyl) phosphate metabolite in the urine of office workers. *Environ Int.* 55:56-61.
- Carignan CC, Mínguez-Alarcón L, Butt CM, Williams PL, Meeker JD, Stapleton HM, Toth TL, Ford JB, Hauser R, for the EST. 2017. Urinary concentrations of organophosphate flame retardant metabolites and pregnancy outcomes among women undergoing in vitro fertilization. *Environ Health Persp.* 125(8):087018.
- Carignan CC, Mínguez-Alarcon L, Williams PL, Meeker JD, Stapleton HM, Butt CM, Toth TL, Ford JB, Hauser R, Team ES. 2018. Paternal urinary concentrations of organophosphate flame retardant metabolites, fertility measures, and pregnancy

- outcomes among couples undergoing in vitro fertilization. *Environ Int.* 111:232-238.
- Carletti E, Schopfer LM, Colletier JP, Froment MT, Nachon F, Weik M, Lockridge O, Masson P. 2011. Reaction of cresyl saligenin phosphate, the organophosphorus agent implicated in aerotoxic syndrome, with human cholinesterases: Mechanistic studies employing kinetics, mass spectrometry, and x-ray structure analysis. *Chem Res Toxicol.* 24(6):797-808.
- Carr RL, Chambers JE. 1996. Kinetic analysis of the in vitro inhibition, aging, and reactivation of brain acetylcholinesterase from rat and channel catfish by paraoxon and chlorpyrifos-oxon. *Toxicol Appl Pharmacol.* 139(2):365-373.
- Carrington CD, Abou-Donia MB. 1988. Variation between three strains of rat: Inhibition of neurotoxic esterase and acetylcholinesterase by tri-o-cresyl phosphate. *J Toxicol Environ Health.* 25(3):259-268.
- Casida JE. 1964. Esterase inhibitors as pesticides. *Science.* 146(3647):1011-1017.
- Casida JE, Quistad GB. 2004. Organophosphate toxicology: Safety aspects of nonacetylcholinesterase secondary targets. *Chem Res Toxicol.* 17(8):983-998.
- Castorina R, Bradman A, Stapleton HM, Butt C, Avery D, Harley KG, Gunier RB, Holland N, Eskenazi B. 2017a. Current-use flame retardants: Maternal exposure and neurodevelopment in children of the chamacos cohort. *Chemosphere.* 189:574-580.
- Castorina R, Butt C, Stapleton HM, Avery D, Harley KG, Holland N, Eskenazi B, Bradman A. 2017b. Flame retardants and their metabolites in the homes and urine of pregnant women residing in california (the chamacos cohort). *Chemosphere.* 179:159-166.
- Cequier E, Marce RM, Becher G, Thomsen C. 2014. A high-throughput method for determination of metabolites of organophosphate flame retardants in urine by ultra performance liquid chromatography-high resolution mass spectrometry. *Anal Chim Acta.* 845:98-104.
- Chanda SM, Mortensen SR, Moser VC, Padilla S. 1997. Tissue-specific effects of chlorpyrifos on carboxylesterase and cholinesterase activity in adult rats: An in vitro and in vivo comparison. *Fundam Appl Toxicol.* 38(2):148-157.
- Chapman DE, Michener SR, Powis G. 1991. Metabolism of the flame retardant plasticizer tris(2-chloroethyl)phosphate by human and rat liver preparations. *Fundam Appl Toxicol.* 17(2):215-224.
- Chen G, Jin Y, Wu Y, Liu L, Fu Z. 2015a. Exposure of male mice to two kinds of organophosphate flame retardants (opfrs) induced oxidative stress and endocrine disruption. *Environ Toxicol Pharmacol.* 40(1):310-318.
- Chen G, Zhang S, Jin Y, Wu Y, Liu L, Qian H, Fu Z. 2015b. Tpp and tcep induce oxidative stress and alter steroidogenesis in tm3 leydig cells. *Reprod Toxicol.* 57:100-110.

- Chen Y, Fang J, Ren L, Fan R, Zhang J, Liu G, Zhou L, Chen D, Yu Y, Lu S. 2018. Urinary metabolites of organophosphate esters in children in south china: Concentrations, profiles and estimated daily intake. *Environ Pollut.* 235:358-364.
- Choo G, Cho HS, Park K, Lee JW, Kim P, Oh JE. 2018. Tissue-specific distribution and bioaccumulation potential of organophosphate flame retardants in crucian carp. *Environ Pollut.* 239:161-168.
- Costa LG. 2006. Current issues in organophosphate toxicology. *Clin Chim Acta.* 366(1-2):1-13.
- Cristale J, Aragão Belé TG, Lacorte S, Rodrigues de Marchi MR. 2018. Occurrence and human exposure to brominated and organophosphorus flame retardants via indoor dust in a brazilian city. *Environmental Pollution.* 237:695-703.
- Cui YJ, Cheng X, Weaver YM, Klaassen CD. 2009. Tissue distribution, gender-divergent expression, ontogeny, and chemical induction of multidrug resistance transporter genes (*mdr1a*, *mdr1b*, *mdr2*) in mice. *Drug Metab Dispos.* 37(1):203-210.
- Ding J, Xu Z, Huang W, Feng L, Yang F. 2016. Organophosphate ester flame retardants and plasticizers in human placenta in eastern china. *Science of The Total Environment.* 554-555:211-217.
- Dishaw LV, Hunter DL, Padnos B, Padilla S, Stapleton HM. 2014. Developmental exposure to organophosphate flame retardants elicits overt toxicity and alters behavior in early life stage zebrafish (*danio rerio*). *Toxicol Sci.* 142(2):445-454.
- Dodson RE, Perovich LJ, Covaci A, Van den Eede N, Ionas AC, Dirtu AC, Brody JG, Rudel RA. 2012. After the pbde phase-out: A broad suite of flame retardants in repeat house dust samples from california. *Environ Sci Technol.* 46(24):13056-13066.
- Du Z, Wang G, Gao S, Wang Z. 2015. Aryl organophosphate flame retardants induced cardiotoxicity during zebrafish embryogenesis: By disturbing expression of the transcriptional regulators. *Aquatic Toxicology.* 161:25-32.
- Eldefrawi AT, Mansour NA, Brattsten LB, Ahrens VD, Lisk DJ. 1977. Further toxicologic studies with commercial and candidate flame retardant chemicals. Part ii. *Bull Environ Contam Toxicol.* 17(6):720-726.
- Elias CF, Aschkenasi C, Lee C, Kelly J, Ahima RS, Bjorbaek C, Flier JS, Saper CB, Elmquist JK. 1999. Leptin differentially regulates npy and pomc neurons projecting to the lateral hypothalamic area. *Neuron.* 23(4):775-786.
- Ellman GL, Courtney KD, Andres V, Jr., Feather-Stone RM. 1961. A new and rapid colorimetric determination of acetylcholinesterase activity. *Biochem Pharmacol.* 7:88-95.
- EPA. 2008. Child-specific exposure factors handbook. Washington, DC: U.S. Environmental Protection Agency, National Center for Environmental Assessment, Office of Research and Development. <http://purl.access.gpo.gov/GPO/LPS112624>.

- EPA. 2015. TSCA work plan chemical problem formulation and initial assessment chlorinated phosphate ester cluster flame retardants.
- Farhat A, Buick JK, Williams A, Yauk CL, O'Brien JM, Crump D, Williams KL, Chiu S, Kennedy SW. 2014. Tris(1,3-dichloro-2-propyl) phosphate perturbs the expression of genes involved in immune response and lipid and steroid metabolism in chicken embryos. *Toxicol Appl Pharmacol.* 275(2):104-112.
- Fromme H, Lahrz T, Kraft M, Fembacher L, Mach C, Dietrich S, Burkardt R, Volkel W, Goen T. 2014. Organophosphate flame retardants and plasticizers in the air and dust in German daycare centers and human biomonitoring in visiting children (IuPe 3). *Environ Int.* 71:158-163.
- Gao M, Bu L, Ma Y, Liu D. 2013. Concurrent activation of liver X receptor and peroxisome proliferator-activated receptor  $\alpha$  exacerbates hepatic steatosis in high fat diet-induced obese mice. *PLoS One.* 8(6):e65641.
- Garretson JT, Teubner BJ, Grove KL, Vazdarjanova A, Ryu V, Bartness TJ. 2015. Peroxisome proliferator-activated receptor  $\gamma$  controls ingestive behavior, agouti-related protein, and neuropeptide Y mRNA in the arcuate hypothalamus. *J Neurosci.* 35(11):4571-4581.
- Geary N, Asarian L, Korach KS, Pfaff DW, Ogawa S. 2001. Deficits in ER $\alpha$ -dependent control of feeding, weight gain, and cholecystokinin satiation in ER $\alpha$  null mice. *Endocrinology.* 142(11):4751-4757.
- Gorres BK, Bomhoff GL, Morris JK, Geiger PC. 2011. In vivo stimulation of oestrogen receptor  $\alpha$  increases insulin-stimulated skeletal muscle glucose uptake. *J Physiol.* 589(Pt 8):2041-2054.
- Gottsch ML, Popa SM, Lawhorn JK, Qiu J, Tonsfeldt KJ, Bosch MA, Kelly MJ, Ronnekleiv OK, Sanz E, McKnight GS et al. 2011. Molecular properties of kiss1 neurons in the arcuate nucleus of the mouse. *Endocrinology.* 152(11):4298-4309.
- Greaves AK, Letcher RJ. 2016. A review of organophosphate esters in the environment from biological effects to distribution and fate. *Bull Environ Contam Toxicol.*
- He C, Toms LL, Thai P, Van den Eede N, Wang X, Li Y, Baduel C, Harden FA, Heffernan AL, Hobson P et al. 2018. Urinary metabolites of organophosphate esters: Concentrations and age trends in Australian children. *Environ Int.* 111:124-130.
- Herr DW, Sanders JM, Matthews HB. 1991. Brain distribution and fate of tris(2-chloroethyl) phosphate in Fischer 344 rats. *Drug Metab Dispos.* 19(2):436-442.
- Hewitt SC, Kissling GE, Fieselman KE, Jayes FL, Gerrish KE, Korach KS. 2010. Biological and biochemical consequences of global deletion of exon 3 from the ER $\alpha$  gene. *FASEB J.* 24(12):4660-4667.
- Hill JW, Elias CF, Fukuda M, Williams KW, Berglund ED, Holland WL, Cho YR, Chuang JC, Xu Y, Choi M et al. 2010. Direct insulin and leptin action on pro-

- opiomelanocortin neurons is required for normal glucose homeostasis and fertility. *Cell Metab.* 11(4):286-297.
- Hodgson E, Rose RL. 2006. Organophosphorus chemicals: Potent inhibitors of the human metabolism of steroid hormones and xenobiotics. *Drug Metab Rev.* 38(1-2):149-162.
- Hoffman K, Butt CM, Webster TF, Preston EV, Hammel SC, Makey C, Lorenzo AM, Cooper EM, Carignan C, Meeker JD et al. 2017a. Temporal trends in exposure to organophosphate flame retardants in the united states. *Environ Sci Technol Lett.* 4(3):112-118.
- Hoffman K, Daniels JL, Stapleton HM. 2014. Urinary metabolites of organophosphate flame retardants and their variability in pregnant women. *Environ Int.* 63:169-172.
- Hoffman K, Garantziotis S, Birnbaum LS, Stapleton HM. 2015. Monitoring indoor exposure to organophosphate flame retardants: Hand wipes and house dust. *Environ Health Perspect.* 123(2):160-165.
- Hoffman K, Lorenzo A, Butt CM, Adair L, Herring AH, Stapleton HM, Daniels JL. 2017b. Predictors of urinary flame retardant concentration among pregnant women. *Environment International.* 98:96-101.
- Honkakoski P, Palvimo JJ, Penttilä L, Vepsäläinen J, Auriola S. 2004. Effects of triaryl phosphates on mouse and human nuclear receptors. *Biochem Pharmacol.* 67(1):97-106.
- Hou R, Xu Y, Wang Z. 2016. Review of opfrs in animals and humans: Absorption, bioaccumulation, metabolism, and internal exposure research. *Chemosphere.* 153:78-90.
- Hu X, Zhang J, Jiang Y, Lei Y, Lu L, Zhou J, Huang H, Fang D, Tao G. 2014. Effect on metabolic enzymes and thyroid receptors induced by bde-47 by activation the pregnane x receptor in hepg2, a human hepatoma cell line. *Toxicol In Vitro.* 28(8):1377-1385.
- Jones-Otazo HA, Clarke JP, Diamond ML, Archbold JA, Ferguson G, Harner T, Richardson GM, Ryan JJ, Wilford B. 2005. Is house dust the missing exposure pathway for pbdes? An analysis of the urban fate and human exposure to pbdes. *Environmental science & technology.* 39(14):5121-5130.
- Kim HS, Hwang YC, Koo SH, Park KS, Lee MS, Kim KW, Lee MK. 2013. Ppar-gamma activation increases insulin secretion through the up-regulation of the free fatty acid receptor gpr40 in pancreatic beta-cells. *PLoS One.* 8(1):e50128.
- Kim JW, Isobe T, Muto M, Tue NM, Katsura K, Malarvannan G, Sudaryanto A, Chang KH, Prudente M, Viet PH et al. 2014. Organophosphorus flame retardants (pfrs) in human breast milk from several asian countries. *Chemosphere.* 116:91-97.
- King AM, Aaron CK. 2015. Organophosphate and carbamate poisoning. *Emerg Med Clin North Am.* 33(1):133-151.

- Klaassen CD, Aleksunes LM. 2010. Xenobiotic, bile acid, and cholesterol transporters: Function and regulation. *Pharmacol Rev.* 62(1):1-96.
- Kodaira H, Kusuhara H, Ushiki J, Fuse E, Sugiyama Y. 2010. Kinetic analysis of the cooperation of p-glycoprotein (p-gp/abcb1) and breast cancer resistance protein (bcpr/abcg2) in limiting the brain and testis penetration of erlotinib, flavopiridol, and mitoxantrone. *J Pharmacol Exp Ther.* 333(3):788-796.
- Kojima H, Takeuchi S, Itoh T, Iida M, Kobayashi S, Yoshida T. 2013. In vitro endocrine disruption potential of organophosphate flame retardants via human nuclear receptors. *Toxicology.* 314(1):76-83.
- Krumm EA, Patel VJ, Tillery TS, Yasrebi A, Shen J, Guo GL, Marco SM, Buckley BT, Roepke TA. 2017. Organophosphate flame-retardants alter adult mouse homeostasis and gene expression in a sex-dependent manner potentially through interactions with era. *Toxicological Sciences.* kfx238-kfx238.
- Kubota N, Terauchi Y, Miki H, Tamemoto H, Yamauchi T, Komeda K, Satoh S, Nakano R, Ishii C, Sugiyama T et al. 1999. Ppar gamma mediates high-fat diet-induced adipocyte hypertrophy and insulin resistance. *Mol Cell.* 4(4):597-609.
- Kurebayashi H, Tanaka A, Yamaha T. 1985. Metabolism and disposition of the flame retardant plasticizer, tri-p-cresyl phosphate, in the rat. *Toxicol Appl Pharmacol.* 77(3):395-404.
- Kurt-Karakus P, Alegria H, Birgul A, Gungormus E, Jantunen L. 2017. Organophosphate ester (opes) flame retardants and plasticizers in air and soil from a highly industrialized city in turkey. *Sci Total Environ.* 625:555-565.
- Kwong TC. 2002. Organophosphate pesticides: Biochemistry and clinical toxicology. *Ther Drug Monit.* 24(1):144-149.
- Lanning CL, Fine RL, Sachs CW, Rao US, Corcoran JJ, Abou-Donia MB. 1996. Chlorpyrifos oxon interacts with the mammalian multidrug resistance protein, p-glycoprotein. *J Toxicol Environ Health.* 47(4):395-407.
- Li J, Yu N, Zhang B, Jin L, Li M, Hu M, Zhang X, Wei S, Yu H. 2014. Occurrence of organophosphate flame retardants in drinking water from china. *Water Res.* 54:53-61.
- Lin HV, Plum L, Ono H, Gutierrez-Juarez R, Shanabrough M, Borok E, Horvath TL, Rossetti L, Accili D. 2010. Divergent regulation of energy expenditure and hepatic glucose production by insulin receptor in agouti-related protein and pomc neurons. *Diabetes.* 59(2):337-346.
- Lipscomb ST, McClelland MM, MacDonald M, Cardenas A, Anderson KA, Kile ML. 2017. Cross-sectional study of social behaviors in preschool children and exposure to flame retardants. *Environ Health.* 16(1):23.



- Liu LY, He K, Hites RA, Salamova A. 2016a. Hair and nails as noninvasive biomarkers of human exposure to brominated and organophosphate flame retardants. *Environ Sci Technol*. 50(6):3065-3073.
- Liu X, Ji K, Choi K. 2012. Endocrine disruption potentials of organophosphate flame retardants and related mechanisms in h295r and mvln cell lines and in zebrafish. *Aquatic Toxicology*. 114-115:173-181.
- Liu X, Ji K, Jo A, Moon HB, Choi K. 2013. Effects of tdcpp or tpp on gene transcriptions and hormones of hpg axis, and their consequences on reproduction in adult zebrafish (*danio rerio*). *Aquat Toxicol*. 134-135:104-111.
- Liu X, Jung D, Jo A, Ji K, Moon HB, Choi K. 2016b. Long-term exposure to triphenylphosphate alters hormone balance and hpg, hpi, and hpt gene expression in zebrafish (*danio rerio*). *Environ Toxicol Chem*. 35(9):2288-2296.
- Long L, Toda C, Jeong JK, Horvath TL, Diano S. 2014. Ppargamma ablation sensitizes proopiomelanocortin neurons to leptin during high-fat feeding. *J Clin Invest*. 124(9):4017-4027.
- Lu Q, Cai Z, Fu J, Luo S, Liu C, Li X, Zhao D. 2014. Molecular docking and molecular dynamics studies on the interactions of hydroxylated polybrominated diphenyl ethers to estrogen receptor alpha. *Ecotoxicol Environ Saf*. 101:83-89.
- Lynn RK, Wong K, Dickinson RG, Gerber N, Kennish JM. 1980. Diester metabolites of the flame retardant chemicals, tris(1,3-dichloro-2-propyl)phosphate and tris(2,3-dibromopropyl) phosphate in the rat: Identification and quantification. *Res Commun Chem Pathol Pharmacol*. 28(2):351-360.
- Ma Y, Jin J, Li P, Xu M, Sun Y, Wang Y, Yuan H. 2017. Organophosphate ester flame retardant concentrations and distributions in serum from inhabitants of shandong, china, and changes between 2011 and 2015. *Environ Toxicol Chem*. 36(2):414-421.
- Ma Z, Yu Y, Tang S, Liu H, Su G, Xie Y, Giesy JP, Hecker M, Yu H. 2015. Differential modulation of expression of nuclear receptor mediated genes by tris(2-butoxyethyl) phosphate (tboep) on early life stages of zebrafish (*danio rerio*). *Aquat Toxicol*. 169:196-203.
- Mamounis KJ, Yang JA, Yasrebi A, Roepke TA. 2014. Estrogen response element-independent signaling partially restores post-ovariectomy body weight gain but is not sufficient for 17beta-estradiol's control of energy homeostasis. *Steroids*. 81:88-98.
- Mao Q, Unadkat JD. 2015. Role of the breast cancer resistance protein (bcrp/abcg2) in drug transport--an update. *AAPS J*. 17(1):65-82.
- Matthews HB, Dixon D, Herr DW, Tilson H. 1990. Subchronic toxicity studies indicate that tris(2-chloroethyl)phosphate administration results in lesions in the rat hippocampus. *Toxicology and industrial health*. 6(1):1-15.

- Mauvais-Jarvis F, Clegg DJ, Hevener AL. 2013. The role of estrogens in control of energy balance and glucose homeostasis. *Endocr Rev.* 34(3):309-338.
- Maxwell DM. 1992. The specificity of carboxylesterase protection against the toxicity of organophosphorus compounds. *Toxicol Appl Pharmacol.* 114(2):306-312.
- McGee SP, Konstantinov A, Stapleton HM, Volz DC. 2013. Aryl phosphate esters within a major pentabde replacement product induce cardiotoxicity in developing zebrafish embryos: Potential role of the aryl hydrocarbon receptor. *Toxicol Sci.* 133(1):144-156.
- Meeker JD, Cooper EM, Stapleton HM, Hauser R. 2013a. Exploratory analysis of urinary metabolites of phosphorus-containing flame retardants in relation to markers of male reproductive health. *Endocr Disruptors (Austin).* 1(1):e26306.
- Meeker JD, Cooper EM, Stapleton HM, Hauser R. 2013b. Urinary metabolites of organophosphate flame retardants: Temporal variability and correlations with house dust concentrations. *Environ Health Perspect.* 121(5):580-585.
- Meeker JD, Stapleton HM. 2010. House dust concentrations of organophosphate flame retardants in relation to hormone levels and semen quality parameters. *Environ Health Perspect.* 118(3):318-323.
- Minegishi KI, Kurebayashi H, Nambaru S, Morimoto K, Takahashi T, Yamaha T. 1988. Comparative studies on absorption, distribution, and excretion of flame retardants halogenated alkyl phosphate in rats. *Eisei Kagaku.* 34(2):102-114.
- Mirshamsi S, Laidlaw HA, Ning K, Anderson E, Burgess LA, Gray A, Sutherland C, Ashford ML. 2004. Leptin and insulin stimulation of signalling pathways in arcuate nucleus neurones: Pi3k dependent actin reorganization and katp channel activation. *BMC Neurosci.* 5:54.
- Moller A, Sturm R, Xie ZY, Cai MH, He JF, Ebinghaus R. 2012. Organophosphorus flame retardants and plasticizers in airborne particles over the northern pacific and indian ocean toward the polar regions: Evidence for global occurrence. *Environmental Science & Technology.* 46(6):3127-3134.
- Morris PJ, Medina-Cleghorn D, Heslin A, King SM, Orr J, Mulvihill MM, Krauss RM, Nomura DK. 2014. Organophosphorus flame retardants inhibit specific liver carboxylesterases and cause serum hypertriglyceridemia. *ACS Chemical Biology.* 9(5):1097-1103.
- Moser VC, Padilla S. 2011. Esterase metabolism of cholinesterase inhibitors using rat liver in vitro. *Toxicology.* 281(1-3):56-62.
- Nogueiras R, Williams LM, Dieguez C. 2010. Ghrelin: New molecular pathways modulating appetite and adiposity. *Obes Facts.* 3(5):285-292.
- Nomeir AA, Kato S, Matthews HB. 1981. The metabolism and disposition of tris(1,3-dichloro-2-propyl) phosphate (fyrol fr-2) in the rat. *Toxicol Appl Pharmacol.* 57(3):401-413.

- Noyes PD, Haggard DE, Gonnerman GD, Tanguay RL. 2015. Advanced morphological — behavioral test platform reveals neurodevelopmental defects in embryonic zebrafish exposed to comprehensive suite of halogenated and organophosphate flame retardants. *Toxicological Sciences*. 145(1):177-195.
- OECD. 1995. Risk reduction monograph no. 3: Selected brominated flame retardants background and national experience with reducing risk.
- Oliveri AN, Ortiz E, Levin ED. 2018. Developmental exposure to an organophosphate flame retardant alters later behavioral responses to dopamine antagonism in zebrafish larvae. *Neurotoxicol Teratol*. 67:25-30.
- Ospina M, Jayatilaka NK, Wong LY, Restrepo P, Calafat AM. 2018. Exposure to organophosphate flame retardant chemicals in the u.S. General population: Data from the 2013-2014 national health and nutrition examination survey. *Environ Int*. 110:32-41.
- Pacyniak EK, Cheng X, Cunningham ML, Crofton K, Klaassen CD, Guo GL. 2007. The flame retardants, polybrominated diphenyl ethers, are pregnane x receptor activators. *Toxicol Sci*. 97(1):94-102.
- Patisaul HB, Roberts SC, Mabrey N, McCaffrey KA, Gear RB, Braun J, Belcher SM, Stapleton HM. 2013. Accumulation and endocrine disrupting effects of the flame retardant mixture firemaster(r) 550 in rats: An exploratory assessment. *J Biochem Mol Toxicol*. 27(2):124-136.
- Paxinos G, Franklin KBJ. 2008. The mouse brain in stereotaxic coordinates. Amsterdam ; Boston: Elsevier Academic Press.
- Phillips AL, Chen A, Rock KD, Horman B, Patisaul HB, Stapleton HM. 2016. Editor's highlight: Transplacental and lactational transfer of firemaster® 550 components in dosed wistar rats. *Toxicological Sciences*. 153(2):246-257.
- Phillips AL, Hammel SC, Konstantinov A, Stapleton HM. 2017. Characterization of individual isopropylated and tert-butylated triarylphosphate (itp and tbpp) isomers in several commercial flame retardant mixtures and house dust standard reference material srm 2585. *Environmental Science & Technology*. 51(22):13443-13449.
- Pillai HK, Fang M, Beglov D, Kozakov D, Vajda S, Stapleton HM, Webster TF, Schlezinger JJ. 2014. Ligand binding and activation of ppargamma by firemaster(r) 550: Effects on adipogenesis and osteogenesis in vitro. *Environ Health Perspect*. 122(11):1225-1232.
- Polli JW, Olson KL, Chism JP, John-Williams LS, Yeager RL, Woodard SM, Otto V, Castellino S, Demby VE. 2009. An unexpected synergist role of p-glycoprotein and breast cancer resistance protein on the central nervous system penetration of the tyrosine kinase inhibitor lapatinib (n-{3-chloro-4-[(3-fluorobenzyl)oxy]phenyl}-6-[5-({2-(methylsulfonyl)ethyl}amino )methyl)-2-furyl]-4-quinazolinamine; gw572016). *Drug Metab Dispos*. 37(2):439-442.

- Preston EV, McClean MD, Claus Henn B, Stapleton HM, Braverman LE, Pearce EN, Makey CM, Webster TF. 2017. Associations between urinary diphenyl phosphate and thyroid function. *Environ Int.* 101:158-164.
- Proudan N, Peroski M, Grignol G, Merchenthaler I, Dudas B. 2015. Juxtapositions between the somatostatinergic and growth hormone-releasing hormone (ghrh) neurons in the human hypothalamus. *Neuroscience.* 297:205-210.
- Qiu J, Bosch MA, Jamali K, Xue C, Kelly MJ, Ronnekleiv OK. 2006. Estrogen upregulates t-type calcium channels in the hypothalamus and pituitary. *J Neurosci.* 26(43):11072-11082.
- Qiu J, Fang Y, Ronnekleiv OK, Kelly MJ. 2010. Leptin excites proopiomelanocortin neurons via activation of trpc channels. *J Neurosci.* 30(4):1560-1565.
- Qiu J, Zhang C, Borgquist A, Nestor CC, Smith AW, Bosch MA, Ku S, Wagner EJ, Ronnekleiv OK, Kelly MJ. 2014. Insulin excites anorexigenic proopiomelanocortin neurons via activation of canonical transient receptor potential channels. *Cell Metab.* 19(4):682-693.
- Renaud HJ, Cui JY, Khan M, Klaassen CD. 2011. Tissue distribution and gender-divergent expression of 78 cytochrome p450 mrnas in mice. *Toxicol Sci.* 124(2):261-277.
- Roberts JR, Reigart JR. 2013. Recognition and management of pesticide poisonings.
- Rock KD, Horman B, Phillips AL, McRitchie SL, Watson S, Deese-Spruill J, Jima D, Sumner S, Stapleton HM, Patisaul HB. 2018. EDC impact: Molecular effects of developmental fm 550 exposure in wistar rat placenta and fetal forebrain. *Endocr Connect.* 7(2):305-324.
- Roepke TA, Malyala A, Bosch MA, Kelly MJ, Ronnekleiv OK. 2007. Estrogen regulation of genes important for k<sup>+</sup> channel signaling in the arcuate nucleus. *Endocrinology.* 148(10):4937-4951.
- Roepke TA, Qiu J, Smith AW, Ronnekleiv OK, Kelly MJ. 2011. Fasting and 17beta-estradiol differentially modulate the m-current in neuropeptide y neurons. *J Neurosci.* 31(33):11825-11835.
- Roepke TA, Smith AW, Ronnekleiv OK, Kelly MJ. 2012. Serotonin 5-HT<sub>2C</sub> receptor-mediated inhibition of the m-current in hypothalamic POMC neurons. *Am J Physiol Endocrinol Metab.* 302(11):E1399-1406.
- Romano ME, Hawley NL, Eliot M, Calafat AM, Jayatilaka NK, Kelsey K, McGarvey S, Phipps MG, Savitz DA, Werner EF et al. 2017. Variability and predictors of urinary concentrations of organophosphate flame retardant metabolites among pregnant women in Rhode Island. *Environ Health.* 16(1):40.
- Ross MK, Borazjani A. 2007. Enzymatic activity of human carboxylesterases. *Curr Protoc Toxicol.* Chapter 4:Unit 4 24.

- Ross MK, Streit TM, Herring KL. 2010. Carboxylesterases: Dual roles in lipid and pesticide metabolism. *J Pestic Sci.* 35(3):257-264.
- Saboori AM, Lang DM, Newcombe DS. 1991. Structural requirements for the inhibition of human monocyte carboxylesterase by organophosphorus compounds. *Chem Biol Interact.* 80(3):327-338.
- Salamova A, Hermanson MH, Hites RA. 2014a. Organophosphate and halogenated flame retardants in atmospheric particles from a european arctic site. *Environmental Science & Technology.* 48(11):6133-6140.
- Salamova A, Ma YN, Venier M, Hites RA. 2014b. High levels of organophosphate flame retardants in the great lakes atmosphere. *Environ Sci Tech Let.* 1(1):8-14.
- Saper CB, Chou TC, Elmquist JK. 2002. The need to feed: Homeostatic and hedonic control of eating. *Neuron.* 36(2):199-211.
- Sasaki K, Suzuki T, Takeda M, Uchiyama M. 1984. Metabolism of phosphoric-acid triesters by rat-liver homogenate. *B Environ Contam Tox.* 33(3):281-288.
- Sasaki K, Takeda M, Uchiyama M. 1981. Toxicity, absorption and elimination of phosphoric acid triesters by killifish and goldfish. *Bull Environ Contam Toxicol.* 27(6):775-782.
- Schmittgen TD, Livak KJ. 2008. Analyzing real-time pcr data by the comparative c(t) method. *Nat Protoc.* 3(6):1101-1108.
- Schreder ED, Uding N, La Guardia MJ. 2016. Inhalation a significant exposure route for chlorinated organophosphate flame retardants. *Chemosphere.* 150:499-504.
- Schwartz MW, Woods SC, Porte D, Jr., Seeley RJ, Baskin DG. 2000. Central nervous system control of food intake. *Nature.* 404(6778):661-671.
- Shen B, Whitehead TP, Gill R, Dhaliwal J, Brown FR, Petreas M, Patton S, Hammond SK. 2017. Organophosphate flame retardants in dust collected from united states fire stations. *Environ Int.* 112:41-48.
- Shi L, Bian X, Qu Z, Ma Z, Zhou Y, Wang K, Jiang H, Xie J. 2013. Peptide hormone ghrelin enhances neuronal excitability by inhibition of kv7/kcnq channels. *Nat Commun.* 4:1435.
- Soubry A, Hoyo C, Butt CM, Fieuws S, Price TM, Murphy SK, Stapleton HM. 2017. Human exposure to flame-retardants is associated with aberrant DNA methylation at imprinted genes in sperm. *Environmental Epigenetics.* 3(1):dvx003-dvx003.
- Stapleton HM, Klosterhaus S, Eagle S, Fuh J, Meeker JD, Blum A, Webster TF. 2009. Detection of organophosphate flame retardants in furniture foam and u.S. House dust. *Environ Sci Technol.* 43(19):7490-7495.

- Stapleton HM, Klosterhaus S, Keller A, Ferguson PL, van Bergen S, Cooper E, Webster TF, Blum A. 2011. Identification of flame retardants in polyurethane foam collected from baby products. *Environ Sci Technol*. 45(12):5323-5331.
- Staskal DF, Diliberto JJ, DeVito MJ, Birnbaum LS. 2005. Toxicokinetics of bde 47 in female mice: Effect of dose, route of exposure, and time. *Toxicol Sci*. 83(2):215-223.
- Stieger B, Gao B. 2015. Drug transporters in the central nervous system. *Clin Pharmacokinet*. 54(3):225-242.
- Su G, Crump D, Letcher RJ, Kennedy SW. 2014. Rapid in vitro metabolism of the flame retardant triphenyl phosphate and effects on cytotoxicity and mrna expression in chicken embryonic hepatocytes. *Environ Sci Technol*. 48(22):13511-13519.
- Sueyoshi T, Li L, Wang H, Moore R, Kodavanti PR, Lehmler HJ, Negishi M, Birnbaum LS. 2014. Flame retardant bde-47 effectively activates nuclear receptor car in human primary hepatocytes. *Toxicol Sci*. 137(2):292-302.
- Suhring R, Diamond ML, Scheringer M, Wong F, Pucko M, Stern G, Burt A, Hung H, Fellin P, Li H et al. 2016. Organophosphate esters in canadian arctic air: Occurrence, levels and trends. *Environmental Science & Technology*. 50(14):7409-7415.
- Sun L, Xu W, Peng T, Chen H, Ren L, Tan H, Xiao D, Qian H, Fu Z. 2016. Developmental exposure of zebrafish larvae to organophosphate flame retardants causes neurotoxicity. *Neurotoxicol Teratol*. 55:16-22.
- Sundkvist AM, Olofsson U, Haglund P. 2010. Organophosphorus flame retardants and plasticizers in marine and fresh water biota and in human milk. *J Environ Monit*. 12(4):943-951.
- Suzuki T, Sasaki K, Takeda M, Uchiyama M. 1984. Metabolism of tributyl-phosphate in male-rats. *J Agr Food Chem*. 32(3):603-610.
- Thomas MB, Stapleton HM, Dills RL, Violette HD, Christakis DA, Sathyanarayana S. 2017. Demographic and dietary risk factors in relation to urinary metabolites of organophosphate flame retardants in toddlers. *Chemosphere*. 185:918-925.
- Tung EWY, Ahmed S, Peshdary V, Atlas E. 2017. Firemaster(r) 550 and its components isopropylated triphenyl phosphate and triphenyl phosphate enhance adipogenesis and transcriptional activity of peroxisome proliferator activated receptor (ppargamma) on the adipocyte protein 2 (ap2) promoter. *PLoS One*. 12(4):e0175855.
- Van den Eede N, Dirtu AC, Neels H, Covaci A. 2011. Analytical developments and preliminary assessment of human exposure to organophosphate flame retardants from indoor dust. *Environment International*. 37(2):454-461.
- Van den Eede N, Maho W, Erratico C, Neels H, Covaci A. 2013a. First insights in the metabolism of phosphate flame retardants and plasticizers using human liver fractions. *Toxicology Letters*. 223(1):9-15.

- Van den Eede N, Neels H, Jorens PG, Covaci A. 2013b. Analysis of organophosphate flame retardant diester metabolites in human urine by liquid chromatography electrospray ionisation tandem mass spectrometry. *J Chromatogr A*. 1303:48-53.
- van der Veen I, de Boer J. 2012. Phosphorus flame retardants: Properties, production, environmental occurrence, toxicity and analysis. *Chemosphere*. 88(10):1119-1153.
- Vora DD, Dastur DK, Braganca BM, Parihar LM, Iyer CG, Fondekar RB, Prabhakaran K. 1962. Toxic polyneuritis in bombay due to ortho-cresyl-phosphate poisoning. *J Neurol Neurosurg Psychiatry*. 25:234-242.
- Wang D, Zhu W, Chen L, Yan J, Teng M, Zhou Z. 2018. Neonatal triphenyl phosphate and its metabolite diphenyl phosphate exposure induce sex- and dose-dependent metabolic disruptions in adult mice. *Environmental Pollution*. 237:10-17.
- Wang Q, Lai NL, Wang X, Guo Y, Lam PK, Lam JC, Zhou B. 2015a. Bioconcentration and transfer of the organophorous flame retardant 1,3-dichloro-2-propyl phosphate causes thyroid endocrine disruption and developmental neurotoxicity in zebrafish larvae. *Environ Sci Technol*. 49(8):5123-5132.
- Wang Q, Lam JC-W, Man Y-C, Lai NL-S, Kwok KY, Guo Yy, Lam PK-S, Zhou B. 2015b. Bioconcentration, metabolism and neurotoxicity of the organophorous flame retardant 1,3-dichloro 2-propyl phosphate (tdcpp) to zebrafish. *Aquatic Toxicology*. 158:108-115.
- Wang Q, Lam JC, Han J, Wang X, Guo Y, Lam PK, Zhou B. 2015c. Developmental exposure to the organophosphorus flame retardant tris(1,3-dichloro-2-propyl) phosphate: Estrogenic activity, endocrine disruption and reproductive effects on zebrafish. *Aquat Toxicol*. 160:163-171.
- Wei GL, Li DQ, Zhuo MN, Liao YS, Xie ZY, Guo TL, Li JJ, Zhang SY, Liang ZQ. 2015. Organophosphorus flame retardants and plasticizers: Sources, occurrence, toxicity and human exposure. *Environ Pollut*. 196:29-46.
- Wen X, Gibson CJ, Yang I, Buckley B, Goedken MJ, Richardson JR, Aleksunes LM. 2014. Mdr1 transporter protects against paraquat-induced toxicity in human and mouse proximal tubule cells. *Toxicol Sci*. 141(2):475-483.
- Woods SC. 2009. The control of food intake: Behavioral versus molecular perspectives. *Cell Metab*. 9(6):489-498.
- Xu LL, Long CY, Wang JL, Yu M, Chen JX. 2016. Involvement of oxidative stress in tri-ortho-cresyl phosphate-induced liver injury in male mice. *Hum Exp Toxicol*. 35(10):1093-1101.
- Xu Q, Wu D, Dang Y, Yu L, Liu C, Wang J. 2017. Reproduction impairment and endocrine disruption in adult zebrafish (*danio rerio*) after waterborne exposure to tboep. *Aquat Toxicol*. 182:163-171.

- Yan S, Wu H, Qin J, Zha J, Wang Z. 2017. Halogen-free organophosphorus flame retardants caused oxidative stress and multixenobiotic resistance in asian freshwater clams (*corbicula fluminea*). *Environmental Pollution*. 225:559-568.
- Yang F, Ding J, Huang W, Xie W, Liu W. 2014. Particle size-specific distributions and preliminary exposure assessments of organophosphate flame retardants in office air particulate matter. *Environ Sci Technol*. 48(1):63-70.
- Yang JA, Mamounis KJ, Yasrebi A, Roepke TA. 2016a. Regulation of gene expression by 17beta-estradiol in the arcuate nucleus of the mouse through ere-dependent and ere-independent mechanisms. *Steroids*. 107:128-138.
- Yang JA, Yasrebi A, Snyder M, Roepke TA. 2016b. The interaction of fasting, caloric restriction, and diet-induced obesity with 17beta-estradiol on the expression of kndy neuropeptides and their receptors in the female mouse. *Mol Cell Endocrinol*. 437:35-50.
- Yang W, Zhao F, Fang Y, Li L, Li C, Ta N. 2018. 1h-nuclear magnetic resonance metabolomics revealing the intrinsic relationships between neurochemical alterations and neurobehavioral and neuropathological abnormalities in rats exposed to tris(2-chloroethyl)phosphate. *Chemosphere*. 200:649-659.
- Yasrebi A, Hsieh A, Mamounis KJ, Krumm EA, Yang JA, Magby J, Hu P, Roepke TA. 2016. Differential gene regulation of ghrelin signaling pathway in the arcuate nucleus and npy neurons by fasting, diet-induced obesity, and 17beta-estradiol. *Mol Cell Endocrinol*. 422:42-56.
- Yasrebi A, Rivera JA, Krumm EA, Yang JA, Roepke TA. 2017. Activation of estrogen response element-independent  $\alpha$  signaling protects female mice from diet-induced obesity. *Endocrinology*. 158(2):319-334.
- Yu L, Jia Y, Su G, Sun Y, Letcher RJ, Giesy JP, Yu H, Han Z, Liu C. 2017. Parental transfer of tris(1,3-dichloro-2-propyl) phosphate and transgenerational inhibition of growth of zebrafish exposed to environmentally relevant concentrations. *Environmental Pollution*. 220:196-203.
- Yuan L, Li J, Zha J, Wang Z. 2016. Targeting neurotrophic factors and their receptors, but not cholinesterase or neurotransmitter, in the neurotoxicity of tdcpp in chinese rare minnow adults (*gobiocypris rarus*). *Environmental Pollution*. 208:670-677.
- Zabeau L, Lavens D, Peelman F, Eyckerman S, Vandekerckhove J, Tavernier J. 2003. The ins and outs of leptin receptor activation. *FEBS Lett*. 546(1):45-50.
- Zhao F, Chen M, Gao F, Shen H, Hu J. 2017. Organophosphorus flame retardants in pregnant women and their transfer to chorionic villi. *Environmental Science & Technology*. 51(11):6489-6497.
- Zhou L, Zhang W, Xie W, Chen H, Yu W, Li H, Shen G. 2017. Tributyl phosphate impairs the urea cycle and alters liver pathology and metabolism in mice after short-term exposure based on a metabolomics study. *Science of The Total Environment*. 603-604:77-85.



Zhu Y, Ma X, Su G, Yu L, Letcher RJ, Hou J, Yu H, Giesy JP, Liu C. 2015. Environmentally relevant concentrations of the flame retardant tris(1,3-dichloro-2-propyl) phosphate inhibit growth of female zebrafish and decrease fecundity. *Environ Sci Technol.* 49(24):14579-14587.